Aix Marseille Université

NNT : 0000AIXM0000

THÈSE DE DOCTORAT

Soutenue à Aix-Marseille Université
le 5 décembre 2024 par

Sofia TUMMINIA

Nouveau Modèle de Presynapse sur Verre pour Étudier la Nanostructure et Fonction de l'Actine Présynaptique

A New Presynapse-on-glass Model to Study the Nanostructure and Function of Presynaptic Actin

Discipline
Biologie santé

Spécialité
Neuroscience

École doctorale
62

Laboratoire/Partenaires de recherche
Institut de NeuroPhysiopathologie

Composition du jury

Pirta HOTULAINEN — Rapportrice
Minerva Institute for Medical Research, University of Helsinki, Helsinki, Finland

Lydia DANGLOT — Rapportrice
IPNP, Université Paris Cité, Paris, France

François DEVRED — Président du jury
INP, Aix-Marseille Université, Marseille, France

Christophe Leterrier — Directeur de thèse
INP, Aix-Marseille Université, Marseille, France

Marie-Jeanne PAPANDRÉOU — Membre Invité
INP, Aix-Marseille Université, Marseille, France

Affidavit

Je soussignée, Sofia Tumminia, déclare par la présente que le travail présenté dans ce manuscrit est mon propre travail, réalisé sous la direction scientifique de Christophe Leterrier et Marie-Jeanne Papandréou, dans le respect des principes d'honnêteté, d'intégrité et de responsabilité inhérents à la mission de recherche. Les travaux de recherche et la rédaction de ce manuscrit ont été réalisés dans le respect à la fois de la charte nationale de déontologie des métiers de la recherche et de la charte d'Aix-Marseille Université relative à la lutte contre le plagiat.

Ce travail n'a pas été précédemment soumis en France ou à l'étranger dans une version identique ou similaire à un organisme examinateur.

Fait à Marseille, le 26 août 2024



Cette œuvre est mise à disposition selon les termes de la Licence Creative Commons Attribution - Pas d'Utilisation Commerciale - Pas de Modification 4.0 International.

Affidavit

I, undersigned, Sofia Tumminia, hereby declare that the work presented in this manuscript is my own work, carried out under the scientific supervision of Christophe Leterrier et Marie-Jeanne Papandréou, in accordance with the principles of honesty, integrity and responsibility inherent to the research mission. The research work and the writing of this manuscript have been carried out in compliance with both the French national charter for Research Integrity and the Aix-Marseille University charter on the fight against plagiarism.

This work has not been submitted previously either in this country or in another country in the same or in a similar version to any other examination body.

Place Marseille, August 26, 2024



Cette œuvre est mise à disposition selon les termes de la Licence Creative Commons Attribution - Pas d'Utilisation Commerciale - Pas de Modification 4.0 International.

Liste de publications et/ou brevets et participation aux conférences

1) Liste des publications et/ou brevet [1] réalisées dans le cadre du projet de thèse :

    1. Deciphering the nanoscale architecture of presynaptic actin using a micropatterned presynapse-on-glass model.
    Tumminia S°, Mezache L°, Wiesner T, Vianay B, Thery M, Papandréou MJ*, Leterrier C* (° co-first authors; * co-corresponding authors).
    bioRxiv, 2024 Sep 5. doi: 10.1101/2024.09.05.611287
    Submitted to the Journal of Neuroscience on September 12th, 2024.

2) Participation aux conférences[2] et écoles d'été au cours de la période de thèse :
    1. Doctoral School of Life and Health Science Symposium 2021, October 18-19. Organizer of the event as member of Hippo'Thèse PhDs' Association.
    2. Microscopy For Biology 2021, November 5-12. CNRS Thematic School on Single Molecule Imagery Techniques. Attendee.
    3. NeuroDays 2022, Mens Sana in Corpore Sano. Interdisciplinary Scientific Seminars in Neuroscience, December 1-2. Organizer of the event as member of the NeuroSchool PhD Program. Attendee.
    4. Doctoral School of Life and Health Science Symposium 2023, May 30-31. Oral Presentation. Organizer of the event as member of Hippo'Thèse PhD's Association. Attendee.
    5. Les Doctoriales du Sud 2023, June 26. Intersection of Socioeconomic World and Doctoral Students. Attendee.
    6. NeuroDays 2023, The Brain Chronicles. Interdisciplinary Scientific Seminars in Neuroscience, November 16-17. Attendee. Oral Presentation. Winner of the 1st Place of NeuroSchool PhD Program Contest.
    7. Focus On Microscopy Conference 2024, March 24-27. Oral Presentation.
    8. Federation of European Neuroscience Society Forum 2024, 25-29 June. Poster Presentation.

[1] Cette liste comprend les articles publiés, les articles soumis à publication et les articles en préparation ainsi que les livres, chapitres de livre et/ou toutes formes de valorisation des résultats des travaux propres à la discipline du projet de thèse. La référence aux publications doit suivre les règles standards de bibliographie et doit être conforme à la charte des publications d'AMU.

[2] Le terme « conférence » est générique. Il désigne à la fois « conférence », « congrès », « workshop », « colloques », « rencontres nationales et/ou internationales » … etc.

Indiquer si vous avez fait une présentation orale ou sous forme de poster.

Résumé

Ce manuscrit décrit les connaissances actuelles et les limitations auxquelles les neuroscientifiques sont confrontés pour déchiffrer le cytosquelette d'actine présynaptique dans son contexte naturel. Interroger l'actine au sein de la présynapse reste un défi malgré l'émergence de techniques de microscopie avantageuses, dépassant la limite de diffraction, permettant l'observation de petites structures biologiques. Pour comprendre les rôles potentiels de l'actine dans les fonctions présynaptiques, une partie de mon projet de thèse a été orientée vers la mise en place et l'application d'un nouveau modèle de présynapse sur verre, facilitant l'imagerie des nanostructures d'actine présynaptique à l'aide de la microscopie de localisation de molécules uniques (SMLM). Cette étude utilise la neuroligine-1, une molécule d'adhésion cellulaire postsynaptique, pour induire la formation de présynapses excitatrices. L'impression d'un micro-pattern de cette protéine sur le verre permet d'orienter les présynapses de manière contrôlée et d'obtenir des résultats cohérents. L'utilisation du modèle de présynapse sur verre a confirmé la présence de présynapses enrichies et non enrichies en actine, ainsi que la corrélation entre l'enrichissement en actine, l'agrégation des clusters présynaptiques et l'activité de recyclage présynaptique, en accord avec les travaux précédents réalisés par l'équipe (Bingham et al., 2023). Ce modèle offre un meilleur accès optique aux composants synaptiques, permettant une imagerie détaillée du corral, du maillage et des rails d'actine ainsi que l'activité du cycle vésiculaire. De plus, le manuscrit discute du potentiel futur de ce modèle dans la recherche sur le cytosquelette d'actine, en proposant des études comparatives explorant la distribution des nanostructures d'actine entre différents types synaptiques, combinées à des outils d'analyse d'image avancés pour affiner la segmentation de l'actine et cartographier plus précisément l'architecture du cytosquelette d'actine. Ces recherches ouvriraient la voie à des études pathologiques, pouvant révéler des dysfonctionnements de l'architecture synaptique et de la dynamique de l'actine dans les troubles neurodéveloppementaux menant à des maladies cognitives.

Mots-clés : cytosquelette d'actine présynaptique, présynapse, modèle de présynapse-sur-verre, SMLM, exocytose, l'activité du cycle vésiculaire

Abstract

This manuscript outlines the current knowledge and limitations neuroscientists face to decipher presynaptic actin cytoskeleton in its natural context. Interrogating actin within the presynapse is still a challenge despite the emergence of advantageous microscopy techniques, going beyond the diffraction-limit, allowing observations of small biological components. To understand the roles actin might play in presynaptic functions, part of my PhD project focused on the implementation and application of a new presynapse-on-glass model facilitating imaging presynaptic actin nanostructure using Single Molecule Localization Microscopy (SMLM). This study employs neuroligin-1, a post-synaptic cell-adhesion molecule, used to induce excitatory presynaptic specializations. Printing a micropattern of this protein onto the glass enables controlled presynaptic orientation and achieves consistent results. The use of presynapse-on-glass model confirmed the presence of actin enriched and non-enriched presynapses, and the correlation between actin enrichment, presynaptic cluster aggregation and presynaptic cycling activity, consistent with previous work realized by the team (Bingham et al., 2023). This model allows for increased optical access to synaptic components, enabling detailed imaging of the actin corral, mesh and rails as well as vesicular cycling activity. Additionally, the manuscript discusses the future potential of this model in actin cytoskeleton research. Proposing comparative studies exploring actin nanostructure distribution between different synaptic types, combined with advanced image analysis tools to refine actin segmentation and map the actin cytoskeleton architecture more accurately. These investigations would open the door for pathological studies possibly uncovering synaptic architecture and actin dynamics dysfunctions in neurodevelopmental disorders leading to cognitive diseases.

Key words: presynaptic actin cytoskeleton, presynapse, presynapse-on-glass model, SMLM, vesicular cycling activity

Acknowledgements

I would like to begin by expressing my deepest gratitude to the pillars of my personal life—my family and friends:

Orsola, Pietro, and Giulia, even though I had to leave our home and island to embrace my future, I miss you every step of the way. Despite the distance, you have remained closer to my heart than ever before. Your patience and steadfastness have consistently inspired me to become the best version of myself—the kind fighter and relentless pursuer of my goals. Your unwavering support has motivated me to look ahead, while your shared wisdom has served as a guiding light throughout this adventure. Grazie di esistere e fare parte della mia vita.

Sylviane, Regis, and Guylian, you welcomed me into your family and made me feel as if I had always belonged. For that, I will always be grateful. Your loving understanding and generosity have profoundly inspired me and provided comfort during my studies in this country. For everything you have done, I am truly thankful.

Riad, Martina, Marine, Anais, Louis, Alice, Estelle, Louisa, Eline, Caroline and Albane, thank you for never doubting my skills and perseverance, and for standing by my side through both good and challenging times. Your support has been a source of strength and inspiration throughout this journey. Without you, I would have lost my motivation and joy in pursuing this path.

Next, I want to acknowledge Christophe and Marie-Jeanne, whose influence introduced me to the world of fundamental research. I am grateful for the opportunity to work under your supervision, which allowed me to navigate this field independently and take ownership of my scientific project. The challenges I faced during this time strengthened my resilience and underscored the value of perseverance. I extend my thanks for the chance to pursue my research vision and bring this work to completion.

I also want to express my gratitude to Fanny and Florence. Our coffee break exchanges and shared moments helped me grow personally, but it was through observing and adapting to our professional interactions that I gained a deeper understanding of the importance of a healthy work environment for the well-being of each team member—a value I am proud to have upheld.

To Théresa, Christopher, and Nico, thank you for brightening the atmosphere with your smiles whenever we crossed paths. I am equally grateful to the many others in the Institute who supported me throughout this adventurous journey: Jehanne, Cynthia, Yuhao, Nassab, Laure, Aurélie, Maud, Chiara, Simone, Emanuel, Karoline, Channa. Even if your name is not listed here, you know in your heart that I am referring to you—thank you.

A special mention goes to Ciáran, who joined this journey a few months after I started and has been by my side ever since. Your brave sincerity struck me unexpectedly and filled me with hope when I thought it was long gone. Thank you for making burdens lighter

and turning them into clever jokes. I hope you know I will always be there for you, even if I am no longer a member of Neurocyto.

As someone once said, “the last will be the first,” and so I want to thank you, Louisa, for providing me with the most honest and kind support I have ever received. I feel truly lucky that our paths crossed. Working alongside you during countless hours was a joy, and you brought so much light and understanding during my darkest moments. It has been an honor to learn from you and a gift to work together. Thank you, dear friend.

Lastly, the person I am most thankful for is Yan. You have always supported, encouraged, and believed in me, reminding me of why I embarked on this journey in the first place. Your presence was the fuel that kept my fire burning and the light that illuminated my darkest days. This achievement would not have been possible without your passion and understanding, the laughter we shared, and the kindness of your heart, which helped me heal and regain my strength. Our love has been the foundation that sustained me through this chapter of life, enabling me to pursue my dreams and maintain my passion for neuroscience despite the many obstacles life presented. For standing by me through every loss and transforming pain into strength, I am deeply grateful. Thank you for being my rock and for helping me turn challenges into motivation.

And finally, I want to recognize the journey I undertook. I acknowledge my perseverance, my belief in science, and my determination to reach this moment. Without that commitment, none of this would have been possible.

Table of Content

Affidavit **2**
Affidavit **3**
Liste de publications et/ou brevets et participation aux conférences **4**
Résumé **5**
Abstract **6**
Acknowledgements **7**
Table of Content **9**
Preface **11**
The Nervous System and its building blocks **12**
1.1 Elucidating the Nervous System 12
1.2. Advances leading to Neurobiology 13
2. Building blocks of the Nervous System: Neurons **14**
2.1. Neuronal Compartments 14
2.2. Neuronal Cytoskeleton 15
2.3. Organization of the Neuronal Cytoskeleton 18
2.3.1. Soma 18
2.3.2. Dendrites 19
2.3.3. Axon 19
2.3.4. Membrane-Associated-Periodic Scaffold 20
3. Synapses: Hubs of Intercellular Interaction Ensuring Neuronal Communication **22**
3.1. Synaptic Classification 22
3.2. Synaptic Components and Main Roles 23
3.3. Synaptic Transmission 25
3.3.1. Neurotransmitters Release 26
3.3.2. Postsynaptic Response 26
3.4. Synaptic Plasticity 27
4. Neuronal Actin Cytoskeleton **29**
4.1. Roles in Neurodevelopment 29
4.1.1. Neuronal Developmental Stages 29
4.1.2. Actin Sculpting Membrane Protrusions in Distinct Neurodevelopmental Stages 31
4.2. Roles in Synaptic Formation and Function 33
4.2.1. Postsynaptic Actin 33
4.2.2. Presynaptic Actin 34
5. Impact of Actin Cytoskeleton Impairment on Neurological Health **37**
6. Investigating Presynapses: Tools of the Trade **38**
6.1. Electron Microscopy and Presynaptic Ultrastructure 38

6.2. Cryogenic Electron Tomography and Presynaptic Cytomatrix Components 40
6.3. Fluorescence Microscopy 41
6.3.1. Widefield Fluorescence Microscopy, Confocal Microscopy, and Total Internal Reflection Fluorescence Microscopy 41
6.3.2. Visualizing Presynaptic Actin and Other Components 42
6.4. Single Molecule Localization Microscopy 44
6.4.1. STORM and DNA-PAINT 45
7. Investigating Presynaptic Actin Ultrastructure 46
7.1. Bead-induced Model of Presynapse 47
7.2. Novel Presynapse-on-Glass Model 48
8. Deciphering the nanoscale architecture of presynaptic actin using a micropatterned presynapse-on-glass model 50
9. Discussing Presynapse on Glass Model as The Optimal Tool to Decipher Presynaptic Actin Structure and Functions 66
9.1. Presynapse on Glass Model to Investigate Actin Role in Synaptic Vesicular Release 66
9.2. Structural and Functional Insights into Presynaptic Actin Nanostructures 66
9.2.1. Actin Distribution During Synaptic Vesicular Release 67
9.2.2. Energy Demands of Actin Dynamics Defining Consistency Between Actin-Enriched and Non-Enriched Presynapses? 68
9.2.3. Dynamics of Actin Nanostructures in Neurodevelopment During Different Synaptic States 69
10. Advanced Microscopy Techniques for Real-Time Visualization of Presynaptic Vesicle Release and Actin using the Presynapse on Glass Model 70
10.1. Investigating Presynaptic Actin with STED 71
10.2. MINFLUX and the Presynapse-on-Glass Model for Studying Presynaptic Actin Dynamics 72
11. From Excitatory/Inhibitory Comparisons to Disease Models: Future Explorations of Presynaptic Actin Architectures and Methodology Implementations 73
Conclusions 75
Bibliography 76

Preface

As a neuroscientist, I couldn't start my thesis manuscript without a preface briefly introducing the roots of what constitute my passion: Neuroscience.

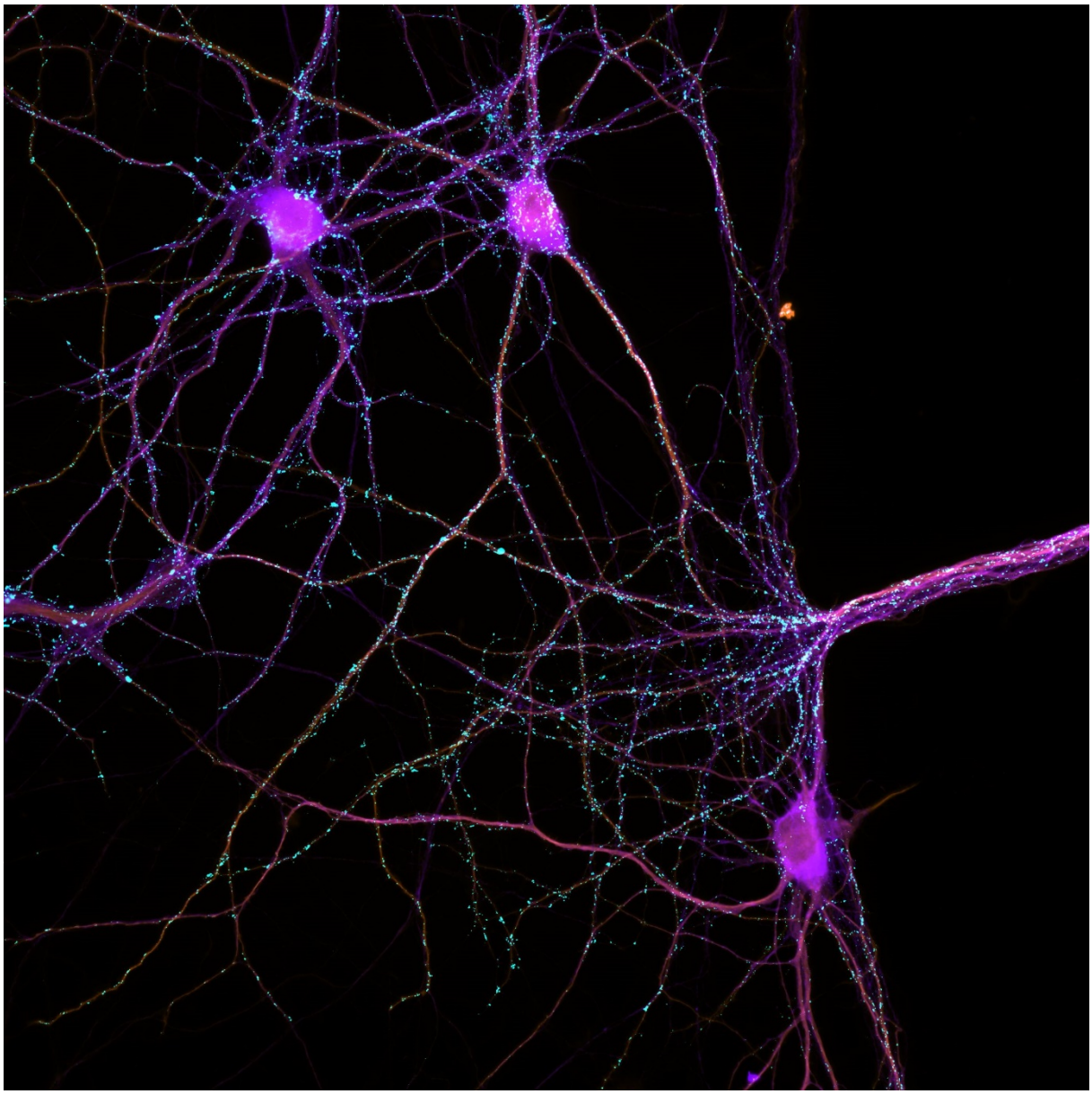

Neuroscience is an interdisciplinary field seeking to understand the structure and functions of the nervous system at several levels in order to decipher behavioral processes and their underlying complex cellular mechanisms.

The Nervous System and its building blocks

1. Elucidating the Nervous System

The Nervous System is divided into the Central Nervous System (CNS) and the Peripheral Nervous System (PNS), and it coordinates the body's sensory and motor functions through a network of nerves. The CNS processes information, while the PNS is in charge of sensory input and motor output. The proper functioning of both systems gives rise to the personal experience of external and internal environments. Stored memories of those perceptions and their associated reactions lead to the behavioral patterns that distinguish each individual from the other.

In order to appreciate the interplay between CNS and PNS and their role in shaping behavior and experience, it is necessary to adopt a holistic approach integrating insights coming from multidisciplinary fields of research. The whole picture though can only be grasped through detailed and parcellated studies in neurobiology, psychology, pharmacology, computer science, and even disciplines such as engineering and physics. The result from each field contributes to giving unique perspectives which together create a deeper comprehension of the nervous system, increasing our ability to address neurological disorders and improve human mental health.

Human fascination with the nervous system has ancient origins. Thousands of years ago, the first known descriptions of the brain came from the Egyptians. They were able to detect impairments in cognitive functions caused by what's now known as epilepsy and astutely linked them to brain malfunctions due to injuries (York & Steinberg, 2009). We had to wait for ancient Greek physicians to obtain comprehensive anatomical studies and speculations about the brain's physiological properties, leading to human sensation and cognition (Stefanou, 2020). Those ancient thinkers allowed the first historical shift from philosophical speculations to empirical scientific evidence laying the groundwork for this distinct scientific discipline, later named neuroscience.

I have briefly pinned these historical events to underline just how old the roots of these scientific beliefs are, considering the brain as the orchestrator of human behavior, even without a clear understanding of the underlying mechanisms.

1.2. Advances leading to Neurobiology

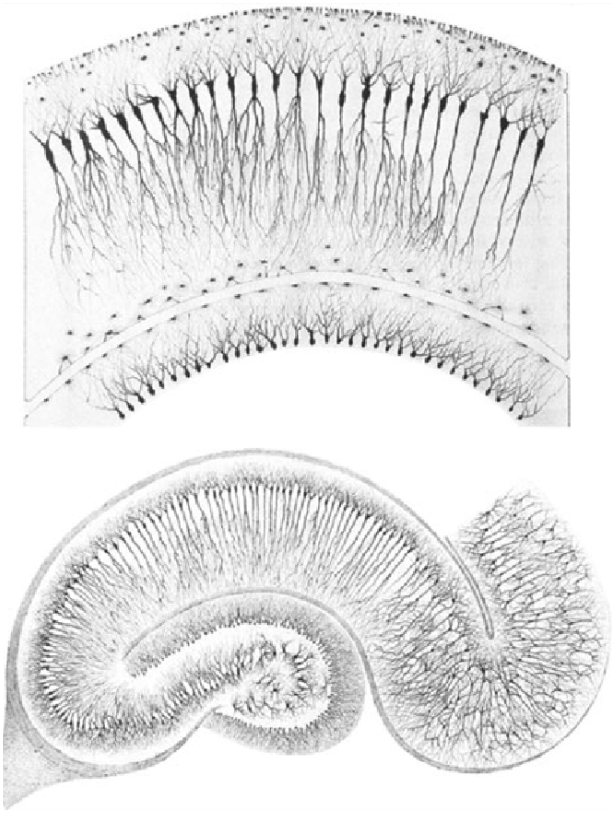

Figure 1. Hippocampal Sections.

Drawing of Histological hippocampal sections of a rabbit (top section) and newborn cat (bottom section). Illustration of the innovative use of the silver chromate staining method in neurocytology. Figure taken from Camillo Golgi's Opera Omnia, 1903

Centuries after these ancient discoveries, the arrival of lenses and later microscopes advanced the study of the nervous system to the cellular level. Camillo Golgi's groundbreaking silver chromate staining technique enabled the meticulous illustration of brain tissues (Fig. 1) (Golgi, 1903). Neurons and their circuit connections were finally revealed and recognized as the building blocks of the nervous system. Their organization in complex networks was highly debated for a whole century (Yuste, 2015). Discoveries concerning their roles in integrating sensory information across different modalities were made by studying the nervous system of different species. Current neuroscience builds on the academic work of the past two centuries, focusing on understanding all aspects of these beautifully mysterious networks. Research in neuroscience uses reductionist models, breaking down the complexities of these systems, in order to study isolated functions of their component parts.

In line with this approach, this thesis investigates the presynaptic actin cytoskeleton using an in vitro model of rat hippocampal culture to reveal the ultrastructure underlying its physiological properties.

2. Building blocks of the Nervous System: Neurons

At the heart of the nervous system lies the neuron, a highly specialized cell responsible for receiving, integrating and transmitting information throughout the body. It is characterized by its peculiar morphology conveying electrical and chemical signals.

2.1. Neuronal Compartments

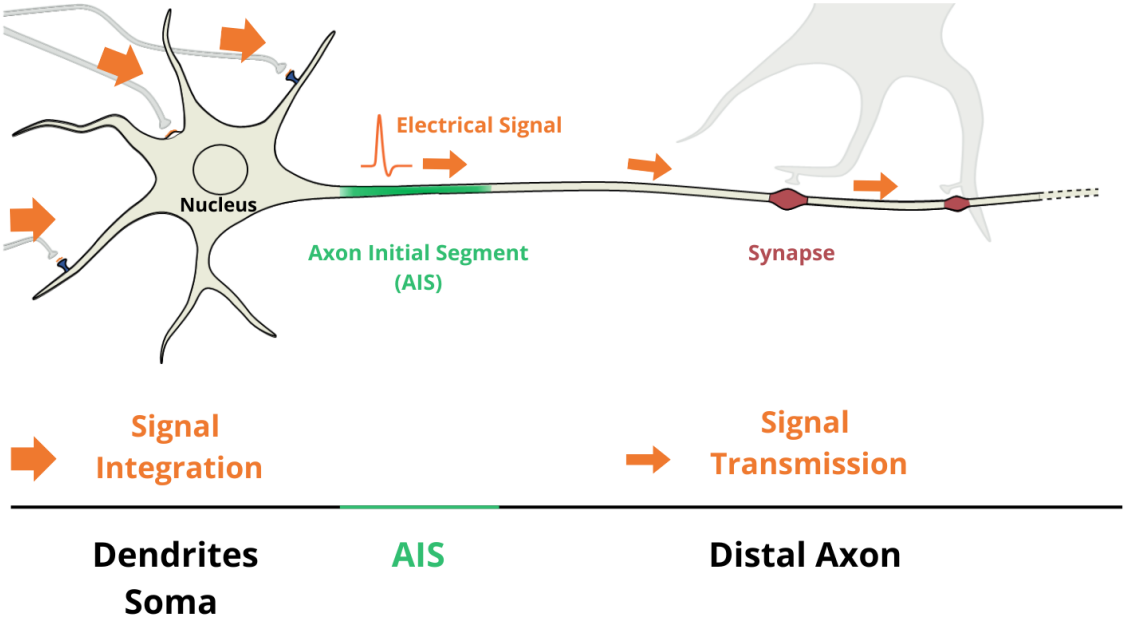

Neurons are polarized cells, comprising branch-like protrusions, dendrites and axons, that extend from the cell body, or soma, which houses the nucleus (Fig. 2). Dendrites, branching in proximity of the cell body, receive information coming from other cells and convey it to the cell body integrating those signals. Axons, consisting of long and slender projections, able to cover great distances, carry the information travelling far from the cell body. The signals can be transmitted to either other neurons or to effector cells.

2.2. Neuronal Cytoskeleton

Neuronal compartments are distinguishable through their morphological features and their associated physiological properties supported by their peculiar cytoskeleton. The neuronal cytoskeleton is a structural element composed of three elements: microtubules, neurofilaments, actin filaments.

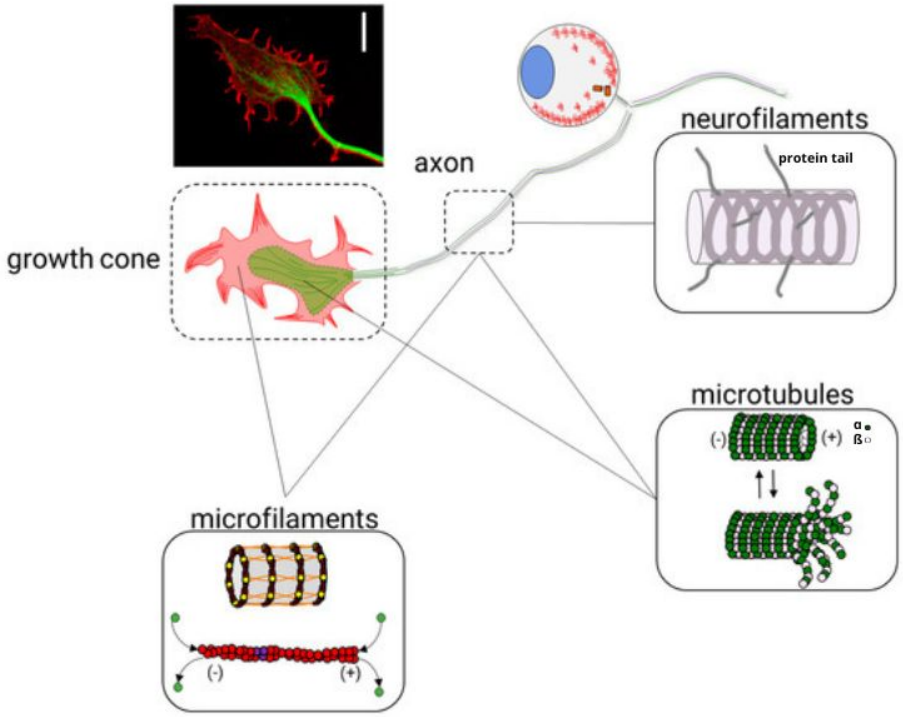

Figure 3. Neuronal Cytoskeletal Components Cytoskeleton Components of a developing neuron undergoing axonal growth. Scale bar 10 µm. *Figure taken from (Munos-Lasso et al., 2020)*

Microtubules are tube-like structures of approximately 25 nm in diameter. Microtubules are composed of polymerized α- and β-tubulin, globular proteins found in eukaryotic cells (Fig. 3). They exist in various isotypes able to interact with each other and form dimers that bind guanosine-5′-triphosphate (GTP) whose hydrolysis is necessary for microtubule dynamics: polymerization and stabilization. Tubulins arrange into organized protofilaments, simple linear structures composed of aligned tubulin subunits. Protofilaments typically assemble into thirteen parallel strands, forming a structure with an internal diameter measuring around 15 nm. They can be intertwined in bundles, their length extending to 25-50 µm (Negi et al., 2015). Within cells, microtubules are metaphorically associated with highways because of their functions in molecular trafficking allowing the transportation of specialized cargoes to precise sites. They can

interact with microtubule-associated proteins (MAPs) involved in their regulation and stabilization. Furthermore, MAPs can affect the binding properties of motor proteins acting as carriers traveling along microtubules (Iwanski & Kapitein, 2023). Microtubule assembly is fundamental for many cellular processes, especially in neurons. As a matter of fact, they are involved in neural migration, maturation and axonal transport (Zocchi et al., 2023).

Neurofilaments are neuron-specific intermediate filaments with an approximately 10 nm diameter filament core surrounded by a layer of protein tails protruding from the core (Fig. 3). Neurofilaments are composed of a large number of distinct subunits assembling into long filamentous structures. Subunits are usually categorized as heavy, medium, and light (Ding & Kumar, 2024). The heavy subunits present a central alpha-helical rod domain for assembly, capped by globular extremities able to interact with other components. The medium subunits are capable of engaging with microtubules and play a role in axonal radial growth. On the other hand, light subunits regulate axonal caliber, synaptic activity and organelle axonal trafficking (Sainio et al., 2022). Therefore, neurofilaments play a vital role in neuronal function and regeneration after injury (Yokobori et al., 2020). Neurofilaments are involved in neuronal caliber regulation and stabilization from neurodevelopmental stages to their maturity (Uchida et al., 2023), and their functions indirectly affect velocity of electric signal conduction in axons (Perge et al., 2012).

Actin Filaments are made of actin monomers, due to their small size, they can be named microfilaments (Fig. 3). Actin, in its monomeric and soluble form, G-actin, is a globular ATPase protein of 375 amino acids. After ATP hydrolysis to ADP, G-actins can polymerize into its filamentous form and constitute the F-actin, a major actor in the actin cytoskeleton (Fig. 4).

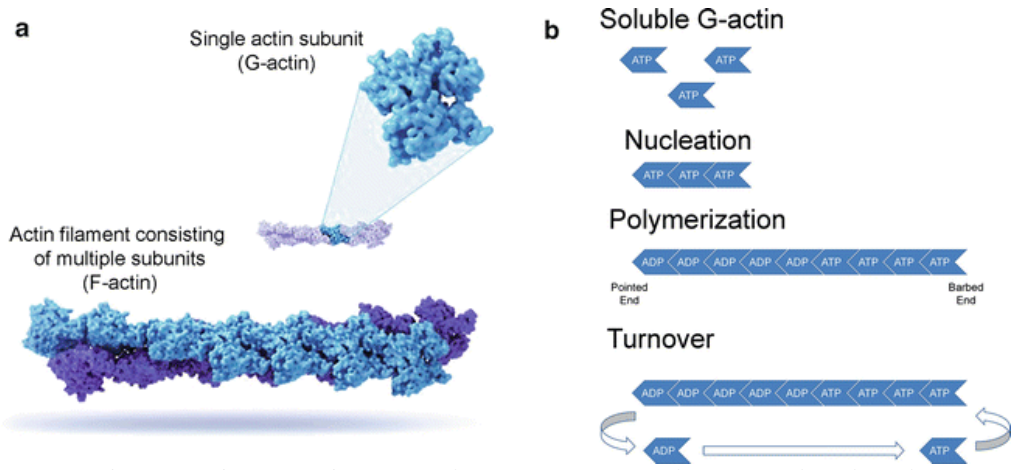

Figure 4. Basics of Actin Dynamics. (a) Actin monomers (G-actin) polymerized into filamentous actin (F-actin). (b) Single actin subunits firstly nucleate, then polymerize hydrolyzing the associated ATP into ADP as elongation occurs. *Figure taken from Gallo, Gianluca (2016). Encyclopedia of Signaling Molecules, ACT (pp1-8)*

Actin filaments have a diameter of approximately 7-10 nm and are characterized by two intertwined and twisted helices of actin monomers (Fig. 4, a) undergoing polymerization at their extremities with different dynamics, the barbed end growing faster than the pointed end (Fig. 4, b). Historically, the actin cytoskeleton has been considered one of the foremost drains of neuronal energy until recently (Bernstein & Bamburg, 2002). Actin dynamics appeared to play a significant role in energy (ATP) depletion and provided further evidence of structural changes in neuronal morphology and vesicle recycling. On the contrary, another study demonstrated that affecting actin dynamics does not impact ATP levels as previously reported (Holland & Gallo, 2023), suggesting that certain compartments such as synapses could represent significant, but local, energy consumption. As a matter of fact, the considerable remodeling of actin filaments involved in synaptic plasticity may explain these contradictory interpretations. Though further investigation is needed to shed light on the subject, the current state of research on the dynamics of neuronal actin cytoskeleton is evolving thanks to the advancement of recent technologies. Understanding the structural properties of the actin cytoskeleton requires considering that actin polymerization depends on additional proteins called actin binding proteins (ABP). There are over 150 ABPs influencing actin filament dynamics and organization within neurons.

Below is displayed a summary of the most known ABP and their respective functions:

ARP2/3 is a protein complex that mediates actin filament nucleation ensuring the branching characteristic of their networks. ARP2/3 is crucial in dendritic spine development and axon branching (Chou & Wang, 2016; Spence et al., 2016).

Formins constitute the unbranched actin nucleators, promoting polymerization of long filaments essential for proper axon development (Breitsprecher & Goode, 2013; Courtemanche, 2018; Zigmond, 2004).

Cofilin-1 regulates actin turnover as one of the major actin depolymerization factors. Involved in neurite and growth cone emergence, as well as activity-dependent remodeling (Bamburg & Bernstein, 2010; Ohashi, 2015; K. Tanaka et al., 2018).

Spectrins are a major component of the neuronal cytoskeleton, providing structural support to the membrane and constituting a scaffold involved in organizing other structural components (Liu & Rasband, 2019; Lorenzo et al., 2023; Unsain et al., 2018).

Adducin participates in regulation of actin filament assembly and stabilization (Hughes & Bennett, 1995; Leite et al., 2016).

The actin cytoskeleton and ABPs are essential in constructing actin submembrane architecture necessary for neuronal development and function (Jung et al., 2020).

The neuronal cytoskeleton forms a three-dimensional scaffold, comprising components and associated proteins vital for neuron development and function. Microtubules are critical for cell division, migration, and axonal growth and regeneration. Furthermore, they ensure synaptic function through their involvement in synaptic protein transport. Neurofilaments help maintain the structural integrity of axons, regulating their diameter and supporting their response to mechanical stress – functions essential for the efficient conduction of electrical signals and synaptic stability. Actin filaments drive rapid cell-shape changes involved in growth cone guidance and play fundamental roles in synaptic formation and function *(See Section 4)*.

Together, the components of the neuronal cytoskeleton, provide mechanical support to axons and dendrites, influencing their functions throughout their life, from neurogenesis through neuron maturation. As a matter of fact, disruption of these components is involved in various neurodevelopmental and neurodegenerative disorders (Liaci et al., 2021). The complexity of the cytoskeletal regulatory pathways and their underlying genetics remain poorly understood and may be targets for innovative therapies (Muñoz-Lasso et al., 2020).

2.3. Organization of the Neuronal Cytoskeleton

The cytoskeleton, comprising the previously referenced cytoskeletal elements and their associated proteins is fundamental to defining the physiological properties of neuronal compartments. Its elaborate framework provides support for various cellular processes. Here we explore the complex organization of its components within the soma, dendrites and axon, with a specific focus on the latter.

2.3.1. Soma

Studies have highlighted microtubules radiating out from the microtubule organizing center (MTOC), which resides close to the nucleus within the soma. During beginning neuronal stages, microtubules are found to orient their fast-polymerizing end toward the cell periphery (Baas et al., 1988) to reorient their polarization in a particular antiparallel manner during maturation (Yau et al., 2016). They often nucleate from structures to which they are attached, creating the “highways” of intracellular transport within the cell body. Microtubule polarity is not restricted to their extremities, but also exists along the lattice length, influencing the trafficking of molecular motor proteins carrying organelles to specialized locations (Baas & Lin, 2011). The synchronicity between microtubules and actin filament extensions is fundamental to cell migration (Tas & Kapitein, 2018). Their polymerization is spatially regulated to drive membrane protrusion from early neurodevelopmental stages to their mature stage in which specialization into dendrites and axons occurs. Meanwhile, neurofilaments further provide structure and mechanical strength to maintain the cell integrity throughout these stages.

2.3.2. Dendrites

The dendritic cytoskeleton is characterized by an abundance of microtubules and their associated proteins MAPs. The specific polarity of these filaments not only orientates the transport of organelles, proteins, and signaling molecules to synaptic sites (Iwanski & Kapitein, 2023; Kapitein & Hoogenraad, 2015), but also plays crucial roles in neuronal plasticity switching rapidly between growth and shrinkage (Penazzi et al., 2016). Neurofilaments and microtubules confer elasticity and structural stability to dendritic architecture. Actin structures are crucial for dendritic spine formation and activity-dependent remodeling underlying synaptic plasticity (Hotulainen et al., 2009), necessary for cognitive processes such as learning and memory (Lamprecht, 2021). Rapid adjustments of actin structures are responsible for morphological variations, translating into modifications of synaptic weight, the strength of connection between the pre- and postsynapse. Moreover, actin filaments influence spine dynamics by modulating synaptic vesicular and receptor transport to and from synaptic sites (Cingolani & Goda, 2008).

2.3.3. Axon

The axonal cytoskeleton is essential for long-distance transport of vesicles, organelles, and proteins, as well as for axon sprouting and regeneration. Within the axonal compartment, microtubules exhibit distinct characteristics from those presented earlier (Baas et al., 1988). Their nucleating extremities are not anchored to any cellular structure, such as the centrosome, a finding that has captured researchers' attention for decades (Brown et al., 1992; Lyser, 1968). Microtubule length ranges from less than 1 µm to over 100 µm (Yu & Baas, 1994), and their polymerization is uniformly oriented toward axon terminals. This orientation facilitates molecular trafficking to replenish the sprouting or regenerating axon and active synapses. Neurofilaments also contribute considerably to axonal functions, influencing the axon diameter and supporting the process of axonal transport through a structured framework (Sainio et al., 2022). Studies on cultured rat neurons have shown that neurofilaments exhibit rapid, anterograde and retrograde movements, frequently interrupted by long pauses (L. Wang et al., 2000). Researchers suggest that this movement pattern slows their axonal transport rate. Actin cytoskeleton participation in organelles and synaptic vesicle axonal transport has also been reported (Morris & Hollenbeck, n.d.; Venkatesh et al., 2020). Actin filaments can be observed as highly dynamic polymers within the axon, able to generate numerous structures throughout neuronal development *(see Section 4)*, but the most known of its nanostructures in mature neurons are the actin rings. Axonal rings of actin polymers are able to interact with other scaffolding or bridging proteins (Xu et al., 2013), conferring mechanical stability and furthermore highly contributing to the organization of voltage-gated-channels or other ionic channels (Letourneau, 2009; Morachevskaya & Sudarikova, 2021).

Microtubules, neurofilaments, and the actin cytoskeleton are vital for neuronal health (Liaci et al., 2021; Muñoz-Lasso et al., 2020). Their complex and sophisticated coordination has caught neuroscientists' attention due to their role in defining physiological properties of axonal sub-compartments and in ensuring their proper function (Alberti et al., 2022; Leterrier, 2021a).

2.3.4. Membrane-Associated-Periodic Scaffold

The unique organization of the membrane associated scaffold within the axon, is important to support its function. Within the cone-shaped area of the protrusion where the axon originates is the axon initial segment (AIS), along which proteins and other cytoskeletal elements begin organizing into a precise membrane-associated periodic scaffold (MPS) since early stages of a neuron life. During neuronal maturation, the MPS extends along the length of the axon and stops at specialized regions called presynapses (Leterrier, 2021b), whose ultrastructure will be discussed later in this manuscript *(See Section 4.2.2)*.

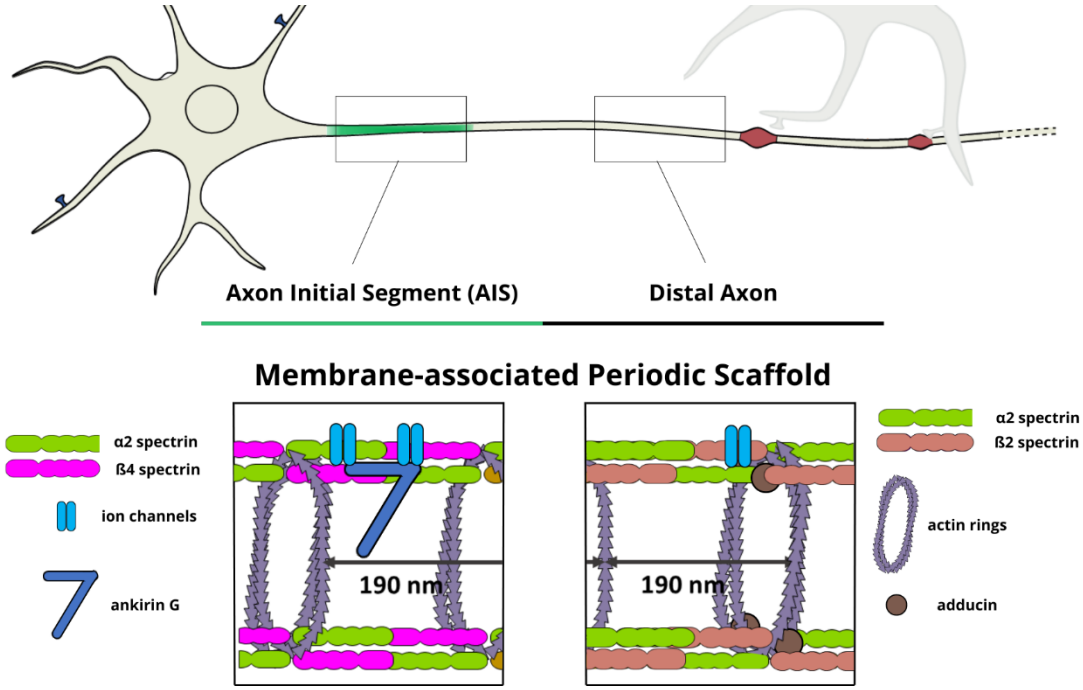

Figure 5. Membrane-associated Periodic Scaffold (MPS). Molecular organization of the MPS within the AIS and the distal axon. Actin rings (purple), α2 spectrin (green), ß4-spectrin (pink), ankyrin G (blue), ß2-spectrin (red), adducin (brown).

A periodic and complex cytoskeletal organization characterizes the AIS (Xu et al., 2013a), firstly providing the critical properties for action potential genesis, secondly constituting a diffusion barrier ensuring the spatial restriction of proteins to their functional compartment (Albrecht et al., 2016). Within the AIS the actin cytoskeleton shows the fundamental arrangement of the MPS, with actin rings found every 190 nm, intercalated by spectrin tetramers composed of α2- and ß4-spectrin. The MPS

arrangement persist along the distal axon, where ß4-spectrin is replaced by ß2-spectrin, and adducin is associated with the periodic actin rings (Leterrier, 2018). The actin/spectrin interaction is extremely organized, giving axons their unique 3D lattice scaffold (Fig. 5)(Albrecht et al., 2016) The cohesive sub-membranous architecture includes ion channels regularly spaced along the axonal length (K. Xu et al., 2013). The effective anchoring of voltage-gated sodium and potassium channels is supported by the periodic architecture of the MPS. These channels are anchored to the membrane through linkers such as the scaffolding proteins ankyrin-G and -B, within the AIS and the distal axon. Additionally, ankyrin-MPS interactions are essential for the evolution of distal axon specialized regions (Komada & Soriano, 2002; Saifetiarova et al., 2017) which ensures the propagation of electrical signals (Poliak & Peles, 2003).

Researchers underlined the importance of MPS and other proteins interactions, in regulating the axon diameter and other MPS functions as axon-axonic and axo-dendritic interconnection (R. Zhou et al., 2022). This periodic scaffold is not a static entity. Indeed, dynamic rearrangement of its components, constantly adapts to the cellular conditions throughout neuronal developmental stages (D'Este et al., 2016). This flexibility allows neurons to adapt to stimuli or injury (Ghose & Pullarkat, 2023; Leite & Sousa, 2016), thus maintaining vital functions. As a matter of fact, in response to extracellular stimuli, the MPS plays the role of a signaling platform where receptors, cell-adhesion and other signaling molecules are recruited to; it provides mechanical support; ensures neuronal physiology and its remodeling is essential for axonal branching and neuronal intercommunication (Bodakuntla et al., 2021; A. R. Costa & Sousa, 2021). MPS organized lattice contributes to maintaining axonal structural integrity necessary for healthy neuronal activity. Researchers explored the MPS and highlighted its ability to resist and respond mechanical tension, depicting the actin-spectrin periodic structures as essential throughout a neuron's life in different neuronal types (D'Este et al., 2015, 2016; Ghose & Pullarkat, 2023; Leterrier et al., 2015; Vassilopoulos et al., 2019).

Somato-dendritic and axonal cytoskeletal elements are highly organized, especially within the MPS, ensuring neuronal physiology and function (Han et al., 2017; Zhong et al., 2014). In a large number of neurodevelopmental and neurodegenerative disorders, disruptions of this organized architecture and aggregations of the cytoskeleton components are recorded (Wurz et al., 2022). Thus, understanding the nanoarchitecture is paramount to further describe and understand the mechanisms in which their disruption is implicated, preparing the path for future innovative therapeutic strategies.

3. Synapses: Hubs of Intercellular Interaction Ensuring Neuronal Communication

Synapses are highly organized cell junctions of the nervous system where communication occurs. They are fundamental for neuronal function, memory storage and information processing, characterized by nanoscopic extracellular gaps, or synaptic clefts, (20 nm) between the axon terminal of an emitting neuron sending signals and a juxtaposed membrane of the receiving cell.

3.1. Synaptic Classification

Observations of CNS neuronal synapses have led to various simplified classification used since the middle of the twentieth century. Synapses can be distinguished by their anatomical features, such as the point of contact of the axon terminal, defining axosomatic, axodendritic and axoaxonic synapses (Krstić, 1985). An alternative classification categorizes synapses by the chemical properties of the neurotransmitters used in communication between the pre- and post-synaptic neuron, distinguishing them as excitatory or inhibitory synapses. Excitatory synapses release neurotransmitters such as glutamate, which typically induce depolarization of the postsynaptic membrane. On the other hand, inhibitory synapses release neurotransmitters like GABA, which generally cause hyperpolarization of the postsynaptic membrane.

Recent investigations demonstrated the significant molecular diversity within a single synaptic category, revealing their highly complex protein composition and expression levels, expanding our knowledge and advancing synaptic categorization. (O'Rourke et al., 2012) Nowadays, modern research techniques, investigating synaptic structural, physiological and genetic characteristics, expand on old classifications. Together, these classifications serve as reductionist and simplified reference points in fundamental research, providing a template for comprehensive understanding for the community.

This manuscript will concentrate on the study of the CNS most common type of synapse: the axodendritic excitatory synapse.

3.2. Synaptic Components and Main Roles

Axodendritic synapses are a type of synaptic connection involving the axon terminal of one neuron (presynaptic neuron) and the dendritic spine of another neuron (postsynaptic neuron). The former constitutes the compartment called the presynapse, while the latter is the postsynapse (Fig. 6).

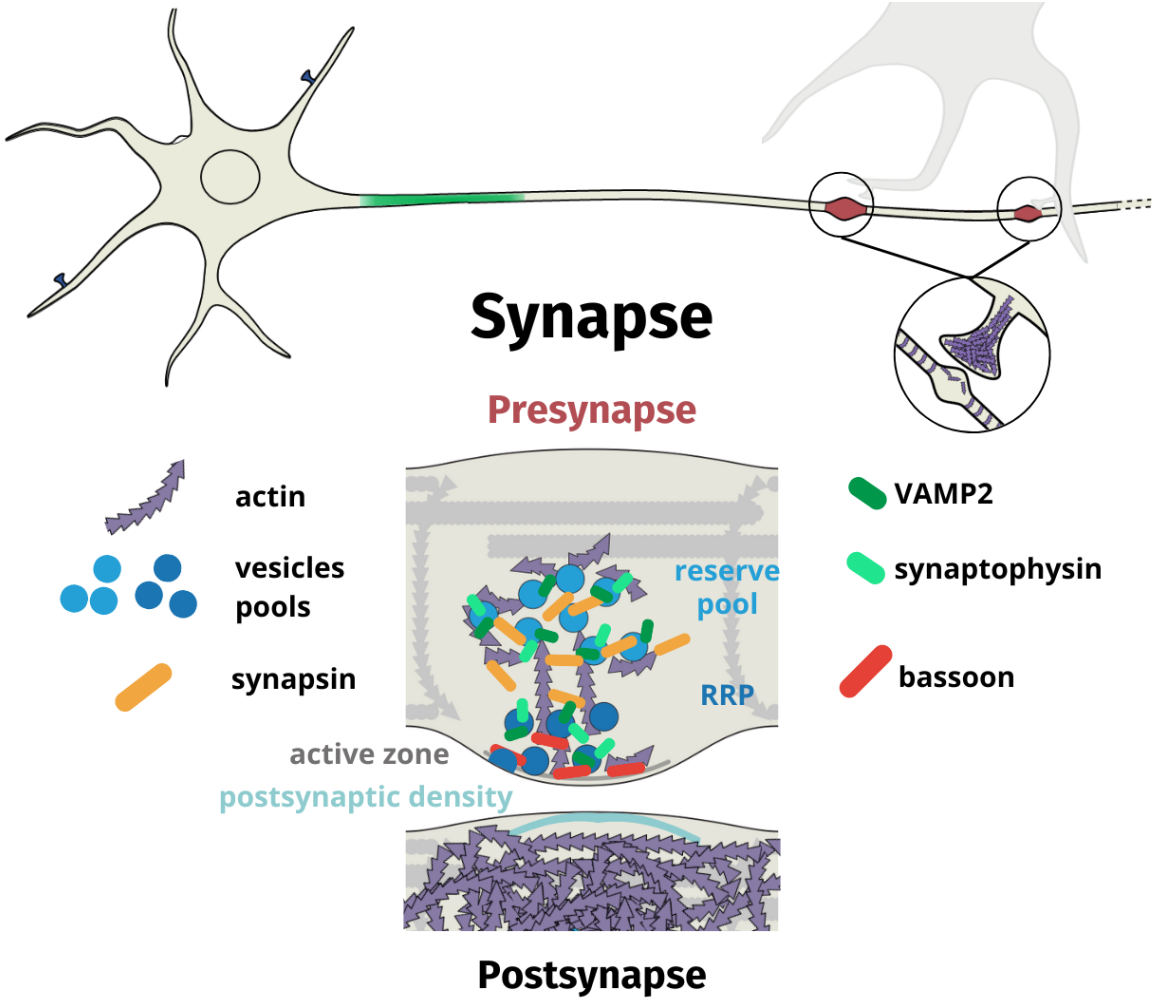

Figure 6. Synaptic Compartments and Major Components. Schematic representing a synapse zoomed on the right. The presynaptic components are highlighted. Actin filaments (purple), synaptic vesicles of the reserve pool (light blue), synaptic vesicles of the ready releasable pool (dark blue), synapsin (orange), VAMP2 (dark green), synaptophysin (light green), bassoon (red)

The presynapse is where hundreds of vesicles containing neurotransmitters are gathered before their release. These vehicles are divided into two pools: the reserve pool and the ready releasable pool (RRP). The RRP is found at the active zone, a specialized region of the presynaptic membrane, where vesicles are docked and primed for release. Multiple distinct releasing sites can be found within a synaptic terminal. This area is enriched with proteins such as bassoon, RIM, synaptotagmin and Munc. Bassoon is known

to be a scaffolding protein of the active zone (Südhof, 2012). The others are recognized to be critical in vesicle fusion along with SNAP-25, Syntaxin-1, VAMP2 (synaptobrevin), part of the SNARE complex, tightly regulating vesicle exocytosis (Südhof & Rizo, 2011; Q. Zhou et al., 2017).

The postsynapse also involves a dense network of proteins. This membrane, in close apposition to the presynaptic terminal, presents a wide range of receptors, scaffolding proteins, and signaling molecules. The postsynaptic membrane also presents a specialized region called the postsynaptic density (PSD) with its own complex organized structure, playing critical roles in postsynaptic response by regulating synaptic strength and plasticity involved in learning processes and memory (Sheng & Hoogenraad, 2007).

Excitatory synapses have dynamic structures undergoing rapid morphological changes in response to synaptic activity. Synaptic proteins localization has been found to organize into nanocolumns aligning between presynaptic and postsynaptic compartment to ensure the efficiency of synaptic transmission. (Tang et al., 2016). Those morphological transformations are supported by the cytoskeleton, especially actin cytoskeleton, which plays vital roles in maintaining the structure of both pre and postsynapse (Gentile et al., 2022). Actin dynamics are also known to be of high importance for vesicular trafficking at the presynaptic terminals and for the remodeling of dendritic spines at postsynaptic sites, through synaptic activity-dependent reorganization. (Insuk Song, 2002; Sankaranarayanan et al., 2003; Spence & Soderling, 2015; Venkatesh et al., 2020).

3.3. Synaptic Transmission

The biological process ensuring neuronal communication is called synaptic transmission. Axodendritic synapses send signals using chemical compounds called neurotransmitters, which are released from the presynapse of an emitting neuron into the synaptic cleft. The postsynaptic membrane reacts to these chemicals to induce changes in membrane potential, thus triggering an electrical impulse that propagates to the soma of the receiving neuron. Synaptic transmission is crucial for the proper functioning of the nervous system.

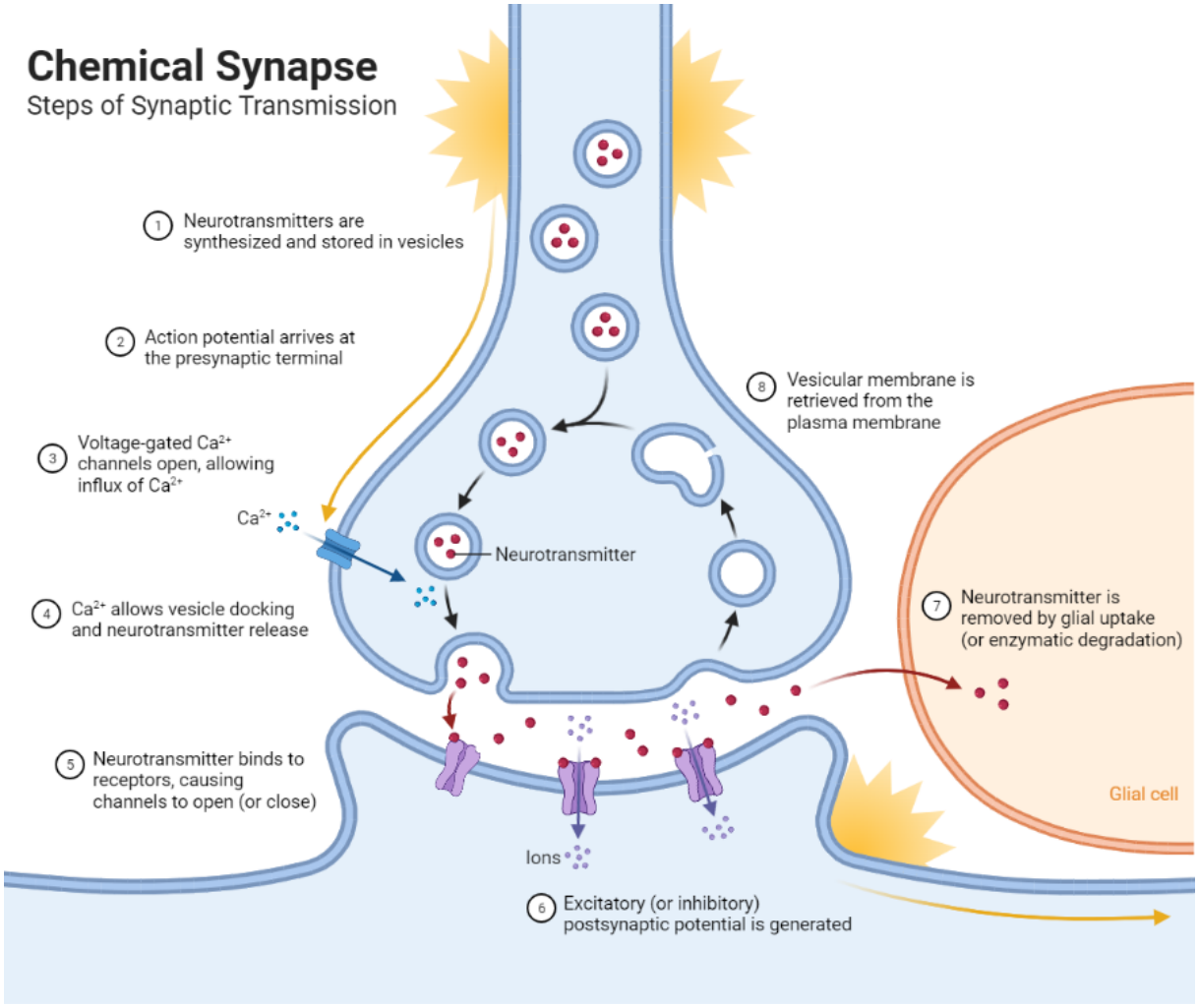

Figure 7. Synaptic Transmission. Steps of synaptic transmission of a chemical synapse
Figure taken from Purves et al. (2018) Neuroscience. 6th Ed. Oxford University Press

3.3.1. Neurotransmitters Release

Neurotransmitters are packaged into synaptic vesicles that travel through the axon to aggregate within presynapses. Changes in axon terminal membrane potential trigger the release of neurotransmitters into the synaptic cleft through the dynamic process called exocytosis. These neurotransmitters then bind receptors of the receiving cell. This is the biological process ensuring synaptic transmission (Krstić, 1985).

Vesicle fusion and subsequent exocytosis of the neurotransmitter is a well-orchestrated series of events still highly studied and debated (Brose et al., 2019) . Different actors are involved in this process (Rizo, 2022), and together stabilize and tether the vesicles to the plasma membrane within the ready releasable pool. Initially, synaptic vesicles containing neurotransmitters are anchored to the plasma membrane of the neuron, with proteins such as synaptobrevin and synaptotagmin-1 embedded in the vesicle membrane. Specialized protein complexes then are responsible for merging and fusing vesicles with the presynaptic membrane, resulting in neurotransmitter release into the synaptic cleft.

3.3.2. Postsynaptic Response

The opening of ionotropic receptors creates driving forces allowing ions such as Na +, K + or Cl- to flow in or out the postsynaptic compartment. The ion flow generates the membrane electrical response, called postsynaptic potential. When Na+ and K+ enter the cell a depolarization of postsynaptic membrane generates the Excitatory Postsynaptic Response (EPSP) which might result in an action potential if the depolarization is significant. If Cl- enters the cell, inducing a hyperpolarization of the membrane potential, it generates the Inhibitory Postsynaptic Potential (IPSP). These responses reduce the membrane potential and their probability of firing by enhancing the amount of current to inject to excite the postsynapse once again (E Bocinelli, 2005).

Other kinds of receptors, coupled with G-proteins, might be activated by the neurotransmitter release. These receptors are called metabotropic as they induce signaling pathways able to modulate various cellular processes leading to channel internalization or externalization, or gene expression modifications. The signal transmission ends when all the postsynaptic receptors are saturated or when the neurotransmitters are removed from the synaptic cleft. Presynaptic or glial cell absorption ensures their removal through neurotransmitter uptake or through enzymatic degradation (Purves et al., 2018). Synaptic vesicles are recycled at the presynaptic compartment after the neurotransmitter release through regulated endocytosis. This process allows formation of new vesicles that might be reused after refill.

3.4. Synaptic Plasticity

Synaptic plasticity is the ability to rapidly change by strengthening or weakening in response to external cues. Essential for memory consolidation, this synaptic ability to adapt through structural modifications is underlined by two distinct processes: Long-Term Potentiation (LTP) and Long-Term Depression (LTD)(Lüscher & Malenka, 2012).

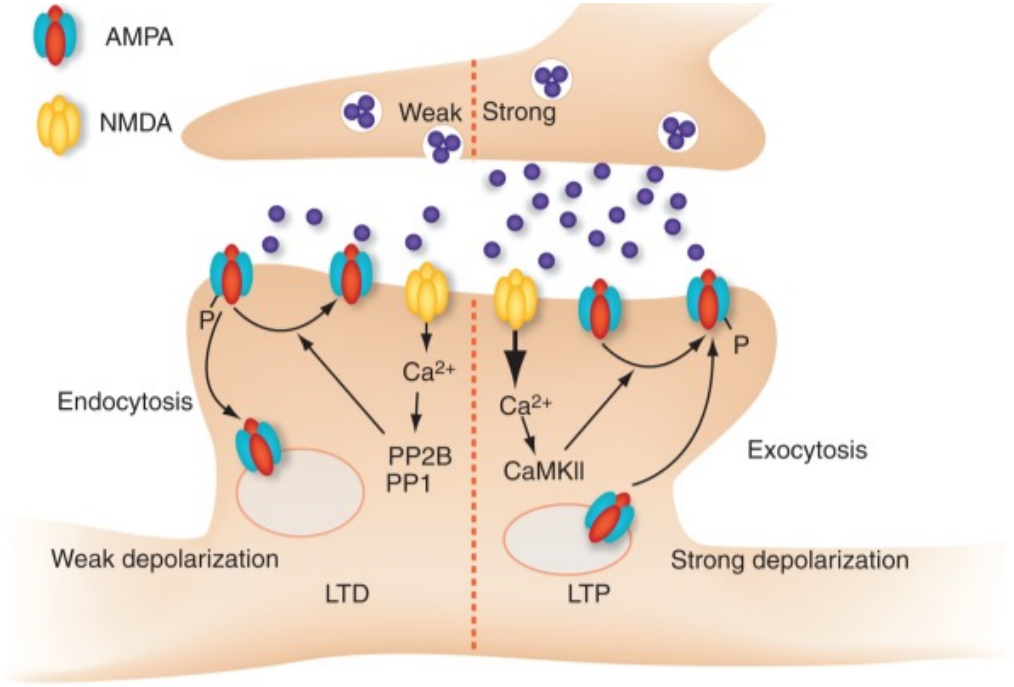

Figure 8. Synaptic Plasticity. Representation of the molecular mechanisms involved in Long-Term Depression (LTD) on the left and Long Term Potentiation (LTP) on the right. *Figure taken from Purves (2018)*

LTP is an increased efficiency of information transmission between the pre and postsynaptic compartments. Synaptic strength is enhanced by the remodeling of its components to increase the probability of generating action potentials. LTP is achieved through the insertion and stabilization of AMPA (α-amino-3-hydroxy-5-methyl-4-isoxazolepropionic acid) receptors within the postsynaptic membrane. The process is initiated by the activation of NMDA (N-methyl-D-aspartate) receptors which are permeable to calcium ions (Ca^{2+}). Repeatedly activated postsynaptic membrane undergoes sufficient depolarization to remove the magnesium ions (Mg^{2+}) inhibiting their channel activity. Subsequent calcium influx triggers an intracellular signaling cascade promoting AMPA receptors externalization at the plasma membrane (Fig. 8, right). The molecular machinery stimulates a boost of the postsynaptic response to neurotransmitter release resulting in an increase in the amplitude of the excitatory postsynaptic potentials, thereby potentiating synaptic transmission. This enhancement in synaptic efficacy is supported by structural changes of the synapse morphology such as the growth of the

dendritic spines as well as the formation of new synaptic connection further enhancing the synaptic response to the neurotransmitter release (Purves et al., 2018).

On the contrary, LTD decreases efficiency of synaptic transmission, weakening the synaptic strength. In less active synapses depletion of AMPA receptors is provoked by a moderate, but prolonged activation of NMDA receptors. This kind of calcium flux activates a different signaling pathway leading to the AMPA receptor endocytosis (Fig. 8, left). The morphological changes result in a shrinkage of dendritic spines contributing to the synaptic strength weakening (Q. Zhou et al., 2004). This process is essential to prune unnecessary connections.

Synaptic plasticity is crucial for regulating neuronal network modifications throughout development. The nervous system undergoes drastic changes from the first stages of life, until the very last ones, and those modifications of the neuronal network are the ones underlying learning and behavioral cognitive processes.

These intricate modifications at a macroscopic level can only be achieved thanks to the contribution of several actors at a microscopic level such as Cell Adhesion Molecules (CAMs), scaffolding proteins, and cytoskeletal elements. CAMs, such as the presynaptic neurexin and their postsynaptic partner neuroligin, ensure signal transduction, and provide synaptic adhesion and stability, since the first steps of synaptic formation (EL-Husseini et al., 2000; Dalva et al., 2007; Südhof, 2008; Südhof & Rizo, 2011). The actin cytoskeleton is subjected to rapid remodeling to support changes in morphology and synaptic strength essential for synaptic signaling and plasticity observed in LTP and LTD. This underlies the well-orchestrated interplay between these molecules in regulating synaptic function and plasticity.

4. Neuronal Actin Cytoskeleton

The actin cytoskeleton within the nervous system is required for proper neuronal development function. Affecting a neuron's morphology, the actin cytoskeleton plays a vital role throughout all the stages of neuronal development, from the outgrowth of membrane protrusions, their specialization in axons and dendrites, to synaptogenesis (Gallo, 2016).

4.1. Roles in Neurodevelopment

Researchers have provided evidence describing actin filament reorganization and membrane protrusions. Actin treadmilling, involving the continuous addition of actin monomers at one end and their dissociation from the other end, generates forces that propel membrane edges (Carlsson, 2018; Wen et al., 2016), supporting the idea that actin nanoarchitecture is responsible for the changes of neuronal membrane shape throughout its development.

4.1.1. Neuronal Developmental Stages

Pioneering observations of neuronal membrane protrusions were made with *in vitro* studies conducted by Banker and his colleagues (Dotti et al., 1988).

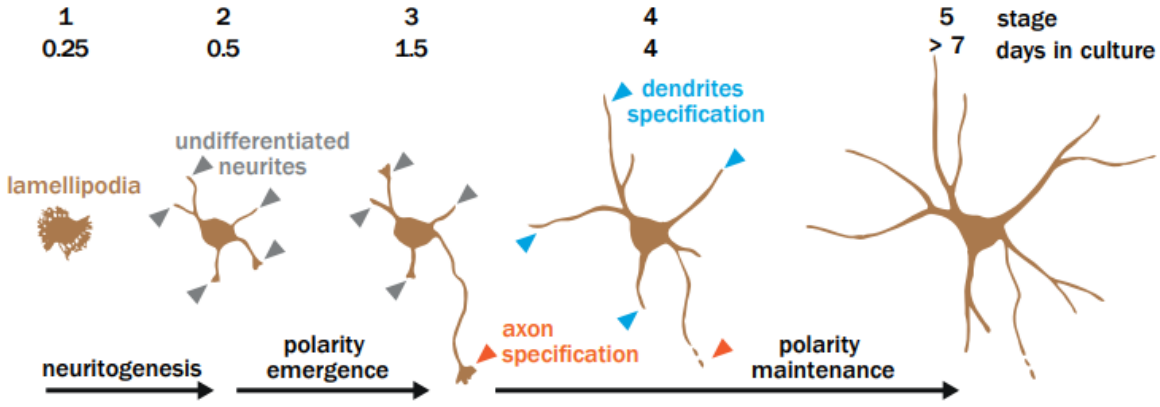

Fig.9 Developmental Stages of Neuronal Polarity. Schematic of the developmental stages of a neuron. *C. Leterrier, with permission*

The researchers defined five stages neurons must pass before the establishment of the final cellular polarity (Fig. 9). The first stage is characterized by the outgrowth of neurite precursors, lamellipodia. These unspecialized membrane protrusions, initially show uniform lengths, giving the cell a multipolar appearance (Fig. 9, 0.25-0.5 days in culture). During the second stage, one of the neurites starts to exhibit rapid growth and soon will

be distinguishable from the others due to its length; it can be identified as the future axon (Fig. 9, 0.5-1 days in culture). The remaining neurites can retract or slowly grow specializing into dendrites in the future. The axon specification occurs and define the third stage (Fig. 9, 1.5 days in culture). The longest neurite extends considerably and establishes the functional neuronal polarity permitting a proper signal transmission. The fourth stage involves dendritic growth and branching letting the cell acquire its characteristic morphology (Fig. 9, 4 days in culture). The fifth and final stage is reached when development of axons and dendritic arborizations are completed (Fig. 9, 7 or plus days in culture). During this stage, synaptic connections are formed and neuronal maturation and functional polarity is achieved (Banker, 2018).

Actin involvement is crucial in regulating the morphological changes neuron undergoes in each of the five stages leading to neuronal polarity.

4.1.2. Actin Sculpting Membrane Protrusions in Distinct Neurodevelopmental Stages

Neuritogenesis refers to the initiation of neuronal membrane protrusions, their extension and branching. Dynamic patterns of extensions and retraction of the plasma membrane are supported by actin and other cytoskeletal actors sculpting its architecture. The developmental stage occurring during the first step of a neuron life requires morphological transformations induced by fast cytoskeletal remodeling.

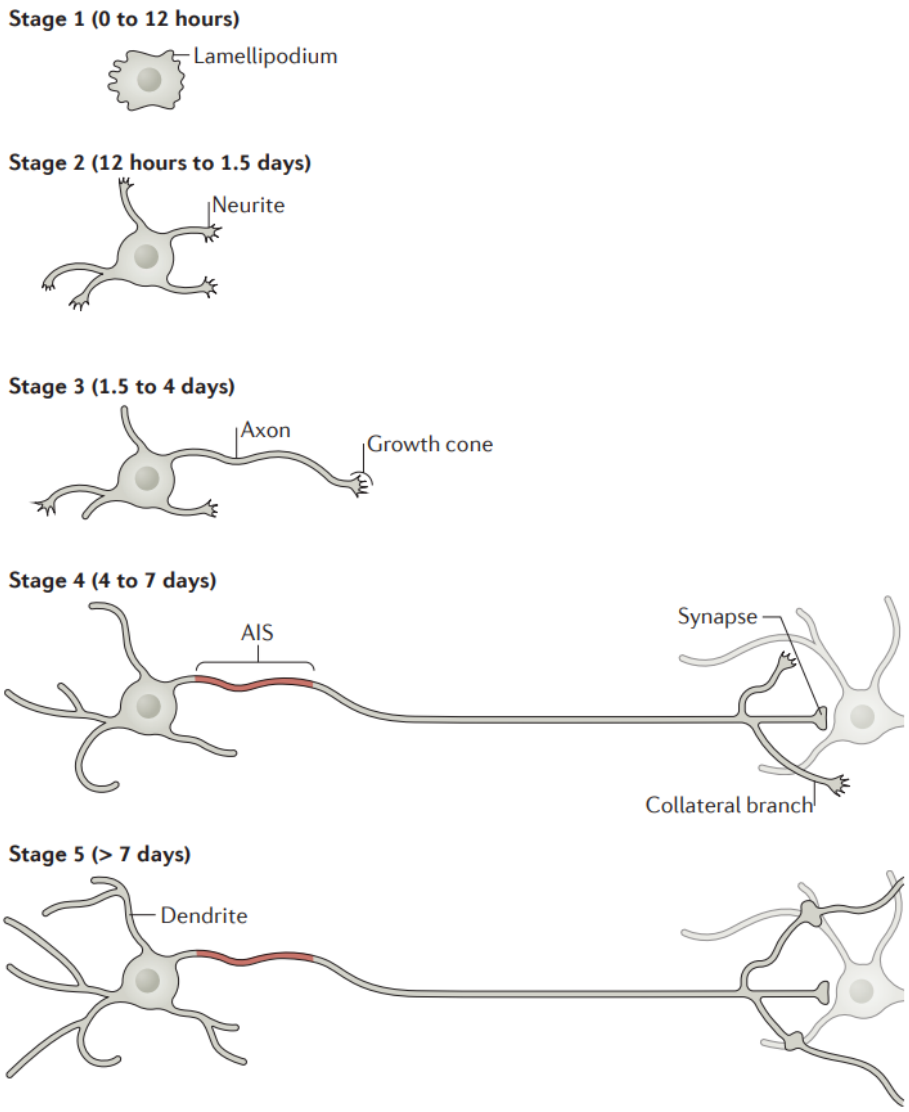

Figure 10. Neurodevelopmental Stages and Membrane Protrusions. Schematic of membrane protrusions and their associated neurodevelopmental stages, C. Leterrier, with permission

Freshly plated neurons exhibit a spherical morphology, but a few hours later, near the neuronal microtubule-organizing center, microtubules and actin filament nucleation and polymerization widen the surface of the cell and the first protrusions appear.

Filopodia and lamellipodia are the two nascent cellular structures, sensing the extracellular environment during the first stages of the neuron life. Filopodia are slender protrusions with a unique finger-like aspect composed of parallel bundles of tightly packed actin filaments. The bundle formation is regulated by actin binding proteins (ABPs), such as fimbrin and villin, ensuring their formation. Meanwhile, lamellipodia are extremely flat membrane protrusions resembling ''veils'' characterized by dense reticular structures composed of branched filaments creating the actin network (Fig. 10 Stage 1) (Flynn et al., 2012).

Neuritogenesis is effective under the influence of extracellular cues able to activate this reaction. During the second stage, membrane protrusion elongation is more prominent and actin treadmilling is highly active preceding growth cone emergence. Actin filaments polymerize, pushing forward the plasma membrane to enable the exploration of the extracellular environment (Fig. 10 Stage 2). No significant distinction between neurites is yet noticeable during this stage. To predict which neurite would become an axon, pioneering studies were conducted using cytochalasin-D, an actin depolymerizing drug. Short-term exposure of cultured neurons to this drug resulted in destabilization of actin hastened the outgrowth of a single axon revealed that actin needs to be destabilized within the future axon growing extremity to hasten its fast outgrowth (Frank Bradke & Calros G. Dotti, 1999; S. X. Zhang et al., 2016).

During the third stage one of the neurite present different growing dynamics. APBs accumulate within a neurite, influencing actin dynamics; when one of the neurites outgrows the others, it specializes into a rapidly elongating axon (Fig. 10, Stage 3). Early observations demonstrated morphological differences could be noticed in premature axon such as larger growing cone presenting microtubule protrusions within its periphery. Later, researchers demonstrate that microtubules trigger more rapid actin treadmilling (Zhao et al., 2017).

The axon specialization is achieved once the AIS starts assuming its properties and presynaptic markers begin to accumulate within the axonal compartment, processes that are essential for neural transmission (Fig. 10, Stage 4). The periodic actin rings start to assemble from the proximal axon *(See Section 2.3.4.)*, and the axon starts branching into several terminals and simultaneously initiates synaptogenesis. *In vitro* studies of hippocampal neurons have demonstrated actin branches sprouting from lamellipodia referred to as growth cone like “waves” (Ruthel & Banker, 1999). The frequency of actin waves increases in elongating neurites around stage 2-3, and observations in hippocampal slices showed that waves induce neurite branching. It has been suggested that these growth cone-like waves are an actively propagating mechanism delivering material essential for the growth cone outgrow and branching (Flynn et al., 2009). Disrupting actin filaments results in a significant decrease in branching. Further experiments have helped establish that growth cone local assembly of F-actin is crucial for axonal branching as well as for presynapse formation (Sasaki, 2020; F. Schneider et

al., 2023). These two events have been suggested to be two parallel processes triggered by the interaction between cell-adhesion molecules and a regulator of actin cytoskeleton (Chia et al., 2014) essential for neuronal maturation. This confirms that the actin cytoskeleton plays different roles also in synaptic formation and function which will be further elucidated in the following sections.

4.2. Roles in Synaptic Formation and Function

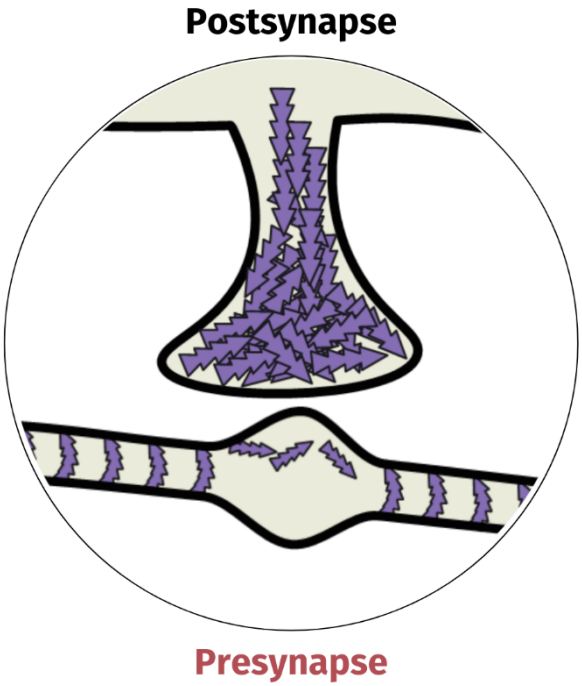

Figure 11. Synaptic Actin. Actin (purple) cytoskeleton within an axodendritic synapse.

4.2.1. Postsynaptic Actin

Actin cytoskeleton has long been examined in dendritic spines and F-actin functions in spines has been extensively investigated (Bär et al., 2016; Fischer et al., 1998; Markham & Fifkova, 1986; Matus et al., 1982; Steffens et al., 2021). Actin structural meshwork is needed for postsynapse morphogenesis, its dynamic remodeling establishes spine size, shape and its stability over time. The orchestrated cooperation of actin binding proteins and their regulatory activities is required to ensure actin nucleation, actin polymerization into filaments, its constant treadmilling between the monomeric and filamentous form and its branching (Hotulainen et al., 2009; Lei et al., 2016). Studies have observed filopodia-like structures, recognized as dendritic spine precursors. These unbranched filaments emerge perpendicular to the dendritic shaft and later elongate into dendritic spine necks. The developed spine head presents complex networks of branched actin structures (Markham & Fifkova, 1986). *In vitro* studies of rat hippocampal neurons have shown the considerable enrichment of actin at dendritic spines (Fischer et al., 1998). Under high-frequency stimulation inducing long-term potentiation, a correlated increase

in spine surface or density is observed. On the contrary, during long term depression, a shrinkage of spine neck is recorded (Q. Zhou et al., 2004). Serving as a dynamic scaffold, the actin cytoskeleton helps organize synaptic nanodomains such as the postsynaptic density (PSD). Essential compartmentalization of signaling molecules, such as glutamate receptors (AMPA and NMDA), guarantees signal transduction and amplification in activity-dependent manner (Cingolani & Goda, 2008; Frost et al., 2010; Okamoto et al., 2004). The long-suspected involvement of actin cytoskeleton in these spatial organizations (Allison et al., 1998; Nonaka et al., 2006) has been demonstrated observing rapid rearrangements in PSD proteins following the application of drugs disrupting F-actin in dendritic spines (Kuriu et al., 2006). This is the case for AMPA and NMDA receptors, where proper anchoring at the plasma membrane provides key mechanisms crucial for synaptic strength and plasticity. Actin is thought to recruit extrasynaptic AMPA receptors during LTP in order to increase the synaptic strength (Hanley, 2014; Opazo et al., 2012; Stockwell et al., 2024).

Dendritic cytoskeletal components interact with actin to coordinate the intracellular transport of synaptic vesicles and other organelles. This traffic is fundamental to bring the molecules needed to form postsynapse (Kapitein & Hoogenraad, 2015). Studies have interrogated actin involvement in the activity-dependent transport of NMDA receptors and have suggested a model of chemical activation through kinase activity leading to increased density of these receptors. This was inhibited after disruption of actin filaments (Bu et al., 2015). Recent investigations have revealed a crucial NMDA-dependent actin remodeling mechanism specific to dendritic submembrane lattice reorganization. In rat hippocampal cultured neurons, dendrites present a periodic scaffold whose momentaneous disappearance is observed following NMDA receptor activation. The membrane-associated actin rings are disrupted and restructured into intracellular fibers to support different processes such as membrane remodeling to accommodate the lateral movements of receptors, signaling via vesicular cycling, and overall spine formation. These modifications are not observed within axons, whose sub-membranous organization is stable in response to enhanced neuronal activity (Lavoie-Cardinal et al., 2020).

4.2.2. Presynaptic Actin

A critical question explored in my research is how the actin cytoskeleton shapes the presynaptic compartment. Current knowledge indicates that the actin network plays key roles in the overall organization of presynaptic components into functional nanodomains and in orchestrating them to ensure proper synaptic transmission. It is responsible for vesicle trafficking, synaptic vesicle tethering, and exocytosis and endocytosis. Actin is a predominant component of the presynaptic compartment of all synapses (Kudryashova, 2021). Investigations into actin architecture and dynamics within this compartment will

provide a better understanding of the molecular mechanisms by which synaptic transmission is modulated and maintained throughout a neuron's life (Gentile et al., 2022; Papandréou & Leterrier, 2018).

Actin acts as a molecular scaffold to constrain the proteins involved in the regulation of vesicular cycling (Bloom et al., 2003; Fenster et al., 2003; W. Zhang & Benson, 2001a). The actin cytoskeleton has also been recognized as a major actor in VGCCs transport to the presynapse and in their retention at the active zone, as shown by impaired delivery when the cytoskeleton is disrupted or their persistence when stabilized (Cunningham & Littleton, 2023; W. Zhang & Benson, 2001a).

The actin filaments surrounding the active zones gather these elements together in close proximity to the postsynaptic density, thus facilitating synaptic transmission. The structural frame made of actin is characterized by filaments surrounding and interconnecting the vesicle pools and eventually anchoring them at the plasma membrane (Siksou et al., 2007). The reserve pool located in the inner-most regions of the presynapse is distinct from the ready releasable pool (RRP), which gathers around the active zone where synaptic vesicles fuse with the plasma membrane. Actin creates a dome shaped structure flattening at RRP periphery where vesicles can be endocytosed and recycled (Bloom et al., 2003).

Researchers have revealed actin involvement in presynaptic dynamics. ARP2/3, an actin binding protein, together with Rac1 and Rho, mediators of actin assembly, play a role in the dynamics of neurotransmitter release and pool replenishment through negative regulation. Meanwhile, Rac1 deletion enhanced the frequency of vesicular replenishment. These results together highlight actin dependent dynamics which are vital for presynaptic functions (O'neil et al., 2021). Previous literature provided contradictory findings concerning actin roles in presynaptic exocytosis. Application of actin-perturbing agents in cultured neurons revealed either reduced or increased exocytosis, underlying possible opposing roles of the presynaptic actin scaffold in presynaptic processes (Cole JC et al., 2000; Morales et al., 2000; Sankaranarayanan et al., 2003).

Structurally, the periodic actin-spectrin scaffold is interrupted at the axon terminal, where the presynaptic actin cytoskeleton changes to accommodate vesicular pools and presynaptic infrastructure (Papandréou & Leterrier, 2018; Sidenstein et al., 2016). Three main nanostructures have been previously identified by our lab: the corrals, the mesh and the rails (Bingham et al., 2023). Actin corrals englobe the entire presynaptic compartment, dense branched actin filaments create a sub-membranous architecture supporting the presynapse shape; the actin mesh appears as a less dense structure often localized in proximity to active zone components such as bassoon; the rails are linear structures extending between ready releasable and reserve pools. Inhibiting the ARP2/3 complex showed a reduction of actin corral and actin mesh, indicating that these nanostructures rely on this actin binding protein to mediate branched nucleation.

Conversely, the use of formin inhibitors disrupted the rails, confirming the linear nature of their nucleation process (Bingham et al., 2023). In this work, Bingham et al. suggest that these nanostructures are engaged in distinct processes. The structural features of the corral surrounding the presynaptic compartment is seemingly linked to orchestrating the dispersal of synaptic vesicles and other organelle, organizing them into specific locations to facilitate vesicle recycling (Bloom et al., 2003). The presence of actin mesh at the active zone is proposed to both guide and prevent exocytosis events. This is in accordance with previous studies suggesting the restrictive role of the cytoskeleton in presynapses, where scientists using depolymerizing agents showed that actin disruption causes increased neurotransmitter release (Morales et al., 2000; Trouillon & Ewing, 2014). Meanwhile, rail orientation between the different pools of vesicles and the known involvement of actin cytoskeleton in organelle and vesicular traffic, induce the assumption that these structures might facilitate vesicle transport between the reserve and the releasable pools (Anggono & Huganir, 2012; Chenouard et al., 2020; Letourneau, 2009; Venkatesh et al., 2020). Distinct nanostructure might play different roles justifying the precedent contradictory results following actin dysregulation.

The actin cytoskeleton in presynapses clusters, mobilizes, and docks synaptic vesicles at the active zone, thus enabling efficient synaptic transmission. Thus, studying actin dynamics in such a compartment will be enriching for insight into the molecular mechanisms involved in the modulation and maintenance of synaptic transmission. These processes are of critical importance since perturbations in actin dynamics impair neuronal communication and perhaps underlie a number of neurodevelopmental and psychiatric disorders.

5. Impact of Actin Cytoskeleton Impairment on Neurological Health

The dysfunction of actin is increasingly recognized as an important feature of many neurodevelopmental and neurodegenerative disorders such as Alzheimer's and Charcot Marie Tooth diseases, and autism spectrum disorder. Aggregation of actin, most notably in the form of cofilin–actin rods, has been described post-mortem in Alzheimer's disease patients (Bamburg & Bernstein, 2016; Maloney et al., 2005). These aggregates impair axonal transport, leading to synaptic loss and cognitive decline, thereby underscoring actin dysregulation as a driver of disease progression. Another disease, such as Charcot-Marie-Tooth, further underscores actin's role. Different classes of mutations affecting the actin-interacting proteins, such as spectrin and inverted formin-2, cause neuronal morphological defects together with impaired myelination. Besides neurodegeneration, actin malfunction is also associated with neurodevelopmental disorders, for instance, autism spectrum disorder where recent studies have shed light on the neuronal actin contribution to the neurophysiological dysregulations. Genetic variations of the spectrum are found to be associated with actin cytoskeleton impairment and the widespread effects on neuronal connectivity which provokes developmental defects (Gilman et al., 2011).

Altogether, these findings shed light on the essential participation of actin in both the pathogenesis of neurodegenerative diseases and the proper development of the nervous system, identifying it as a key target for new therapeutic interventions (Liaci et al., 2021).

6. Investigating Presynapses: Tools of the Trade

Imaging actin cytoskeleton nanostructures, per se, raises many challenges associated with the intrinsic complexity of the synaptic environment. One of the main difficulties is that a dense expression of actin is observed within the postsynaptic compartment, obscuring the nanostructures of the juxtaposed presynapse. Various microscopy techniques have provided critical insights into the presynaptic cytoskeletal composition and dynamics. However, considering the extremely small size of actin nanostructures, most of the technological approaches still present limitations (Jung et al., 2020). The following sections expose the emergence of different methodologies employed to investigate presynaptic actin nano-architecture.

6.1. Electron Microscopy and Presynaptic Ultrastructure

Ultrastructural studies have shed light on the distribution and organization of actin within synapses. Quick-freeze electron microscopy was among the first tools used to visualize and describe actin filaments in detail within chemical synaptic terminals. Early observations focused primarily on the presynaptic ultrastructure, shedding light on the organization of vesicle pools and other components.

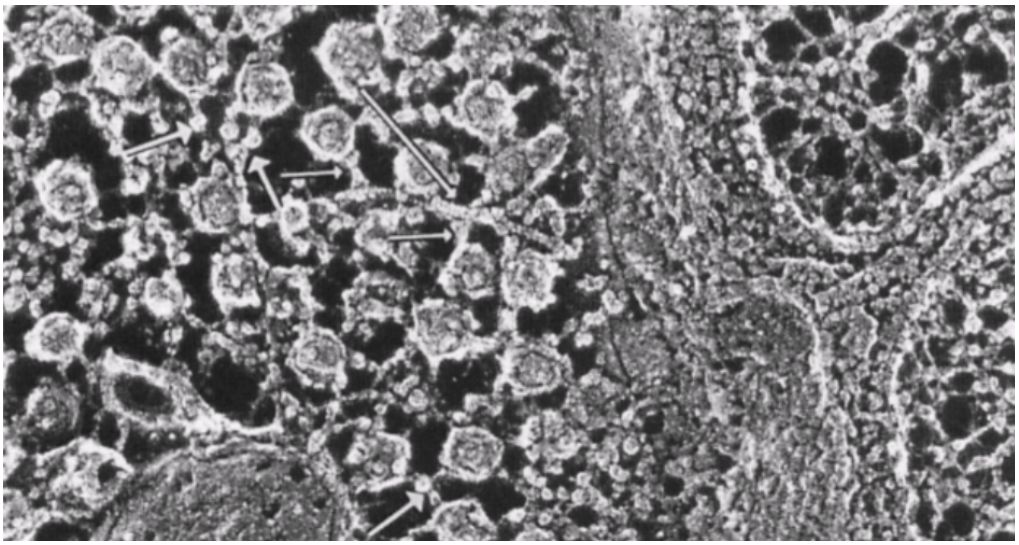

Figure 12. Cytoskeletal Architecture of a Presynaptic Terminal of a Frog Neuromuscular Junction. Observation of 20-30 nm strands (short arrows) between actin filaments (long arrows) and synaptic vesicles. synaptic vesicle short linking strands or globular structures are found (thick arrows). Adapted from (Hirokawa et al., 1989)

This complex imaging technique uncovered the close relationship between the actin cytomatrix and vesicular organization (Fig. 12). These structural data elucidated the synapsin-mediated interconnection between vesicles and actin filaments (Hirokawa et al., 1989). The average amount of vesicles per presynapse in mouse hippocampal neurons has been estimated at over 200, with a range of 40 to 801. A small fraction of these vesicles was observed to be docked at the active zone (Schikorski & Stevens, 1997). These researchers captured 71 synapses. The majority (90%) displayed a single active zone, a small portion (8%) showed two releasing sites, and only one synapse (2%) showed 3 active zone. More insight regarding the presynaptic ultrastructure was obtained when Landis and colleagues provided interesting arguments regarding tissue preparation methods and how they may influence the interpretation of such nanoscopic structures within presynaptic junctions (Landis et al., 1988). They compared different fixation methods with rapid freezing, and determined that all preservation methods are appropriate for examining various presynaptic structural features. Aldehyde fixations, for example, showcase electron dense membranes and materials of the synaptic cleft as well as presynaptic linear actin fibers. On the other hand, ethanol diminishes the membrane staining for better visualization of other components.

6.2. Cryogenic Electron Tomography and Presynaptic Cytomatrix Components

Cryogenic electron tomography (cryo-ET) is a vanguard imaging technique that emerged in the late 1990s from EM and developed during the past decades to grant three-dimensional (3D) visualization of biological structures at the nanometer-scale(Doerr, 2016). Cryo- ET requires taking a series of images with different angles to create a 3D rendering of the imaged sample, suitable for analyzing synaptic components. Structures like vesicles fusing with the presynaptic membrane, which typically fade with chemical fixations are preserved, enabling visualization of the fine filaments interconnecting them (Fernández-Busnadiego et al., 2010; Siksou et al., 2007).

Three-dimensional (3D) reconstruction of the presynaptic terminal cytomatrix was achieved using cryo-ET (Fig. 13).

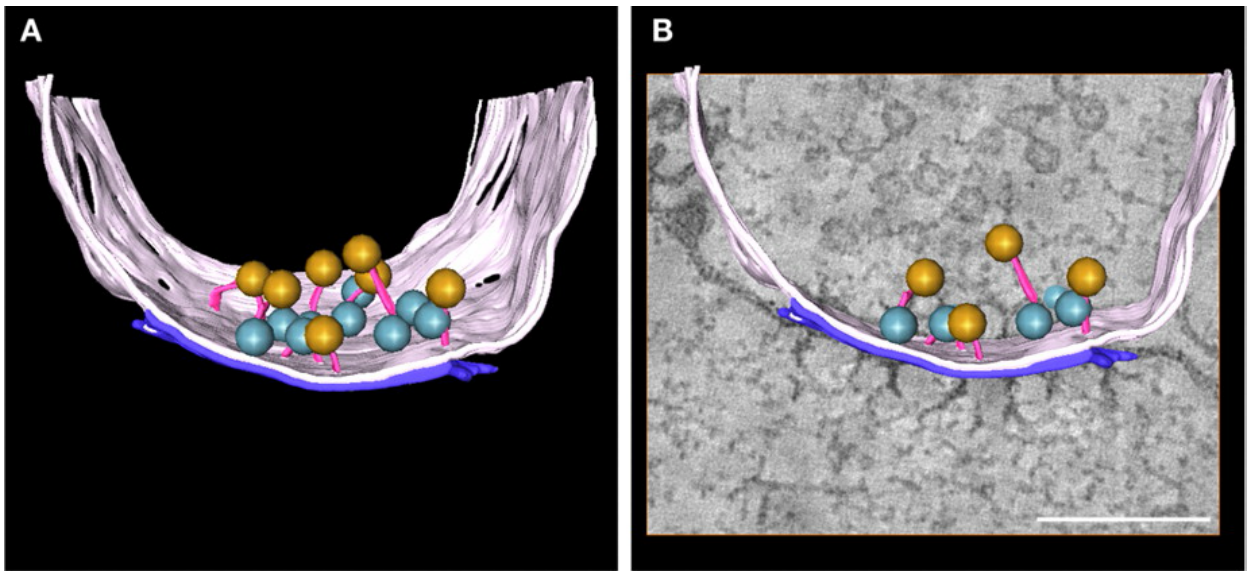

Figure 13. 3D Reconstruction of Presynaptic Compartment Electron Tomography Acquisition. A. Presynaptic bouton rendering. B. Intermediate reconstruction step. Plasma membrane (light pink), docked vesicles (blue), filaments (pink) connecting vesicles (yellow) to the plasma membrane. Scale bar : 200 nm. *Adapted from*

Cryo-ET can achieve a resolution lower than 0.1 nm. Providing images of the biological complexes in their natural states requires thin sample slices and extensive preparations, including delicate protocols of fixation, quick freezing, and precise sectioning (Benoît Zuber et al., 2005). Cryo-ET requires a time-consuming and complex data acquisition process, but it allows for 3D reconstructions of cellular structures, offering detailed and precise observations. Nevertheless, the necessity of specialized equipment and expertise in sample preparation makes it a highly tedious technique (J. Schneider & Jasnin, 2022). More importantly, the lack of molecular specificity associated with cryo-ET prevents a complete description of actin cytoskeletal and presynaptic cytomatrix components.

6.3. Fluorescence Microscopy

Further advancements in understanding the spatial arrangement of presynaptic components came with the emergence of fluorescence microscopy. This technique provided molecular specificity by using fluorescent dyes, antibodies, and genetically encoded fluorescent proteins to label specific proteins and molecules, overcoming the limitations of EM (Renz, 2013).

6.3.1. Widefield Fluorescence Microscopy, Confocal Microscopy, and Total Internal Reflection Fluorescence Microscopy

Widefield fluorescence microscopy (WF), confocal microscopy, and total internal reflection fluorescence microscopy (TIRF) allow the visualization of multiple fluorescent-labeled targets. The typical spatial resolution is limited to 200-300 nm laterally and to 500-700 nm axially for the WF, while an improved axial resolution is achievable (~500 nm) with confocal microscopy. TIRF involves illuminating a small portion of the sample just at the glass surface, yielding an axial resolution of 100-200 nm (Fish, 2009). These imaging techniques are commonly employed to observe fixed samples and are also extremely useful in the real time study of biological processes in living organisms. In fact, live-cell WF imaging is a relatively simple technique, illuminating the whole specimen and acquiring dynamic signals within a broad field of view (Rao et al., 2022). It is well suited for observing fast processes such as synaptic vesicle dynamics, exocytosis or endocytosis because it can provide high-speed imaging, although sometimes the resulting acquisition might be blurred by the out of focus light when the samples are thick. In these cases, confocal live-cell imaging produces sharper acquisitions allowing a better resolution of tiny elements such as vesicles or actin structures. It is successful in tracking vesicular kinetics and actin dynamics, all the while minimizing the photobleaching and phototoxicity by limiting the sample exposure to a specific imaging plane. Confocal microscopy improves spatial resolution compared to WF microscopy, but its ability to capture events happening on shorter timescales, such as vesicular fusion, is restricted by its lower temporal resolution. TIRF constitutes a compromise providing an enhanced resolution in a small sample depth and minimizing the background noise, by exciting just the fluorophores of the illuminated field. It is capable of recording processes occurring near the cell-membrane, making it the most adapted technique to observe synaptic vesicle dynamics such as docking, priming, exo/endocytosis observed at the active zone. This advantage, though, restricts its use to superficial events and disqualifies it for inner-membrane events.

6.3.2. Visualizing Presynaptic Actin and Other Components

These imaging techniques have revealed the spatial interactions between numerous presynaptic components, from the cytoskeleton to protein distribution (Sakamoto et al., 2018). Multi-color acquisitions combined with segmentation-based analysis affords high versatility of the experimental design. Both fixed and live-cell imaging are possible, allowing observations of time-frozen snapshots and real-time molecular dynamics throughout neurodevelopmental stages. Noteworthy, on hippocampal cultured neurons, the immunofluorescence analysis of pre- and post-synaptic markers has facilitated investigations of synaptogenesi (Schätzle et al., 2012) s. Automated quantification reveals that within 7-day-old neurons, presynaptic components are three times less abundant than those of the postsynapse. During this developmental stage, only a few fully formed synapses are observed. Later, 14 day-old cultured neurons show an equal number of elements in both compartments, but only half of them are directly involved in synaptic formations (Fig. 14).

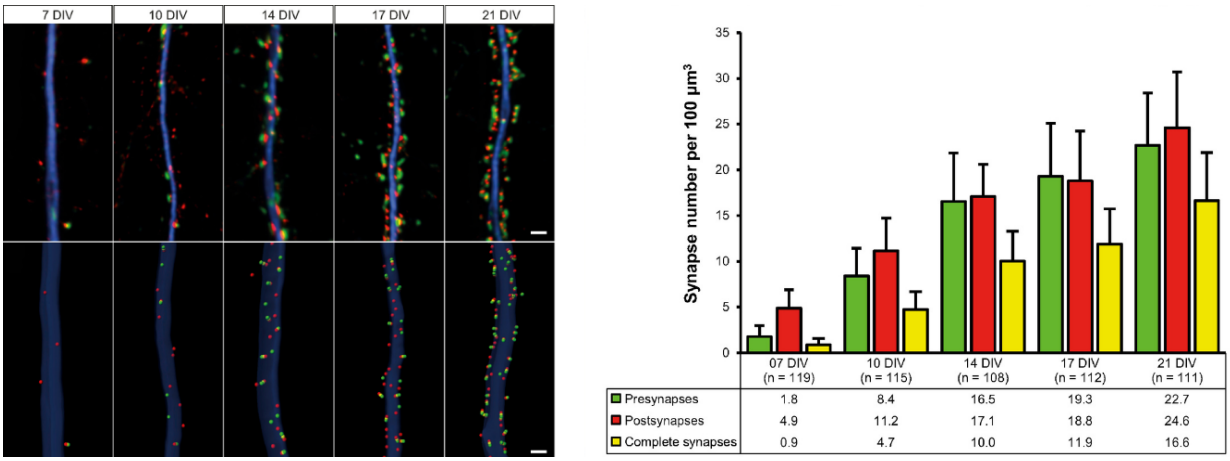

Figure 14. Synaptogenesis of hippocampal cultured neurons. Left image displaying epifluorescence image (upper panel) or 3D representations (lower panel) of MAP2 labeled dendrites (blue) over time of cultivation. The analyzed samples are organized from DIV 7 to DIV 21 and show axodendritic synapses elements density evolution through time. Presynaptic elements are labeled in green and postsynaptic ones in red. Right image summarizes the results obtained through the three-dimensional automated quantification. The presented values are normalized to dendritic volumes. Error bars represent the standard deviation. Scale bars 2µm. Adapted from (Schätzle et al., 2012)

Epifluorescence microscopy is an optical diffraction limited imaging technique, able to offer intensity measurements and help unraveling presynaptic terminal development and molecular dynamics during synaptic formation. The actin cytoskeletal involvement in neurodevelopment was revealed principally due to the technological advancements permitting specific staining of actin filaments and the simultaneous visualization of other cellular components. Since early stages of fluorescence microscopy, phalloidin, a toxin binding specifically to interfacing subunits of actin polymers, was widely used to label and

visualize F-actin in fixed cells. Their use has produced numerous data regarding actin cytoskeleton distribution, organization and functions, within all kind of cells (M. Costa et al., 1997; Desroches & Harris, 2023; McGough et al., 1997; Wulf et al., 1979). Phalloidin still constitutes the gold standard for labeling endogenous actin despite the existence of other labeling techniques using fluorescent-dye-conjugated antibodies or HA-Flag-tagged actin.

To observe dynamic processes *in vitro*, there are several probes using actin binding domains (ABDs), mostly constituted by derivates of fluorescent proteins fused with genetically encoded ABDs. LifeAct-GFP, for example, is derived from yeast and has been specifically designed to bind actin filaments. It is one of the most reliable tools minimally affecting actin polymerization and other cellular functions. LifeAct is very versatile for real-time studies on actin dynamics, allowing the visualization in multi-color imaging experiments according to the conjugated fluorescent protein (Courtemanche et al., 2016a; Riedl et al., 2008a). Live tracking of fluorescent actin has been useful to investigate cytoskeletal modifications neurons undergo throughout their development, such as the activity dependent morphogenesis of dendritic spines, axonal distribution and actin's role in regulating synaptic plasticity processes (Ganguly et al., 2015; Gentile et al., 2022; Leite et al., 2021; Leterrier et al., 2017; Papandréou & Leterrier, 2018).

Fluorescence microscopy has elucidated numerous processes involving the presynapse and its components. Due to live-imaging techniques, a study highlighted the orchestrated signaling events preceding the creation of a presynaptic terminal, the trafficking of both synaptic vesicles and active zone proteins as a mechanism taking place prior to stable synapse formation (Bury & Sabo, 2011). Actin's precise implication into these processes still needs to be elucidated although its influence in these mechanisms has been demonstrated.

In the early 21st century, a study demonstrated that the presence of actin cytoskeleton at presynaptic sites is crucial for the initial stages of neuronal development (W. Zhang & Benson, 2001a). Using fluorescence microscopy and EM microscopy techniques, Zhang and colleagues investigated rat hippocampal cultures labeled for synaptophysin, a protein embedded in synaptic vesicle membranes, whose cluster aggregation is still commonly used to identify presynapses. They also examined their activity by observing dye uptake within vesicles. The application of an actin-depolymerizing agent to one-week old neurons revealed by fluorescence microscopy, resulted in a near-complete loss of synaptophysin clusters, decreased cluster size, and disruption of presynaptic cycling activity. Moreover, EM images showed unrecognizable ultrastructure of presynaptic sites, highlighting the critical role of the actin cytoskeleton in early presynaptic formation. However, in two-week old neurons, presenting more mature presynapses, showed a noticeable reduction in the number and size of synaptophysin-labeled clusters, yet the overall presynaptic morphology remained intact even after actin depolymerization. Zhang findings suggests that maturing presynapses develop increasingly stabilized actin

structures that maintain synaptic architecture despite F-actin disruption. Indeed, in eighteen-day old neurons, synaptophysin clusters and vesicle recycling become more resistant to actin disruptions, indicating mature synapses develop other strategies to maintain their structure and function. Additionally, Zhang and colleagues interrogated this decreased dependence from actin cytoskeleton and found a correlation with the recruitment and retention of key synaptic scaffolding proteins such as bassoon at the active zone. Using fixed and live-cell fluorescence imaging to visualize presynaptic actin structures and dynamics in real-time, actin was detected adjacent to bassoon clusters, confirming actin presence at the presynaptic active zone (Morales et al., 2000). Further, electrophysiological studies revealed increased probability of vesicle release following administration of an actin depolymerizing drug, suggesting that actin influences vesicle exocytosis.

The fluorescence microscopy approaches employed in these studies correlated the actin dynamics with the exocytosis events, providing insight into the actin cytoskeleton's roles in presynaptic structure and function. Fluorescence labelling techniques present significant advantages over EM regarding the specificity of tagging and visualizing molecular components in fixed and living specimens, enhancing the comprehension of dynamic processes unachievable with EM. Moreover, fluorescence microscopy sample preparations are less complicated, and they preserve cell function and viability. However, the diffraction-limited optical features of fluorescence microscopy constrain the observation of presynaptic actin nanostructures and other nanoscopic synaptic components whose dimensions are below the resolution limit. Despite this, both techniques are essential but insufficient to fill the knowledge gap concerning ultrastructural features of the presynaptic actin cytoskeleton.

6.4. Single Molecule Localization Microscopy

Overcoming the optical diffraction limit of traditional microscopy is critical to investigate the molecular organization of the presynapse. Fortunately, over the last three decades, innovative technological advances brought adequate sub-diffraction imaging strategies grouped under the name of single molecule localization microscopy (SMLM). Essential to super-resolve biological structures at a molecular level, two SMLM techniques stand out: stochastic optical reconstruction microscopy (STORM) or point accumulation for imaging in nanoscale topography (PAINT)(Lelek et al., 2021).

These SMLM techniques rely on the stochastic emission of light from a few fluorophores at a time. The random blinking of these fluorophores is essential to isolate and image individual fluorescent molecule emitting signals at different time points. Each frame captures point spread functions (PSFs) of emitting molecules, and by fitting these PSFs to a Gaussian function allow the precise localization at a nanometer-scale resolution. An astigmatic lens deforms the captured PSFs to compute axial coordinates resulting in

3D super-resolved acquisitions. This level of precision makes SMLM a good candidate for the analysis of presynaptic actin nanostructures.

6.4.1. STORM and DNA-PAINT

STORM uses synthetic photo-switchable fluorophores (dyes) that transition between a dark (OFF) state and an emitting one (ON state) to record the precise positioning of single molecules within a biological sample. Affecting the switching probabilities is achievable by modulating the laser irradiation or by affecting the chemical environment in which fluorophores are immersed. STORM requires relatively simple sample preparation, using traditional antibody-based immunostaining techniques and a reducing buffer that forces most dyes into the off state upon excitation. This set up allows only a sparse subset of fluorophores to reach the energy levels needed to emit light at any given time. A related technique, termed point accumulation for imaging in nanoscale topography (PAINT), uses short single DNA strands fused to antibodies to obtain similar results. The SMLM technique entails the use of fluorescent dyes conjugated to DNA strands. The complementary DNA strand is conjugated to the primary antibody bound to the target protein of interest. The ON and OFF states are generated by the binding and unbinding of the complementary DNA strands. DNA-PAINT is particularly advantageous for multicolor SMLM acquisitions. Apart from the distinct labeling strategies, DNA-PAINT and STORM allow the reconstruction of super-resolved images with a lateral resolution down to ~20 nm and 50-70 nm axial resolution (Rust et al., 2006; Sharonov & Hochstrasser, 2006). These characteristics are crucial for detail visualization of small molecular structures, highlighting the advantages of their applications in various biological fields such as neuroscience (Igarashi et al., 2018), where comprehensive analysis allowed detailed description of the presynaptic active zone cytomatrix (Dani et al., 2010; Glebov et al., 2017). Taking advantage of the high throughput imaging capabilities of STORM 3D multicolor acquisitions, Dani and colleagues analyzed the spatial distribution of ten pre- and postsynaptic proteins. They highlighted the existing variations in synapse morphology and composition using 3D structural analysis and revealed STORM as an appropriate tool for investigating the synaptic architecture and related functions. These methodologies are primarily specialized quantitative systems designed to objectively measure and analyze spatial arrangements of proteins to determine nanoscale changes in their clusters (Glebov et al., 2017).

7. Investigating Presynaptic Actin Ultrastructure

Despite the advantages made in these microscopy techniques, it remains challenging to visualize presynaptic actin cytoskeleton in its natural context. The greater expression of actin within the postsynaptic compartment considerably contributes to the challenges associated with visualizing presynaptic actin, even with super-resolution microscopy (Nosov et al., 2020). Researchers have tried to avoid these constraints by using genetically encoded fluorescent tags such as GFP labeled actin. For instance, the use of LifeAct-GFP has been essential to observe actin behavior in biological processes such as neuronal polarization (Riedl et al., 2008a), as well as exocytosis and endocytosis (Jang et al., 2012; L. G. Wu & Chan, 2022). However, studies have reported that the use of these fluorescent probes requires cautious titration as they induce concentration-dependent effects on actin assembly in cultured cells (Courtemanche et al., 2016a). Despite the selective labeling of presynaptic compartments to minimize the interference from postsynaptic actin expression (Reshetniak & Rizzoli, 2019), this approach yields low labeling densities in order to avoid any perturbative effects on endogenous functions. These observations have led our team to develop alternatives approaches to afford optimal actin labeling densities in a model of isolated presynapses.

7.1. Bead-induced Model of Presynapse

The use of a validated model of bead-induced presynapses overcame postsynaptic obstructions in visualizing actin cytoskeleton (Fig. 15)(Bingham et al., 2023). This method triggers rapid presynaptic boutons formation upon contact with poly-L-lysine coated beads (Burry & Matthew, 1986; Lucido et al., 2009).

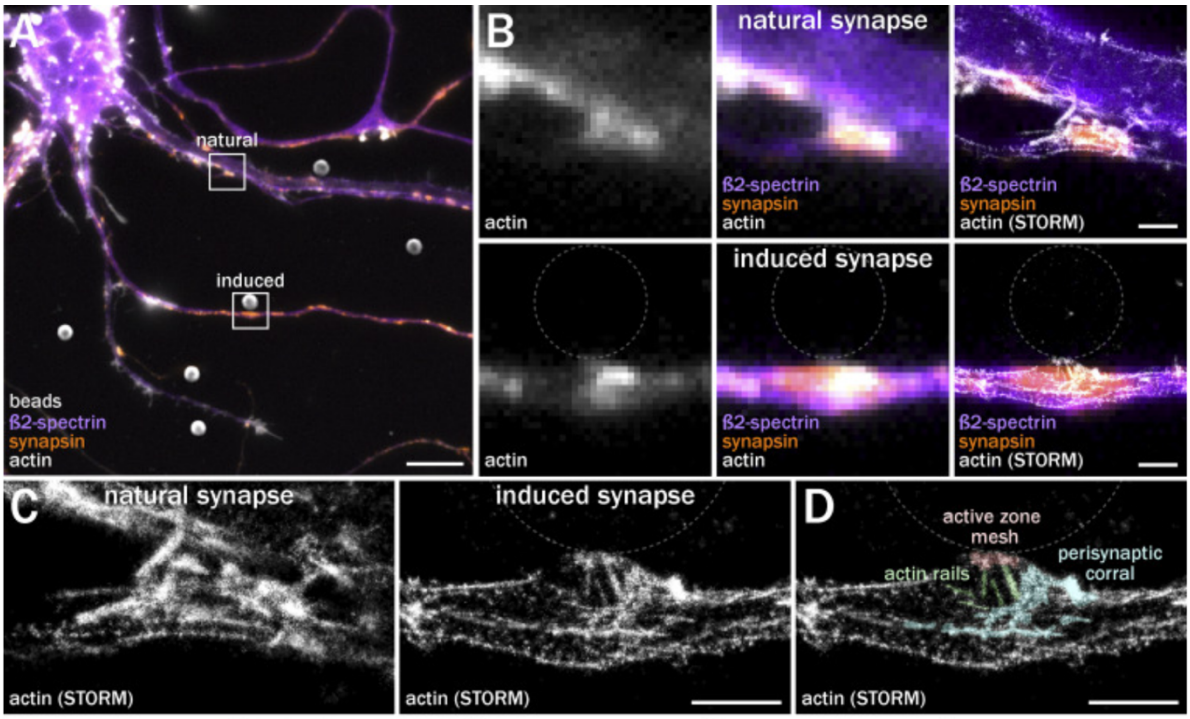

Figure 15. Actin Nanostructures Visualization at Bead-induced Presynapse. (A)Widefield image of a n axo-dendritic and a bead-induced synapse labeled for ß2-spectrin (purple), synapsin (orange), and actin (gray). (B) Zoomed regions highlighted in A. (C) Zoomed STORM images of the natural synapse (left) and bead-induced presynapse (right). (D) Presynaptic actin structures highlights: active zone mesh (red), actin rails (green), corral (blue). Scale bars in A, 10 µm; in B–D, 1 µm. Adapted from (Bingham et al., 2023).

Phalloidin labeling and diffraction-limited microscopy allowed our team to visualize and characterize actin in bead-induced presynapses. Using the bead-model, were identified two distinct populations of induced presynapses: actin-enriched and non-enriched, with a total of ~70% actin-enriched and ~30% non-enriched presynapses observed. These findings highlight the heterogeneity in presynaptic actin distribution (Bingham et al., 2023). Actin enriched presynapses showed enhanced synaptic vesicular cycling, suggesting the implication of presynaptic actin nanostructures in ensuring normal synaptic function. Nanoscale reconstruction of presynaptic actin organization using super-resolution microscopy technique STORM, revealed the presence of three actin nanostructures present in both actin enriched and non-enriched presynapses: corrals, mesh, and rails. The nucleating features of these nanostructures was further determined using pharmacological perturbations to reveal branched corrals and mesh and linear rails. Disruption of rail nucleation resulted in significantly reduced synaptic vesicular cycling, pointing to their potential role in the trafficking of vesicles from the

reserve pool toward the active zone release site (Maschi et al., 2018). However, due to the heterogeneity in the shape and orientation of bead-induced presynapses, the presynapse-on-bead model is not the optimal tool to investigate actin structures and dynamics.

To interrogate the roles of corrals, mesh, and rails in exocytosis, a more appropriate tool is necessary to trigger presynaptic formation in such a way that more closely represents the physiological environment and that improves optical accessibility of these nanostructures.

7.2. Novel Presynapse-on-Glass Model

Recent techniques involved coating the entire surface of glass coverslips with a postsynaptic cell-adhesion molecule, Neuroligin, to induce presynaptic active zone formations (Funahashi et al., 2018; Kim et al., 2016). However, the presynaptic distribution onto the whole coated area is difficult to distinguish from traveling vesicles that carry the presynaptic markers used to identify induced presynapses. Additionally, this method of covering the entire surface impedes the natural conditions neurons face in living organisms, where aggregations of neuroligin are observed on sparse postsynaptic sites.

Restricting the coated regions to ~2 µm diameter dots onto the glass provides a more physiological environment, mimicking the size and approximate shape of dendritic spines. Micropatterned substrates have emerged as useful tools for spatially controlled

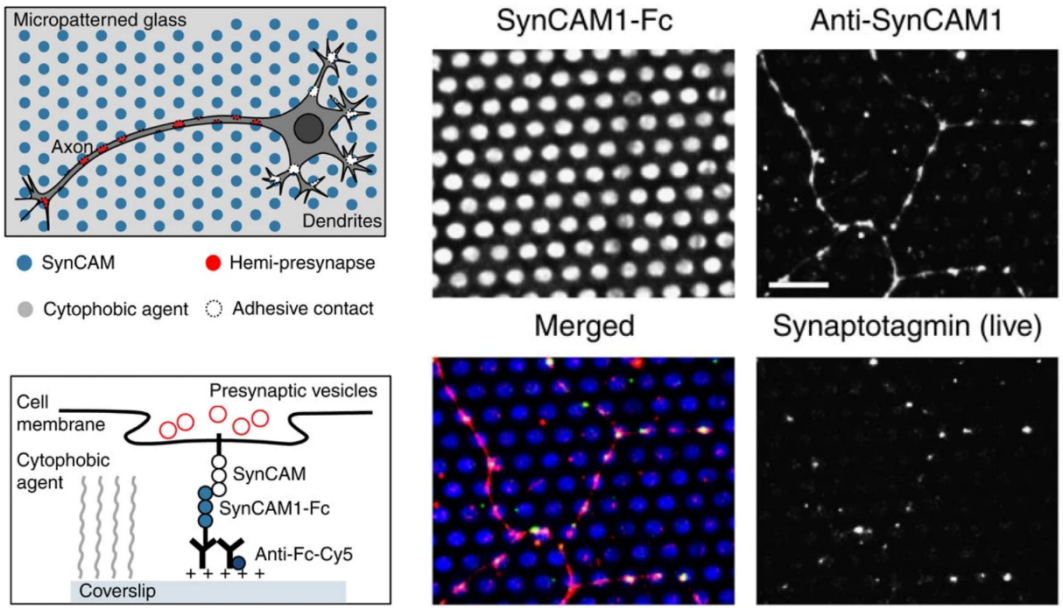

Figure 16. Presynapse formation on a synCAM1-coated micropattern. Top left schematic view of a neuron (dark gray) plated on micropatterned substrate of synCAM1 (blue) and cytophobic environment (gray) presenting adhesive contacts (white) and hemi-presynapse (red). Bottom left schematic of the synCAM induced presynaptic formation. Righ panel showing the synCAM1-coated micropattern and axonal segment labeled with anti-synCAM1 (ref) and synaptotagmin (green). Scale bar 10 µm.
Adapted from (Czöndor et al., 2013).

synaptic formation in cultured neurons, such as induced presynapses formed on dots of synCAM1 (Fig. 16)(Czöndör et al., 2013).

These techniques require coating the coverslips with cytophobic reagents. Perforated masks are then layered over the coated coverslips, after which lasers are used to degrade the cytophobic layer in precise spots. The coverslips are subsequently recovered with the cell-adhesion molecules (CAMs) of interest which reside within the engineered holes of the cytophobic coat. Micropatterned substrates provide advantages in promoting controlled presynaptic formation in targeted locations forcing axons to develop on top of the cytophilic dots of CAMs.

In contrast to these methods, the novel presynapse-on-glass model presented in this thesis uses stamps to print arrays of spots, approximately 1.8 μm diameter, coated with neuroligin directly onto the glass (Fig. 17). Importantly, our model avoids restricting axon attachment. Instead, the glass is coated with poly-L-lysine and laminin to promote more natural neuronal development. This environment induces presynaptic formation toward the glass, an optimal orientation for imaging studies. The flat glass surface provides enhanced optical accessibility to visualize actin cytoskeleton nanostructures and investigate their roles in vesicle exocytosis.

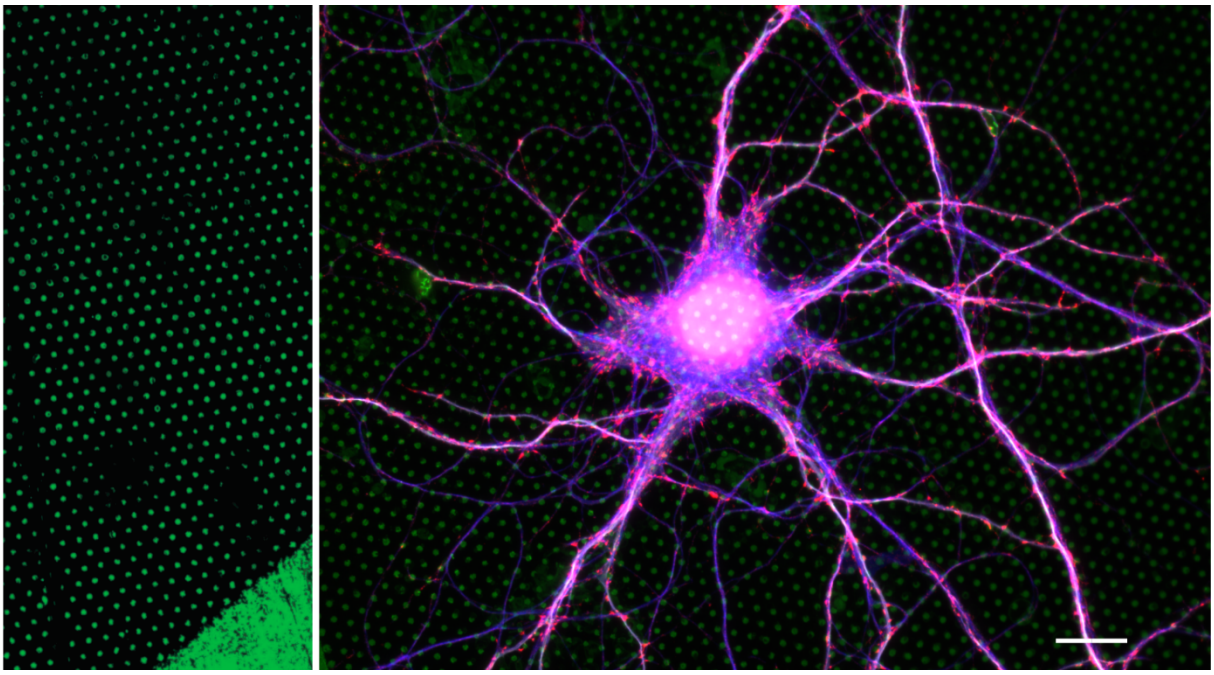

Figure 17. Novel Presynapse-on-glass Model. Neuroligin-dots micropattern on the left panel. Neuron cultured onto the novel presynapse-on-glass model (right panel). Neuroligin (green), presynaptic marker (red), dendritic marker (white), axonal marker (blue). Scale bar 20 μm.

8. Deciphering the nanoscale architecture of presynaptic actin using a micropatterned presynapse-on-glass model

Tumminia S°, Mezache L°, Wiesner T, Vianay B, Thery M, Papandréou MJ*, Leterrier C* (° co-first authors; * co-corresponding authors).

bioRxiv, 2024 Sep 5. doi: 10.1101/2024.09.05.611287
Submitted to the Journal of Neuroscience on September 12th, 2024

Deciphering the nanoscale architecture of presynaptic actin using a micropatterned presynapse-on-glass model

Sofia Tumminia[1°], Louisa Mezache[1°], Theresa Wiesner[1], Benoit Vianay[2], Manuel Théry[2,3], Marie-Jeanne Papandréou[1*], Christophe Leterrier[1*]

[1] Aix Marseille Université, CNRS, INP UMR7051, NeuroCyto, 13005 Marseille, France.

[2] CytoMorpho Lab, LPCV, UMR5168, Université Grenoble-Alpes, CEA/INRA/CNRS, Interdisciplinary Research Institute of Grenoble, 38054 Grenoble, France.

[3] CytoMorpho Lab, CBI, UMR8132, Université Paris Sciences et Lettres, CEA/CNRS, École Supérieure de Physique et Chimie Industrielles de la Ville de Paris, Institut Pierre Gilles De Gennes, 75005, Paris France.

° These authors contributed equally.

* Correspondence: marie-jeanne.papandreou@univ-amu.fr and christophe.leterrier@univ-amu.fr.

Abstract

Chemical synapses are fundamental units for the transmission of information throughout the nervous system. The cytoskeleton allows to build, maintain and transform both pre- and postsynaptic contacts, yet its organization and the role of its unique synaptic nanostructures are still poorly understood. Here we present a presynapse-on-glass model where presynaptic specializations are robustly induced along the axons of cultured neurons by micropatterned dots of neuroligin, allowing the controlled orientation and easy optical visualization of functional induced presynapses. We demonstrate the relevance and usefulness of this presynapse-on-glass model for the study of presynaptic actin architecture, showing that a majority of induced presynapses are enriched in actin, with this enrichment being correlated to higher synaptic cycling activity. We confirm our previous results on bead-induced presynapses by identifying the same distinct actin nanostructures within presynapses: corrals, rails and mesh. Furthermore, we leverage the controlled orientation of the presynapse-on-glass model, visualizing the arrangement of these actin structures relative to the active zone nanoclusters using multicolor 3D Single Molecule Localization Microscopy (SMLM), and relative to the sub-diffractive localization exocytic events using a correlative live-cell and SMLM approach.

Introduction

Neuronal communication is a complex process involving coordinated interactions between cell-adhesion molecules, signaling complexes, and cytoskeletal elements, which are essential for precise signal transmission across chemical synapses (McAllister, 2007; Togashi et al., 2009). Noteworthy is the actin cytoskeleton, which is crucial in maintaining neuronal structure and shaping neurons throughout their development. It provides the essential framework that supports neuron morphology and enables dynamic changes necessary for growth and function during both early development and maturity (Luo, 2002; Coles and Bradke, 2015). Disruptions in these dynamics can impair neuronal polarization and axonal guidance, leading to ineffective neuronal communication and potentially contributing to neurodevelopmental and psychiatric disorders (Bernstein et al., 2010; Yan et al., 2016).

In addition to its structural role, actin dynamics are vital for neuronal function and synaptic transmission (Cingolani and Goda, 2008; Papandréou and Leterrier, 2018; Gentile et al., 2022). The actin cytoskeleton plays a significant role in presynaptic vesicle clustering, mobilization, and docking, which are essential for maintaining synaptic efficacy (Bernstein and Bamburg, 1989; Kim and Lisman, 1999; Doussau and Augustine, 2000). Actin is also important for endocytosis and the generation of synaptic vesicles at presynapses (Shupliakov et al., 2002; Watanabe et al., 2013; Ogunmowo et al., 2023). As regards the exocytic process, studies using short-term application of actin-perturbing agents have led to contradictory findings of reduced (Cole et al., 2000) or enhanced (Cole et al., 2000; Sankaranarayanan et al., 2003) vesicular release, suggesting that actin acts as a meshwork that gathers vesicles before exocytosis, or as a physical barrier within the presynaptic subdomains. These opposing claims underscore the need for further research to clarify its mechanisms (Li et al., 2018a).

A better understanding of actin's roles at the presynapse requires knowledge of its structural architecture (Papandréou and Leterrier, 2018). Early ultrastructural studies using electron microscopy have provided significant insights into the distribution and organization of actin within synapses, revealing a dense meshwork of actin in dendritic spines (Matus et al., 1982), and shedding light on presynaptic components and actin interconnections within synaptic vesicular clusters (Landis et al., 1988; Hirokawa et al., 1989) and at the active zone periphery (Bloom et al., 2003). However, electron microscopy studies are limited by the difficulty distinguishing actin from other cytoskeletal elements, the complex sample preparation leading to potential damage, and the restrained molecular specificity inhibiting a comprehensive model of presynaptic architecture.

Fluorescence microscopy techniques have expanded our knowledge about the spatial relationship between presynaptic components due to their better molecular specificity, despite its diffraction-limited resolution being inadequate to resolve presynaptic cytoskeletal and molecular nanostructures. Fortunately, super-resolution microscopy approaches can overcome the diffraction limit and allow nanoscale imaging studies (Jacquemet et al., 2020; Werner et al., 2021). Among these, Single Molecule Localization Microscopy (SMLM) techniques such

as Stochastic Optical Reconstruction Microscopy (STORM) and DNA-Point Accumulation in Nanoscale Topography (PAINT), which rely on stochastic blinking of single fluorophores followed by their precise localization, have refined our knowledge of presynaptic organization (Dani et al., 2010; Glebov et al., 2017; Carvalhais et al., 2021).

Despite those advances, the dense expression of actin at the postsynapse makes presynaptic actin imaging quite challenging in its natural context (Reshetniak and Rizzoli, 2019; Nosov et al., 2020). To overcome these obstacles, our team has recently used a model of bead-induced isolated presynapses (Burry, 1980; Lucido et al., 2009). By visualizing actin within isolated presynapses by SMLM, we characterized three distinct presynaptic actin nanostructures: a faint active zone mesh, linear actin rails found between the active zone and the reserve pools, as well as actin corrals that surround the presynaptic compartment (Bingham et al., 2023). However, presynapses formed on ~5 μm spherical beads result in heterogeneous orientation and sizes of induced presynapses. This limits optical accessibility and unambiguous localization of the active zone, impeding the analysis of actin structure roles in dynamic processes like presynaptic exo-endocytosis. An alternative is to induce the formation of presynapses directly on the glass, using postsynaptic adhesion proteins such as neuroligin applied on the whole coverslip (Funahashi et al., 2018) or on micropatterns of SynCAM1 separated by cytophobic regions (Czöndör et al., 2013).

In this study, we designed and optimized a presynapse-on-glass model to orient presynaptic formation toward patterned dots displaying the extracellular domain of neuroligin-1 (nlgn) in addition to a continuous layer of polylysine and laminin. This allowed unrestricted growth of neuronal processes as well as robust induction of presynaptic specialization near the patterned nlgn. We demonstrate how this model recapitulates actin distribution and the nanoscale organization we observed in bead-induced and endogenously tagged presynapses (Bingham et al., 2023). Furthermore, presynapses-on-glass allow to refine the 3D visualization of actin nano-architecture at presynapses, and to combine the visualization of synaptic vesicle exocytosis in living neurons with the nanoscopy of presynaptic components to link actin nano-architecture to the precise location of vesicle exocytosis.

Results

Micropatterned neuroligin induces axonal presynaptic marker clustering and actin aggregation

To improve optical accessibility and homogeneity of presynaptic formation, we adapted a validated method of presynaptic induction, where coating the coverslip with the extracellular domain of a postsynaptic cell-adhesion molecule, neuroligin-1 fused to the N-terminal of human immunoglobulin-Fc region (nlgn) induces the formation of excitatory presynapses onto the glass (Funahashi et al., 2018). We used micro-contact printing (Théry, 2010) of a PDMS stamp with 1.8 μm diameter pillars to generate an array of ~2 μm dots on the coverslip. To induce presynapses, the pillars were coated with nlgn together with fluorescent BSA for pattern visualization (nlgn dots). After printing, the coverslips were coated with a uniform layer of polylysine and laminin, so that axons and dendrites could grow freely and react when crossing printed dots. Rat hippocampal neurons were then cultured onto printed coverslips, and subsequently fixed and immunolabeled for presynaptic markers after 14-15 days in vitro (div) to examine presynaptic formation. Isolated axons containing at least three successive induced presynapses on neuroligin dots were classified as "patterned axons". The formation of patterned axons was assessed (as the percentage of total length of isolated axons over the field of view) for two presynaptic proteins: the active zone scaffolding protein bassoon (Dieck et al., 1998) and the synaptic vesicle membrane protein synaptophysin (Jahn et al., 1985; Wiedenmann and Franke, 1985). In addition, active vesicular cycling was evaluated using feeding with a synaptotagmin antibody against an extracellular epitope that accumulates in presynapses through constitutive vesicular cycling (Kraszewski et al., 1995). Representative fluorescence images demonstrate aggregation of bassoon, synaptophysin and synaptotagmin uptake into axonal clusters near nlgn dots (Fig. 1A-F). All three markers yielded comparable occurrences of patterned axons along nlgn dots patterns (23 ± 3% with bassoon, 16 ± 3% with synaptophysin, and 23.3 ± 2% with synaptotagmin, Fig. 1G), while neurons cultured on patterns of dots containing a human Fc without fused neuroligin or outside of the micropatterned areas resulted in almost no patterned axons (1.5 ± 0.4%, Fig. S1).

On zoomed views, the morphology of bassoon (Fig. 1B), synaptophysin (Fig. 1D), and synaptotagmin uptake (Fig. 1F) clusters are similar between nlgn dot-induced presynapses (noted S+) and natural synapses (noted NS) between axon and dendrites of the same culture. We quantified the signal intensity of each presynaptic marker at ngln dot-induced presynapses and compared it to natural synapses and neighboring axonal segments devoid of presynaptic clusters (noted S-, Fig. 1H). Induced presynapses (S+) had a lower intensity compared to NS for bassoon (0.89 ± 0.02) and synaptophysin (0.77 ± 0.02), and the synaptotagmin intensity was not significantly different (0.88 ± 0.04). Control axonal segment (S-) showed very low values of presynaptic component intensity (Fig. 1H). We then measured the actin content of induced presynapses: as expected, the high concentration of postsynaptic actin resulted in an actin intensity being almost 3 times lower in induced presynapses S+ normalized to natural synapses NS (0.38 ± 0.02), but two times higher than in non-synaptic axonal segments S- (0.19 ± 0.01, Fig. 1H), confirming the relative concentration of axonal actin at presynapses (Morales et al., 2000). Altogether, these data show that we can reliably induce the formation of presynapses on micropatterned dots of neuroligin in a minimally perturbed neuronal culture, validating our presynapse-on-glass model.

Figure 1: Micropatterned neuroligin induces axonal presynaptic marker clustering and actin aggregation. **See next page >>**
A. Widefield fluorescence image of cultured neurons on top of the nlgn micropattern (gray) fixed at 15 div, labeled for adducin (purple), bassoon (cyan) and map2 (orange). **B.** Zooms corresponding to the areas highlighted in A. Top row: natural synapses (NS) at axo-dendritic contacts; middle row: induced presynapses at isolated axon-micropattern dots (S+); bottom row: isolated axon with no induced presynapse (S-). **C.** Widefield fluorescence image of cultured neurons on top of the nlgn micropattern (gray) fixed at 15 div, labeled for β2-spectrin (purple), synaptophysin (cyan), and map2 (orange). **D.** Zooms corresponding to the NS, S+ and S- highlighted in C. **E.** Widefield fluorescence image of cultured neurons on top of the nlgn micropattern (gray) fixed at div 15, labeled for actin (purple), feeding with anti-synaptotagmin antibody (syt) during constitutive vesicular cycling (cyan) and map2 (orange).

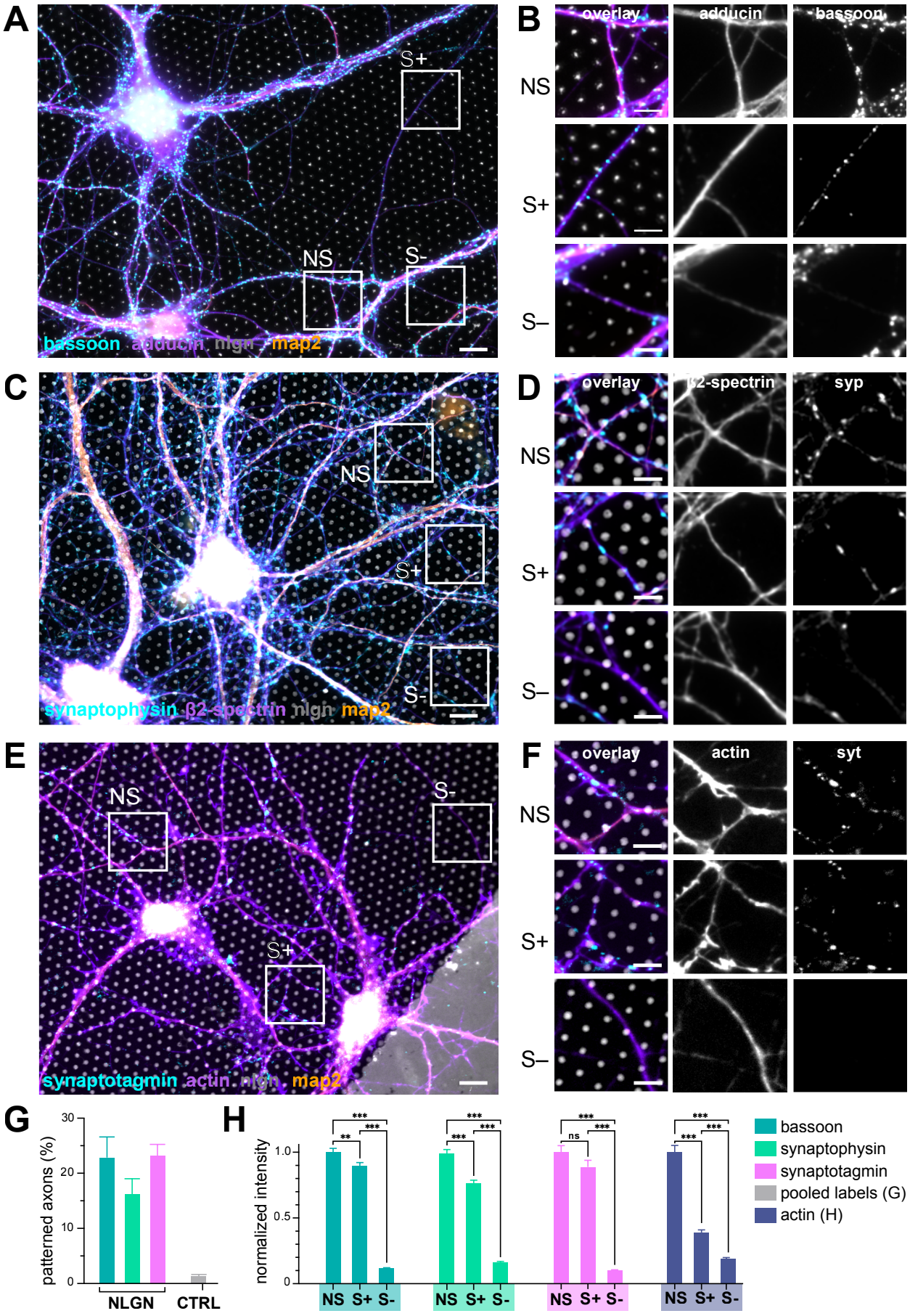

<< See Figure 1 captions on previous page.

F. Zooms corresponding to the NS, S+, and S- highlighted in E. Scale bars for A, C, E: 20 µm. Scale bars for B, D, F: 10 µm. **G.** Proportion of the length of isolated axons showing presynaptic specializations following the nlgn micropattern (patterned axon) over the total length of isolated axons selected within the experimental conditions (bassoon, synaptophysin, synaptotagmin) compared to controls (pooled labels, see Fig. S1). **H.** Mean intensity for bassoon (dark cyan, N=2; n>100), synaptophysin (light green, N=4; n>200), synaptotagmin (pink; N=5, n>200) and actin (blue) at natural synapses (NS), induced presynapses (S+), and isolated axon devoid of presynapse (S-), normalized to natural synapses.

Actin enrichment correlates with increased presynaptic component concentration at nlgn dot-induced presynapses

Previous work by our group on bead-induced and natural axon-dendrite presynapses revealed that two categories exist: presynapses showing actin enrichment compared to the surrounding axon (A+) and presynapses lacking actin enrichment (A-). Furthermore, actin enrichment was associated with a higher concentration of presynaptic components and higher cycling activity (Bingham et al., 2023). Consistent with these findings, on micropatterned nlgn dots, induced presynapses could be categorized into actin-enriched and non-enriched from diffraction-limited images (Fig. 2A-B): A+ induced presynapses representing 63% of nlgn dot-induced presynapses, and A- representing 37% (Fig. 2C). We then quantified the enrichment of actin and presynaptic components at nlgn dot-induced presynapses in each category, measuring the fluorescence intensity in A+ and A- induced presynapses as well as the adjacent axonal shaft as a control (S-). Normalized to its intensity in A+ induced presynapses, actin intensity was reduced in A- presynapses and S- shafts (0.38 ± 0.02 and 0.38 ± 0.1, respectively, Fig. 2D). Moreover, A- presynapses demonstrated a significantly reduced concentration of bassoon and synaptotagmin (0.73 ± 0.05 and 0.66 ± 0.05, respectively). Overall, nlgn dot-induced presynapses recapitulate the presence of a majority of actin-enriched presynapses that contain more presynaptic components than their non-enriched counterpart, further validating our presynapse-on-glass model.

STORM of nlgn dot-induced presynapses reveal discrete actin nanostructures

As noted above, nlgn dot-induced presynapses are visibly distinguishable as A+ and A- at diffraction-limited resolution, particularly when compared side-by-side (Fig. 3A). To further interrogate actin structural organization and assess the presence of the distinct presynaptic actin nanostructures we previously identified in bead-induced presynapses (Bingham et al., 2023), we turned to STORM of actin at nlgn dot-induced presynapses. First, STORM reconstruction confirmed that the periodic actin rings are disrupted at nlgn dot-induced presynapses, as shown previously for the periodic spectrin scaffold at presynapses (He et al., 2016; Sidenstein et al., 2016, Fig. 3B). Furthermore, we were able to identify the three distinct types of actin nanostructures within A+ and A- nlgn dot-induced presynapses (Bingham et al., 2023). Firstly, a large branched and dense structure surrounding the periphery of the presynapse is identified as the actin corral (blue). Secondly, the small linear structures within the bouton often connecting wider and branched structures of the presynapse are classified as actin rails (green). Thirdly, the faint cluster of actin nanostructures colocalizing with the active zone bassoon clusters, is recognized as the actin mesh (Fig. 3B, red). Quantitative analysis of these discrete actin nanostructures showed that all A+ and A- presynapses exhibited a distinguishable peripheral corral. The presence of the fainter rails was detectable in 71% of A+ and 69% of A- presynapses, while the active zone mesh was detected in 83% of A+ and 81% of A- presynapses (Fig. S2). As these numbers were similar for A+ and A- presynapses, we

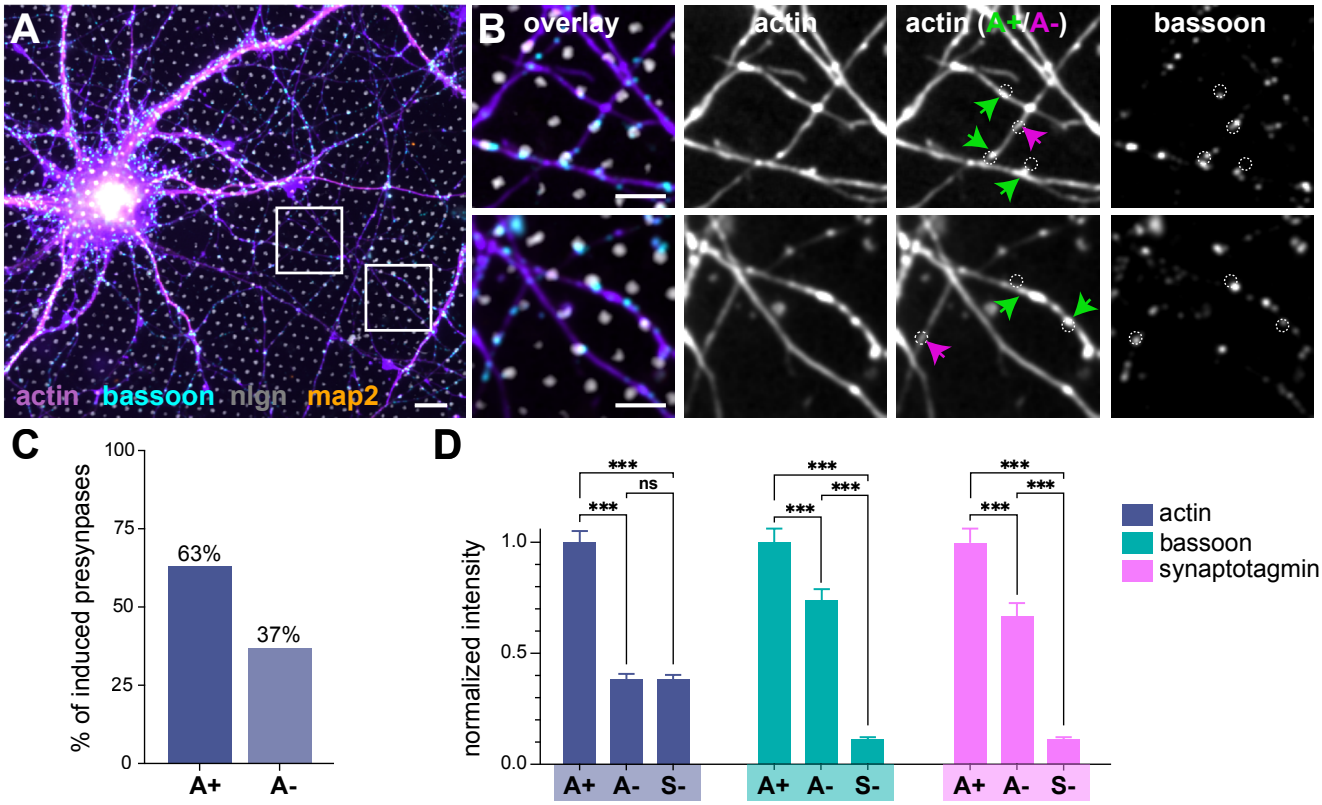

Figure 2: Actin enrichment correlates with increased presynaptic component concentration at nlgn dot-induced presynapses.
A. Widefield fluorescence image of cultured neurons on top of the nlgn micropattern (gray) fixed at 15 div, labeled for actin (purple), bassoon (cyan), nlgn (gray) and map2 (orange). Scale bars, 20 µm. **B.** Zooms corresponding to the areas highlighted in A displaying (from left to right): overlayed channels; actin; nlgn dots (dashed circles) near actin-enriched induced presynapses (A+, green arrows) and non-enriched presynapses (A-, pink arrows); presynaptic marker bassoon and nlgn dots (dashed circles). Scale bars, 10 µm. **C.** Percentage of actin-enriched and non-enriched induced presynapses along axons on nlgn dots. **D.** Mean intensity of actin (blue; N=3, n>300), bassoon (dark cyan; N=2, n>150), and synaptotagmin (pink, N=3, N>130) at actin-enriched presynapses (A+), non-enriched induced presynapses (A-), isolated axons with no induced presynapses (S-), normalized to actin-enriched presynapses.

refined our analysis by measuring the area of each nanostructure on STORM images: only the area of corrals showed a significant difference between A+ and A- induced presynapses, with A+ presynapses being larger (0.23 ± 0.01 µm² for A+ vs 0.17 ± 0.03 µm² for A-, Fig. 3C). The presence of all three nanostructures in nlgn dot-induced presynapses, and the main difference between A+ and A- induced presynapses being the relative size of the actin corral surrounding them are perfectly in line with our previous results on bead-induced presynapses (Bingham et al., 2023).

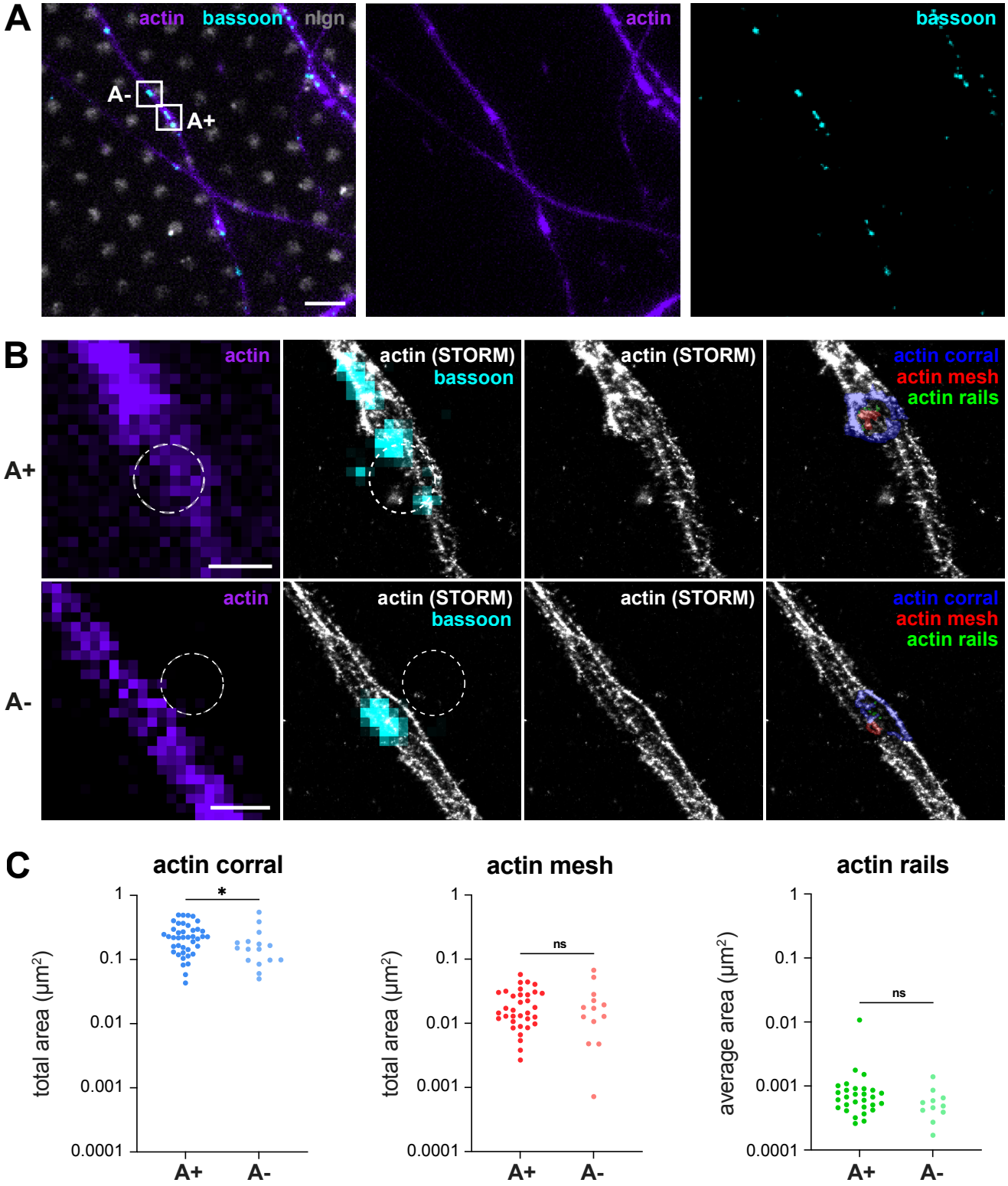

Figure 3: STORM of nlgn dot-induced presynapses reveal discrete actin nanostructures.
A. Widefield fluorescence image of cultured neurons on top of the nlgn micropattern (gray) fixed at 15 div, labeled for actin (purple) and bassoon (cyan). Scale bar, 4 µm. **B.** Zooms corresponding to two distinct induced presynapses highlighted in A. Left column shows the epifluorescence image of actin (purple) and the position of nlgn dots (white dashed circle). Second column displays the STORM image of actin (gray), epifluorescence bassoon (cyan), and the position of nlgn dots (white dashed circle). Third column shows the STORM image of actin alone (gray). Fourth column shows colorized presynaptic actin nanostructures: corrals (blue), mesh (red) and rails (green). Scale bar, 1 µm. **C.** Areas of presynaptic actin nanostructures as measured on STORM images, comparing A+ and A- induced presynapses. Each point represents an individual measurement, N = 3, n=41 for A+ and 16 for A-.

Multicolor localization microscopy of nlgn dot-induced presynapses reveals the arrangement of actin nanostructures relative to the active zone

At this point we confirmed that our presynapse-on-glass model recapitulates the results obtained on the bead-induced presynapse model both in terms of actin content and nanostructures. To further show the usefulness of our nlgn dot-induced presynapse, we leveraged the reproducible and controlled orientation of the induced presynapses to interrogate the relationship between actin nanostructures and presynaptic components at the nanoscale. We performed 2-color localization microscopy at nlgn dot-induced presynapses by sequentially combining STORM of actin and DNA-PAINT of the active zone scaffold protein bassoon, using somatodendritic map2 and axonal ß2-spectrin co-staining to target presynapses along isolated axons near nlgn dots (Fig. 4A). We could thus relate the position of the identified actin nanostructures to the bassoon nanoclusters by examining XY and transverse XZ reconstructions (Fig. 4B) as well as ChimeraX renderings (Fig. 4C). Bassoon labeling was made of distinct nanoclusters, as previously described (Glebov et al., 2017). These clusters were located at the bottom of the axon, consistent with the formation of the presynapse toward the glass. The actin corral outlines the periphery of the presynapse, in continuity with rails branching inwardly toward the central part of the presynapse. The structure identified as the mesh based on diffraction-limited views of presynaptic markers (see Fig. 3) could often be seen above the bassoon clusters rather than below them, interdigitating between the clusters to separate them.

Correlative imaging of the relationship between exocytic sites and presynaptic nanostructures

To further demonstrate the usefulness of our presynapse-on-glass approach, we by took advantage of its controlled *en-face* orientation to set up a live-cell / STORM correlative workflow and resolve the nanoscale environment of synaptic vesicle release events. Neurons were cultured on nlgn-patterned coverslips and transfected with VAMP2-pHluorin, a fusion of the VAMP2/synaptobrevin membrane protein (Baumert et al., 1989) with a pH-sensitive GFP that fluoresces upon exocytosis of the tagged synaptic vesicles (Miesenböck et al., 1998; Burrone et al., 2006), followed by live-cell total internal reflection fluorescence (TIRF) imaging to image spontaneous synaptic vesicle exocytosis at nlgn dots (Fig. 5, first column). The neurons were then fixed and immunolabeled for epifluorescence and single-color STORM imaging of ei-

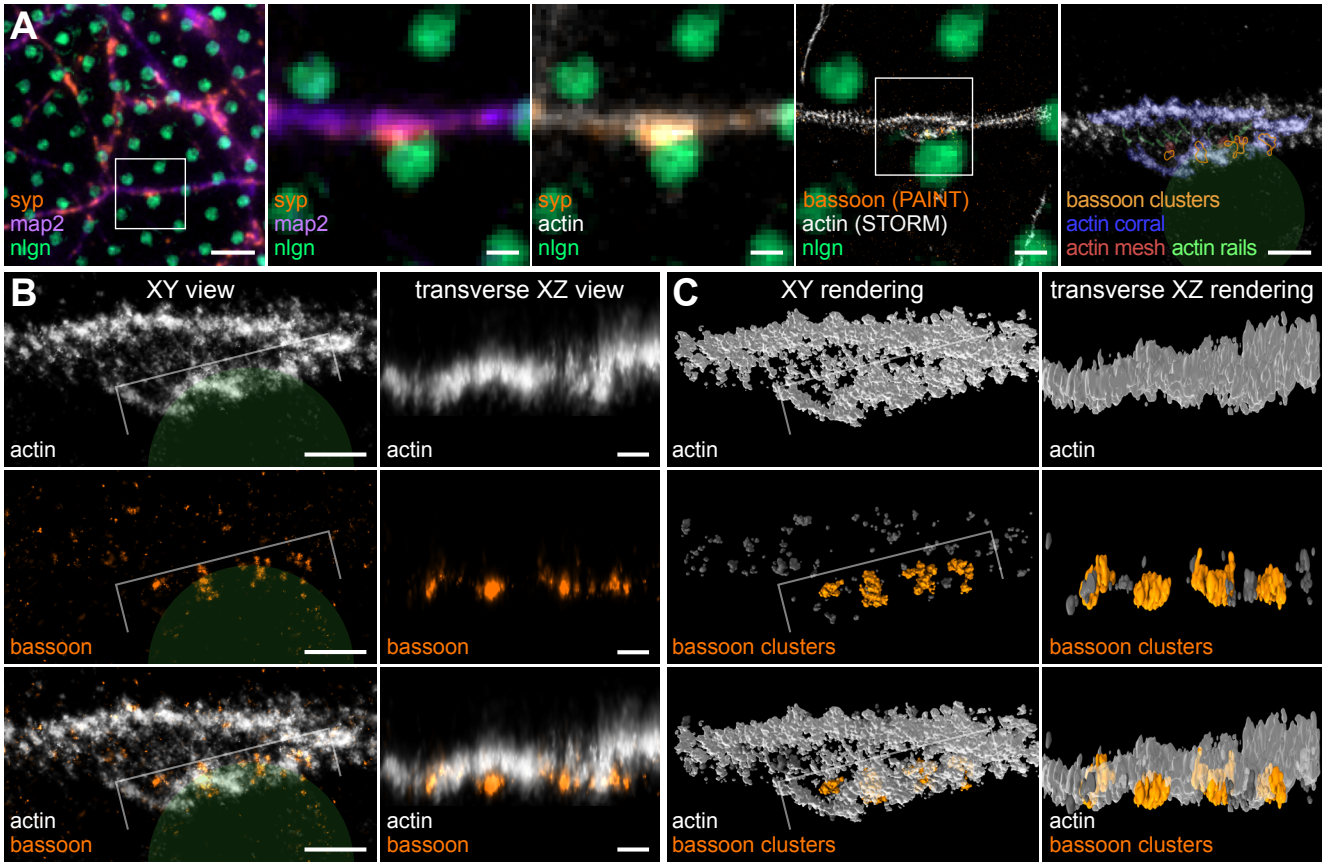

Figure 4: Multicolor localization microscopy of nlgn dot-induced presynapses reveals the arrangement of actin nanostructures relative to the active zone.
A. First to third images, widefield fluorescence image of cultured neurons on top of the nlgn micropattern (green) fixed at 15 div, labeled for map2 (purple), synaptophysin (orange) and actin (gray). Scale bar, 5 µm (first image), 1 µm (second and third images, zooms of the area highlighted on the first image). Fourth image shows the nlgn pattern (green) superimposed with the PAINT image of the bassoon staining (orange) and the STORM image of the actin staining (gray). Scale bar, 1 µm. Fifth image is a zoom of the area highlighted on the fourth image showing the micropattern (green shape), bassoon clusters from the PAINT image (orange contours), and colorized presynaptic actin nanostructures from the STORM image (gray, corral in blue, mesh in red, rails in green). Scale bar, 500 nm. **B.** Zooms of the presynapse shown in A showing the STORM image of actin (gray) and PAINT image of bassoon (orange) in XY (left column) and transverse (XZ with a vertical Z axis, right column) views. The transverse view is taken along the bracket shown on the XY view. Scale bars, 500 nm (XY views), 200 nm (transverse XZ views). **C.** ChimeraX renderings corresponding to the views shown in B with XY (left column) and transverse (right column) views of actin nanostructures (gray) and bassoon nanoclusters (orange). The transverse XZ views show how actin is present above and in-between bassoon nanoclusters.

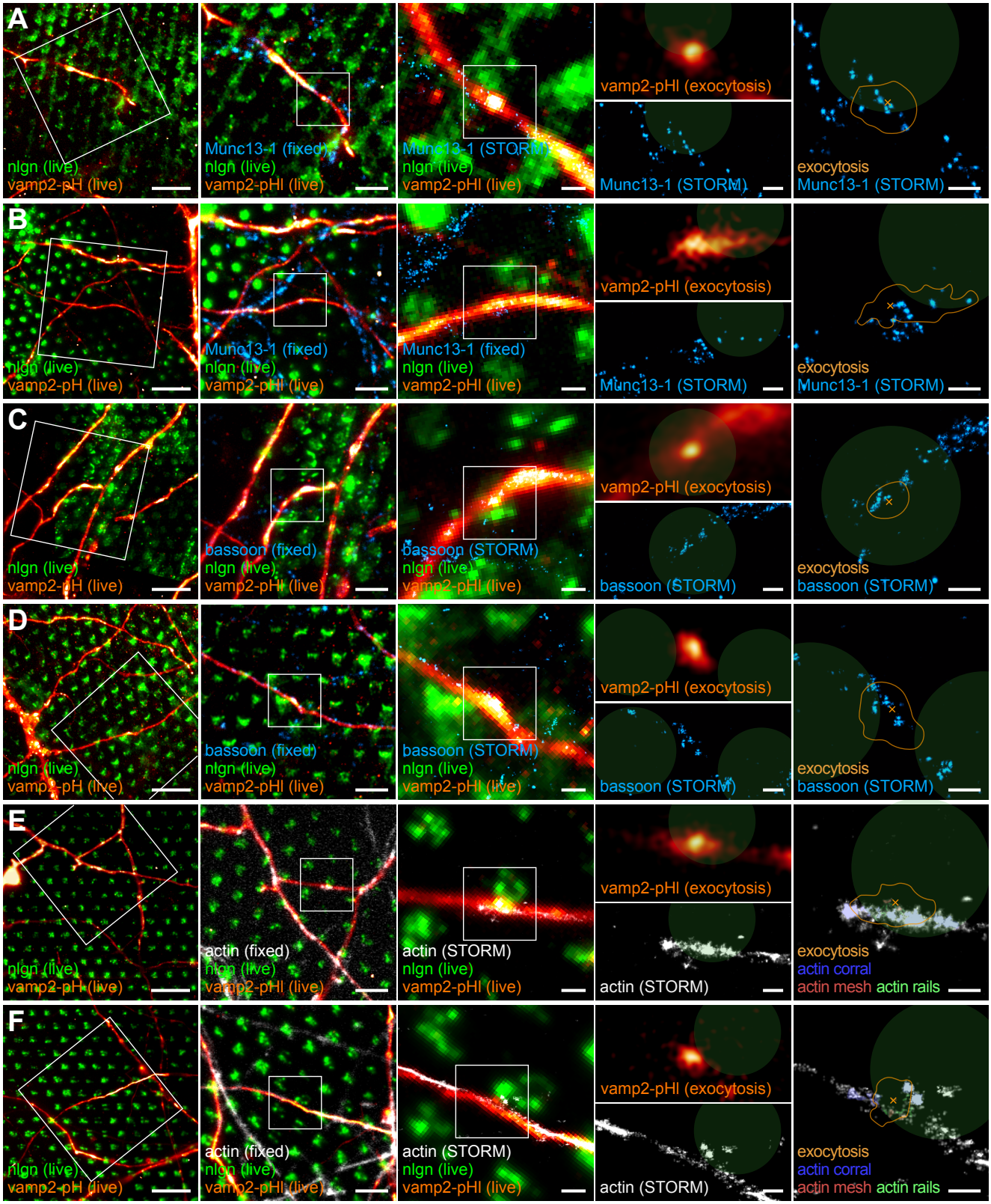

Figure 5: Correlative imaging of the relationship between exocytic sites and presynaptic nanostructures
A-B. First image, live-cell imaging of the axon of a cultured neuron at 15 div on top of the nlgn pattern (green), transfected with VAMP2-pHluorin (VAMP2-pHl, orange). Scale bar, 10 µm. Second and third images, progressive zooms on an induced presynapse labeled for Munc13-1 (blue, epifluorescence on the second image, STORM on the third image) after fixation and aligned with the live-cell image. Scale bars, 5 µm (second image), 1 µm (third image). Right panel shows the first frame of the exocytosis event from the VAMP2-pHluorin movie (orange, top left), the corresponding STORM image of the Munc13-1 labeling (blue, bottom left) and the overlay of the exocytosis event (orange contour) with its fitted center (orange cross) with the Munc13-1 STORM image (blue) and nlgn micropattern (green shapes, right). Scale bars, 500 nm. **C-D.** First image, live-cell imaging of the axon of a cultured neuron at 15 div on top of the nlgn pattern (green), transfected with VAMP2-pHluorin (orange). Scale bar, 10 µm. Second and third images, progressive zooms on an induced presynapse labeled for bassoon (blue, epifluorescence on the second image, STORM on the third image) after fixation and aligned with the live-cell image. Scale bars, 5 µm (second image), 1 µm (third image). Right panel shows the first frame of the exocytosis event from the VAMP2-pHluorin movie (orange, top left), the corresponding STORM image of the bassoon labeling (blue, bottom left) and the overlay of the exocytosis event (orange contour) with its fitted center (orange cross) with the bassoon STORM image (blue) and nlgn micropattern (green shapes, right). Scale bars, 500 nm.
See captions on next page >>

<< See Figure 5 on previous page
E-F. First image, live-cell imaging of the axon of a cultured neuron at 15 div on top of the nlgn pattern (green), transfected with VAMP2-pHluorin (orange). Scale bar, 10 µm. Second and third images, progressive zooms on an induced presynapse labeled for actin (gray, epifluorescence on the second image, STORM on the third image) after fixation and aligned with the live-cell image. Scale bars, 5 µm (second image), 1 µm (third image). Right panel shows the first frame of the exocytosis event from the VAMP2-pHluorin movie (orange, top left), the corresponding STORM image of the actin labeling (gray, bottom left) and the overlay of the exocytosis event (orange contour) with its fitted center (orange cross) with the actin STORM image (gray) with colored nanostructures (blue, corral; red, mesh; green, rails) and nlgn micropattern (green shapes, right). Scale bars, 500 nm.

ther active zone proteins or presynaptic actin, and the precise location of the exocytic event (from fitting the appearing spot on time-lapse images of VAMP2-pHluorin) was correlated to the nanoscale arrangement from the aligned STORM image (Fig. 5).

As a proof of concept, we first contextualized the exocytic event by localizing presynaptic components with STORM images of Munc13-1, a component of the presynaptic release machinery (Augustin et al., 1999), and the active zone scaffold protein bassoon (Südhof, 2012). Sub-resolution fitting of VAMP2-pHluorin flashes at nlgn-induced presynapses resulted in exocytic localizations in close proximity (<50 nm) to small Munc13-1 clusters (Fig. 5A-B), whereas exocytosis was seen to occur further away from the larger, more uniform bassoon clusters (Fig. 5C-D). We then performed a similar experiment, this time combining live-cell imaging of VAMP2-pHluorin with STORM of actin, counterstaining for bassoon to confirm presynapse induction at individual nlgn dots (Fig. 5E-F). Comparing the localization of single spontaneous exocytic events to labeled actin nanostructures revealed that at the nanoscale, exocytosis occurs in presynaptic regions devoid of actin, presumably emerging from areas adjacent to actin mesh (Fig. E-F). These qualitative results together with the 2-color nanoscale imaging of bassoon and actin (Fig. 4) support an emerging model where actin is interspaced with bassoon clusters to structure the active zone in different nanoscale areas, with further segregation within these areas between bassoon scaffold clusters and Munc13-1/RIM-enriched exocytic zones (Glebov et al., 2017).

Discussion

In this study, we designed and optimized a presynapse-on-glass model to more precisely investigate actin nano-architecture in induced presynapses. By printing the extracellular domain of neuroligin-1 before coating the coverslips with polylysine and laminin, we developed a micropatterned substrate that promotes natural development of neurons over the whole coverslip. This contrasts with previous methods that coaxed presynapse induction by overexpressing presynaptic neurexin in addition to coating the coverslip with neuroligin (Funahashi et al., 2018; Tanaka et al., 2023) or restrict axon attachment to small spots separated by cell-repellent substrates (Czöndör et al., 2013). Compared to our previous model of presynapses induced by ~5 µm beads (Bingham et al., 2023), our new model drives presynaptic orientation toward the glass, improving visual accessibility for nanostructure visualization and unbiased exocytosis analysis.

We demonstrate that nlgn dots can induce presynaptic specializations along isolated axons, with concentration of presynaptic components (bassoon, synaptophysin) and active vesicular cycling demonstrated by synaptotagmin antibody uptake. Induced presynapses show a similar morphology, fluorescence intensity of presynaptic components, and vesicular cycling activity compared to natural synapses found at axon-dendrite contacts. The quantification of the fraction of axons exhibiting induced presynapses over nlgn dots might appear low (~20%), but it is a consequence of our stringent criteria for identifying them, excluding segments with less than three successive induced presynapses to avoid over-estimating induction by including spurious clusters. It should be noted that our micropatterning strategy differs from previously published ones, where the presynapse-inducing patterns (1.5 µm-diameter dots) were complementary with a cytophobic substrate (polyethyleneglycol, Czöndör et al., 2013). In our model, an adhesion-promoting coating of polylysine and laminin is present uniformly, superimposed with the nlgn dots to allow natural growth of neurites over the coverslip with induction of presynapses when axons cross the nlgn dots.

Besides their similarity to natural synapses, the absence of the more intense postsynaptic actin at induced presynapses allowed us to distinguish two populations of presynapses: 63% that are actin-enriched (A+) and 37% that are not enriched (A-), a proportion close to the results obtained on bead-induced presynapses (67% and 33%) and actin-tagged natural presynapses (75% and 25%, Bingham et al., 2023). Furthermore, actin-enriched (A+) induced presynapses similarly accumulated ~50% more presynaptic components compared to their A- counterparts, validating our nlgn dots-induced presynapse model.

In addition to closely recapitulating the properties of bead-induced presynapses, the presynapse-on-glass model allowed nanoscale visualization with improved optical accessibility due to the formation of an active zone with a controlled orientation and proximity to the substrate. We could thus refine the characterization of the presynaptic actin nanostructures we previously identified (Bingham et al., 2023). Actin corrals are consistently found distributed at the periphery of presynapses, with the corrals of A+ presynapses being significantly larger than those of A- presynapses. These variations in shape and size and the difference in presynaptic content between A+ and A- presynapses suggests that corrals are the primary remodeled actin structure during presynaptic plasticity (O'Neil et al., 2021). Interestingly, we observed a greater percentage of both actin rails and actin mesh in nlgn dot-induced presynapses compared to the bead-induced presynapses (Bingham et al., 2023). This indicates that nlgn dots-induced presynapses indeed exhibit enhanced visibility and allow to more effectively distinguish between the corrals, rails and mesh nanostructures.

One of the key advantages of the presynapse-on-glass model is the controlled orientation of the induced presynapses that form *en face* to the glass substrate. This allows unambiguous interpretation of the 3D nanoscale architecture, without the need for a postsynaptic marker that is often used to determine synapse orientation (Dani et al., 2010; Tang et al., 2016). We

could verify the orientation of the induced presynapses by imaging the nanoscale arrangement of bassoon together with presynaptic actin architecture: bassoon nanoclusters were consistently found at the bottom of the axon, even when the presynapse formed on one side of the shaft, and this allowed easier identification of actin corrals, rails and mesh within presynapses. Oriented 3D, multicolor SMLM images allowed us to refine our previous results by demonstrating that the actin mesh, previously coated at the active zone (Bingham et al., 2023) is found above and between bassoon clusters rather than below them. This suggests that rather than a submembrane assembly directly shaping the vesicle exocytosis area, the mesh could have a role in organizing nanoclusters within the active zone, in line with the declustering of bassoon previously observed upon latrunculin A treatment (Glebov et al., 2017).

Being able to visualize synaptic vesicle exocytosis in living cells, including rare spontaneous events, and to correlate them with the nano-architecture of presynaptic component is another application we demonstrate of our presynapse-on-glass model. We visualized individual exocytic events that likely correspond to single-vesicle release (Funahashi et al., 2018) and fit their sub-diffraction localization. By correlating with fixed-cell STORM images of components within the same presynapse, we confirmed that exocytosis occurs next to or at Munc13-1 clusters (Sakamoto et al., 2018), while scaffold proteins such as bassoon are present further away from the exocytic location, in line with their proposed complementary segregation in distinct nanoclusters within the active zone (Tang et al., 2016; Glebov et al., 2017). Furthermore, we used this correlative approach to further understand the role of presynaptic actin. We consistently visualized exocytic events away from actin nanostructures, including the actin mesh, confirming that actin seem to be mostly absent from the exocytic points and further suggesting that active zone actin has a role in defining hotspots of vesicular release where it is absent (Morales et al., 2000). Our results on the nanoscale relationship between actin structures and presynaptic components and vesicular release are primarily qualitative at this point, due to the low throughput of our current correlative approach, and will undoubtedly guide future work by helping to refine functional hypotheses about the roles of actin in presynapses.

Acknowledgments

We would like to acknowledge funding by the Fédération pour la Recherche Médicale (FRM Equipe grant EQU202103012966) and Agence Nationale pour la Recherche (ANR grant ANR-20-CE13-0024) to C.L. We would like to thank the Neuro-Cellular Imaging Service and Nikon Center for Neuro-NanoImaging at INP, with funding from CPER-FEDER (PlateForme NeuroTimone PA0014842), the Institut Marseille Imaging and NeuroMarseille for complementary equipment funding from Excellence Initiative of Aix-Marseille University – A*MIDEX, a French "Investissements d'Avenir" program (AMX-19-IET-002). We would like to thank Maxime Cazorla (Institut des Neurosciences de la Timone, INT, Marseille, France) for helping with the use of the plasma cleaner, as well as Stephanie Gupton (UNC, Chapell Hill, USA) and Tomoo Hirano (Department of Biophysics, Kyoto University, Japan) for the gift of plasmids.

Author Contributions

Methodology: S.T., L.M., T.W., B.V., M.T., M.-J.P., C.L.; Formal analysis: S.T., L.M., M.-J.P., C.L.; Investigation: S.T., L.M.; Resources: B.V., M.T.; Writing-Original Draft: S.T., L.M., M.-J.P., C.L.; Writing-Review and Editing: S.T., L.M., T.W., M.T., M.-J.P., C.L.; Visualization: S.T., L.M., C.L.; Conceptualization: M.-J.P, C.L.; Supervision, Project Administration: M.-J.P., C.L.; Funding acquisition: C.L.

Methods

Plasmids

The expression vector for nlgn (gift from T. Hirano, Funahashi et al., 2018) consists of the cDNA encoding the extracellular region (amino acids 1–675) of neuroligin 1 (–A+B) fused to the N-terminal of human immunoglobulin-Fc region in the pCAGplayII expression vector (Kawaguchi and Hirano, 2006). VAMP2-pHluorin (gift from S Gupton, Urbina et al., 2018) consists in the human VAMP2 fused to super-ecliptic pHluorin (Miesenböck et al., 1998).

Fc-neuroligin (nlgn) production

Nlgn production followed published procedures (Tanaka et al., 2014). HEK 293 T cells cultured at 70% confluence in 100 mm diameter dishes were transfected with a mixture of Lipofectamine 3000 (Thermo Fisher Scientific; 16 µL/dish) and nlgn plasmid (8 µg/dish) for 4 h in DMEM. Protein expression was carried out for 2 days in DMEM, 10% ultra-low IgG fetal bovine serum (Thermo Fisher Scientific), 100 UI/mL penicillin/streptomycin. The culture medium was then recovered and centrifuged for 10 min at 3000 g to remove cell debris. 200 µL of protein-A Sepharose beads (Sigma) was added to the 50 mL of supernatant in the presence of anti-protease (Sigma) and incubated overnight at 4°C with stirring. After centrifugation for 5 min at 1200 rpm, the beads were washed three times with phosphate buffer saline (PBS, pH 7.4) and nlgn was eluted with 600 µL of 0.1M glycine buffer, pH 2.6 and immediately buffered to pH 7 with 1M Tris, pH 9. Purified nlgn concentration determined by dot blot was consistently around 250 µg/mL.

Micropatterned substrate onto glass coverslips

18-mm diameter round, #1.5H thickness coverslips were rapidly washed in acetone and ethanol, then affixed with dots made from two-components orthodontics paste (Rotec) as spacers. They were then oxidized in a plasma cleaner (Fento, Diener Electronic). Micro-contact printing was performed using PDMS stamps with 1.8 µm-diameter pillar arrays with 4 µm center-to-center distance (gift of Jianping Fu, University of Michigan, USA, Weng and Fu, 2011) according to a previously published protocol (Théry and Piel, 2009). Stamps were coated and incubated for 40 min at 37°C with a mixture of BSA-Alexa Fluor 488 (80 µg/mL; Thermo Fisher Scientific) and nlgn (25 µg/mL), or with BSA-AF488 (80 µg/mL) mixed with the Fc fragment of human IgG (25 µg/mL; Jackson ImmunoResearch) as a control. PDMS stamps were then inverted onto ionized coverslips and incubated at 37°C for 20 min, then treated overnight with a mixture of laminin (Thermo Fisher Scientific; 10 µg/mL) and poly-L-lysine (Sigma; 38 µg/mL), prior to neuron seeding.

Animals and cell culture

The use of Wistar rats followed the guidelines established by the European Animal Care and Use Committee (86/609/CEE) and was approved by the local ethics committee (agreement G13055). Rat hippocampal neurons were cultured following the Banker method, above a feeder glia layer (Kaech and Banker, 2006). Hippocampi from E18 rat pups were dissected and homogenized by trypsin treatment followed by mechanical trituration and seeded on the patterned coverslips at a density of 4,000-6,000 cells/cm^2 for 3 h in serum-containing plating medium (MEM with 10% FBS, 0.6% glucose, 0.08 mg/mL sodium pyruvate, and 100 UI/mL penicillin/streptomycin). Coverslips were then transferred, cells down, to petri dishes containing confluent glia cultures conditioned in neurobasal medium (NB; Thermo Fisher Scientific) supplemented with 2% B27 (Thermo Fisher Scientific), 100 UI/mL penicillin/streptomycin, and 2.5 µg/mL amphotericin, and cultured in these dishes at 37°C, 5% CO_2. Neurons were fixed at 13-16 days in vitro (div).

Anti-synaptotagmin vesicular cycling assays

Vesicular cycling assays were performed using an antibody directed to an extracellular epitope of synaptotagmin 1 (syt, clone 604.2; Synaptic Systems, Kraszewski et al., 1995) that was fed to neurons before fixation. Neurons were incubated for 1 h at 37°C, 5% CO_2 with the syt antibody at 1.6 µg/µL in HBS medium (136 mM NaCl, 10 mM HEPES, 10 mM glucose, 2 mM $CaCl_2$, 1.3 mM $MgCl_2$). Cells were then washed three times with PBS before fixation.

Antibodies

Primary antibodies used are chicken anti-map2 (1:1,000, ab5392, RRID:AB_2138153; Abcam), mouse anti-ß2-spectrin (1:100, clone 42/aa 2101-2189, #612563, RRID:AB_399854; BD Bioscience), guinea pig anti-synaptophysin (1:400, 101 004, RRID:AB_1210382; Synaptic Systems), mouse anti-synaptotagmin1 (1:600, clone 604.2/aa 1-12, 105 311, RRID:AB_993036; Synaptic Systems), rabbit anti-adducin alpha (1:100, ab40760, RRID:AB_722627; Abcam), mouse anti-bassoon (1:200, clone SAP7F407, ab82958, RRID:AB_1860018; Abcam), rabbit anti-GFP (1:750, ab290, RRID:AB_303395; Abcam), mouse anti-GFP (1:750, clone 9F9.F9, ab1218, RRID:AB_298911; Abcam), rabbit anti-munc13-1 (1:500, 126 103, RRID:AB_887733; Synaptic Systems). Secondary antibodies used were conjugated to Alexa Fluor 488, 555, or 647 (Thermo Fisher Scientific), Atto 643 (Massive Photonics), or DyLight 405 (Rockland) and diluted 1:200-1:400. Actin was labeled with phalloidin Alexa Fluor 647 Plus (1:400, Thermo Fisher Scientific).

Fluorescence immunocytochemistry

Immunocytochemistry of neuronal cultures for widefield microscopy, SMLM and live-cell imaging was performed as in published protocols (Jimenez et al., 2020) with minor modifications. Cells were fixed using 4% PFA in PEM buffer (80 mM PIPES pH 6.8, 5 mM EGTA, 2 mM $MgCl_2$) for 10 min at room temperature (RT). After rinses in 0.1 M phosphate buffer (PB), neurons were blocked for 1-2h at RT in immunocytochemistry buffer (ICC: 0.22% gelatin, 0.1% Triton X-100 in PB), and incubated with primary antibodies diluted in ICC for either 1h30 at RT or overnight at 4°C. After rinses in ICC, neurons were incubated with secondary antibodies diluted in ICC for 1h at RT and rinsed. Actin staining was then performed by incubating in fluorescent phalloidin at 0.5 µM for either 1h at RT or overnight at 4°C. Stained coverslips were kept in PB + 0.02% NaN_3 at 4°C until imaging. For widefield microscopy, coverslips were mounted in ProLong Glass (Thermo Fisher Scientific).

Epifluorescence microscopy

Diffraction-limited epifluorescence images were obtained using an Axio-Observer upright microscope (Zeiss) equipped with a 40X NA 1.4 or 63X NA 1.4 objective and an Orca-Flash 4.0 camera (Hamamatsu). Appropriate hard-coated filters and dichroic mirrors were used for each fluorophore. A thin Z-stack of 3-10 slices spaced by 0.2 µm was acquired to include the signal from all neuronal processes within the whole field of view. For illustration images, image editing was performed using Fiji (Schindelin et al., 2012) with linear contrast adjustment to highlight the faint actin labeling along axons.

Epifluorescence image analysis

Percentage of patterned axon quantifications were performed by defining linear regions of interest (ROIs) and measuring their length using the Fiji software. Patterned axon ROIs were identified along isolated axons (devoid of dendritic contact) as presenting at least three successive presynaptic aggregates next to nlgn dots; other isolated axon segments were defined as non-patterned. The percentage of patterned axons was calculated over the total length (patterned + non-patterned ROIs).

Intensity quantifications were performed on maximum projections of the raw epifluorescence data with no further adjustment. Short linear ROIs were defined onto the presynaptic cluster aggregates at nlgn dot-induced presynapses (S+), at natural (axon-dendrite) synapses (NS), and at the axonal shaft flanking the presynapses as control (S-). Those tracings were translated into Fiji ROIs and refined to the presynaptic cluster (S+ and NS) or axon shaft (S-) using the ProFitFeat script (available at https://github.com/cleterrier/Measure_ROIs/blob/master/Pro_Feat_Fit.js), limiting it to the segment with an intensity above 40% of the maximum intensity along the linear ROI. The background-corrected mean intensity along these ROIs was then measured for each labeled channel. Induced presynapses were visually categorized as "actin enriched" (A+) or "non-enriched" (A–) depending on the relative intensity of actin compared to the neighboring axon shaft (Bingham et al., 2023).

SMLM: STORM and PAINT

Both STORM and DNA-PAINT acquisitions were performed on an N-STORM microscope (Nikon Instruments). The N-STORM system uses an Agilent MLC-400B laser launch with 405 nm (50 mW maximum fiber output power), 488 nm (80 mW), 561 mW (80 mW), and 647 nm (125 mW) solid-state lasers, a 100X NA 1.49 objective, and an Ixon DU-897 camera (Andor). After locating a patterned axon using low-intensity epifluorescence illumination, a STORM or DNA-PAINT acquisition was performed using laser illumination in HiLo (grazing angle) configuration. An astigmatic lens was added to the light path to achieve 3D imaging. For STORM, stained coverslips were mounted in a silicone chamber filled with STORM buffer (Smart Buffer Kit, Abbelight), and 30,000-60,000 images (256 × 256 pixels, 15 ms exposure time) were acquired at 100% 647-nm laser power. Reactivation of fluorophores was performed during acquisition by increasing illumination with the 405-nm laser. For DNA-PAINT, stained coverslips were mounted in a Ludin chamber filled with an imaging buffer (Massive Photonics). Imaging strands conjugated to Atto643 (Massive Photonics)

were added from a starting concentration of 0.1 nM each, then adjusted to optimize blinking density. 30,000-45,000 images (256x256, 40 ms exposure time) were acquired at 50-60% laser power for 647 nm laser excitation.

To obtain optimal STORM images of presynaptic actin, we carefully selected induced presynapses with unambiguous proximity with a nlgn dot along an isolated, continuous axon. We avoided situations where the nlgn dot was partially printed or erased, as well as regions of axons crossing or bundling.

For STORM and DNA-PAINT images, acquired stacks were processed using DECODE (Speiser et al., 2021). Briefly, PSFs were modeled using spline fitting in SMAP (Li et al., 2018b) and used to simulate sequences of blinking events using characteristics (photon number range and lifetime distribution) inferred from real acquisition data from the N-STORM microscope. A PyTorch model was trained to infer the 3D coordinates and uncertainty of the simulated blinking events and then applied to the experimental acquired sequence. The resulting localizations (fitted blinking events) were filtered based on uncertainty, and drift during acquisition was corrected in 3D using a redundant cross-correlation algorithm (Wang et al., 2014) implemented as an independent module of SMAP (Ries, 2020). After translation of the coordinate files, image reconstructions were performed using the ThunderSTORM ImageJ plugin (Ovesný et al., 2014) in Fiji software. Custom scripts and macros were used to translate coordinate files and automate image reconstruction for images at 16 nm/pixel for visualization and at 8 nm/pixel for cluster analysis (https://github.com/cleterrier/ChriSTORM).

STORM image analysis

A high-magnification image (4 nm/pixel) was generated for each induced presynapse image, and manually registered by translation with the corresponding epifluorescence images in other channels, including presynaptic marker. Actin structures present at the induced presynapse were categorized into three types using the following criteria (Bingham et al., 2023):
• actin mesh: a small cluster of actin next to the nlgn dot contact and within the presynaptic active zone marker cluster.
• actin rails: linear structures within the presynaptic marker cluster
• actin corrals: large actin clusters at the periphery or just surrounding the presynaptic marker cluster.
The size of the actin nanostructures was determined using manual outlines on 2D projection of actin STORM images in Fiji, aided by visualization of 3D renderings using ChimeraX software (Goddard et al., 2018).

Neuronal transfection and live-cell imaging

13 div cultured neurons, at a density of 6,000 cells/cm^2, were transfected using Lipofectamine 2000 (Thermo Fisher Scientific) with 0.15 µg of VAMP2–pHluorin. Following 30 min incubation in neurobasal medium (NB; Thermo Fisher Scientific) at 37oC, 5% CO_2, coverslips were returned to their original culture dishes. After 16 h, live-cell imaging of neurons expressing VAMP2–pHluorin was performed on an inverted microscope ECLIPSE Ti2-E (Nikon Instruments) equipped with an ORCA-Fusion sCMOS camera (Hamamatsu Photonics) and a CFI SR HP Apochromat TIRF 100× oil (NA 1.49) objective. The system was equipped with a Nikon Perfect Focus System (PFS) and images were acquired with the NIS-Elements software. Coverslips with neurons were mounted in a Ludin metal chamber in Tyrode's solution (119 mM NaCl, 25 mM HEPES, 2.5 mM KCl, 2 mM $CaCl_2$, 2 mM $MgCl_2$, 30 mM glucose, pH 7.35). Neurons were maintained in a humid chamber at 35.5–37°C for the duration of the experiments using a stage-top incubator (Okolab Inc). To image exocytosis, VAMP2–pHluorin initially present at the plasma membrane was photobleached using high power 488 nm laser light for 15 s before time-lapse imaging to isolate exocytic signal (Yudowski et al., 2007); 100 ms exposure frames were then continuously acquired for 5 min using 488 nm laser light at lower power (1–10%).

Timelapse data processing

Acquired videos were preprocessed using the Filter Timelapse script (available at https://sites.imagej.net/Christopheleterrier/plugins/NeuroCyto%20Lab/Kymographs/), which performed image stabilization using the Image Stabilizer plugin (https://imagej.net/plugins/image-stabilizer) after 2× downscaling, and bleach correction using average intensity compensation for the foreground identified as the top 12% of pixel intensities within each image of the sequence. Exocytosis events along isolated axons across a field of nlgn dots were then identified with the pHusion plugin in ImageTank software (O'Shaughnessy et al., 2024). Exocytotic events were detected by using the Difference of Gaussian (DoG) method using a sigma of 3 and a scaling factor of 1.25. Using the region of interest from the DoG image, a small image series was cropped from the raw image stack taking 5 frames before and 30 after the identified spot. Each image in the series was fitted with a gaussian model. Only events with a goodness of fit for the gaussian model greater than 0.7 were considered. Events that drifted greater than 4 pixels were removed. Identified exocytosis events were subsequently verified by visual inspection of the original timelapse movies in Fiji.

Correlative live-cell/STORM

Live-cell timelapse data and corresponding STORM images were registered with a two-step procedure. First, an RGB merge of the maximum-projected VAMP2-pHluorin movie and nlgn pattern from live-cell data was aligned to an RGB merge of the fixed VAMP2-pHluorin image from the STORM acquisition using a manually-tuned affine transform using the BigDataViewer Fiji plugin (Pietzsch et al., 2015). The resulting affine transform was then applied to the live-cell data using the TransformJ Fiji plugin to align it to STORM reconstructions and corresponding up-sampled epifluorescence channels (at 16 or 4 nm per pixel depending on the zoom level). Vamp2-pHluorin timelapse was up-sampled using a quintic B-spline approach (Meijering et al., 2001), and the exocytic localization was determined on the first frame where the exocytosis signal appeared, as the highest intensity pixel on the image up-sampled to 16 nm per pixel.

Statistics

Individual measurement points (n) from independent experiments (N) were pooled. Intensity profiles, graphs, and statistical analyses were generated using Prism. On bar graphs, dots (if present) are averages of each independent experiment, bars or horizontal lines represent the mean, and vertical lines are the SEM unless otherwise specified. Significances were tested using one-way, non-parametric ANOVA with Šídák post-hoc significance testing between selected conditions (Fig. 1 and 2) or using Wilcoxon rank sum test (Fig. 3). On Figures, the results of the post-hoc significance are indicated as follows: ns or ns, non-significant; *, $p < 0.05$; **, $p < 0.01$; ***, $p < 0.001$.

References

Augustin I, Rosenmund C, Südhof TC, Brose N (1999) Munc13-1 is essential for fusion competence of glutamatergic synaptic vesicles. Nature 400:457–461.

Baumert M, Maycox PR, Navone F, Camilli PD, Jahn R (1989) Synaptobrevin: an integral membrane protein of 18,000 daltons present in small synaptic vesicles of rat brain. EMBO J 8:379–384.

Bernstein BW, Bamburg JR (1989) Cycling of actin assembly in synaptosomes and neurotransmitter release. Neuron 3:257–265.

Bernstein BW, Maloney MT, Bamburg JR (2010) Neurobiology of Actin, From Neurulation to Synaptic Function. Adv Neurobiol 5:201–234.

Bingham D, Jakobs CE, Wernert F, Boroni-Rueda F, Jullien N, Schentarra E-M, Friedl K, Moura JDC, Bommel DM van, Caillol G, Ogawa Y, Papandréou M-J, Leterrier C (2023) Presynapses contain distinct actin nanostructures. J Cell Biol 222:e202208110.

Bloom O, Evergren E, Tomilin N, Kjaerulff O, Löw P, Brodin L, Pieribone VA, Greengard P, Shupliakov O (2003) Colocalization of synapsin and actin during synaptic vesicle recycling. J Cell Biol 161:737–747.

Burrone J, Li Z, Murthy VN (2006) Studying vesicle cycling in presynaptic terminals using the genetically encoded probe synaptopHluorin. Nat Protoc 1:2970–2978.

Burry RW (1980) Formation of apparent presynaptic elements in response to poly-basic compounds. Brain Res 184:85–98.

Carvalhais LG, Martinho VC, Ferreiro E, Pinheiro PS (2021) Unraveling the Nanoscopic Organization and Function of Central Mammalian Presynapses With Super-Resolution Microscopy. Front Neurosci 14:578409.

Cingolani LA, Goda Y (2008) Actin in action: the interplay between the actin cytoskeleton and synaptic efficacy. Nat Rev Neurosci 9:344–356.

Cole JC, Villa BRS, Wilkinson RS (2000) Disruption of actin impedes transmitter release in snake motor terminals. J Physiol 525:579–586.

Coles CH, Bradke F (2015) Coordinating Neuronal Actin–Microtubule Dynamics. Curr Biol 25:R677–R691.

Czöndör K, Garcia M, Argento A, Constals A, Breillat C, Tessier B, Thoumine O (2013) Micropatterned substrates coated with neuronal adhesion molecules for high-content study of synapse formation. Nat Commun 4:2252.

Dani A, Huang B, Bergan J, Dulac C, Zhuang X (2010) Superresolution Imaging of Chemical Synapses in the Brain. Neuron 68:843–856.

Dieck S, Sanmartí-Vila L, Langnaese K, Richter K, Kindler S, Soyke A, Wex H, Smalla K-H, Kämpf U, Fränzer J-T, Stumm M, Garner CC, Gundelfinger ED (1998) Bassoon, a Novel Zinc-finger CAG/Glutamine-repeat Protein Selectively Localized at the Active Zone of Presynaptic Nerve Terminals. J Cell Biol 142:499–509.

Doussau F, Augustine GJ (2000) The actin cytoskeleton and neurotransmitter release: An overview. Biochimie 82:353–363.

Funahashi J, Tanaka H, Hirano T (2018) Visualization of Synchronous or Asynchronous Release of Single Synaptic Vesicle in Active-Zone-Like Membrane Formed on Neuroligin-Coated Glass Surface. Front Cell Neurosci 12:140.

Gentile JE, Carrizales MG, Koleske AJ (2022) Control of Synapse Structure and Function by Actin and Its Regulators. Cells 11:603.

Glebov OO, Jackson RE, Winterflood CM, Owen DM, Barker EA, Doherty P, Ewers H, Burrone J (2017) Nanoscale Structural Plasticity of the Active Zone Matrix Modulates Presynaptic Function. Cell Rep 18:2715–2728.

Goddard TD, Huang CC, Meng EC, Pettersen EF, Couch GS, Morris JH, Ferrin TE (2018) UCSF ChimeraX: Meeting modern challenges in visualization and analysis. Protein Sci 27:14–25.

He J, Zhou R, Wu Z, Carrasco MA, Kurshan PT, Farley JE, Simon DJ, Wang G, Han B, Hao J, Heller E, Freeman MR, Shen K, Maniatis T, Tessier-Lavigne M, Zhuang X (2016) Prevalent presence of periodic actin–spectrin-based membrane skeleton in a broad range of neuronal cell types and animal species. Proc Natl Acad Sci 113:6029–6034.

Hirokawa N, Sobue K, Kanda K, Harada A, Yorifuji H (1989) The cytoskeletal architecture of the presynaptic terminal and molecular structure of synapsin 1. J Cell Biol 108:111–126.

Jacquemet G, Carisey AF, Hamidi H, Henriques R, Leterrier C (2020) The cell biologist's guide to super-resolution microscopy. J Cell Sci 133:jcs240713.

Jahn R, Schiebler W, Ouimet C, Greengard P (1985) A 38,000-dalton membrane protein (p38) present in synaptic vesicles. Proc Natl Acad Sci 82:4137–4141.

Jimenez A, Friedl K, Leterrier C (2020) About samples, giving examples: Optimized Single Molecule Localization Microscopy. Methods 174:100–114.

Kaech S, Banker G (2006) Culturing hippocampal neurons. Nat Protoc 1:2406–2415.

Kawaguchi S, Hirano T (2006) Integrin α3β1 suppresses long-term potentiation at inhibitory synapses on the cerebellar Purkinje neuron. Mol Cell Neurosci 31:416–426.

Kim C-H, Lisman JE (1999) A Role of Actin Filament in Synaptic Transmission and Long-Term Potentiation. J Neurosci 19:4314–4324.

Kraszewski K, Mundigl O, Daniell L, Verderio C, Matteoli M, Camilli PD (1995) Synaptic vesicle dynamics in living cultured hippocampal neurons visualized with CY3-conjugated antibodies directed against the lumenal domain of synaptotagmin. J Neurosci 15:4328–4342.

Landis DMD, Hall AK, Weinstein LA, Reese TS (1988) The organization of cytoplasm at the presynaptic active zone of a central nervous system synapse. Neuron 1:201–209.

Li P, Bademosi AT, Luo J, Meunier FA (2018a) Actin Remodeling in Regulated Exocytosis: Toward a Mesoscopic View. Trends Cell Biol 28:685–697.

Li Y, Mund M, Hoess P, Deschamps J, Matti U, Nijmeijer B, Sabinina VJ, Ellenberg J, Schoen I, Ries J (2018b) Real-time 3D single-molecule localization using experimental point spread functions. Nat Methods 15:367–369.

Lucido AL, Sanchez FS, Thostrup P, Kwiatkowski AV, Leal-Ortiz S, Gopalakrishnan G, Liazoghli D, Belkaid W, Lennox RB, Grutter P, Garner CC, Colman DR (2009) Rapid Assembly of Functional Presynaptic Boutons Triggered by Adhesive Contacts. J Neurosci 29:12449–12466.

Luo L (2002) Actin cytoskeleton regulation in neuronal morphogenesis and structural plasticity. Annu Rev Cell Dev Biol 18:601–635.

Matus A, Ackermann M, Pehling G, Byers HR, Fujiwara K (1982) High actin concentrations in brain dendritic spines and postsynaptic densities. Proc Natl Acad Sci 79:7590–7594.

McAllister AK (2007) Dynamic Aspects of CNS Synapse Formation. Neuroscience 30:425–450.

Meijering EHW, Niessen WJ, Viergever MA (2001) Quantitative evaluation of convolution-based methods for medical image interpolation. Méd Image Anal 5:111–126.

Miesenböck G, Angelis DAD, Rothman JE (1998) Visualizing secretion and synaptic transmission with pH-sensitive green fluorescent proteins. Nature 394:192–195.

Morales M, Colicos MA, Goda Y (2000) Actin-Dependent Regulation of Neurotransmitter Release at Central Synapses. Neuron 27:539–550.

Nosov G, Kahms M, Klingauf J (2020) The Decade of Super-Resolution Microscopy of the Presynapse. Front Synaptic Neurosci 12:32.

Ogunmowo TH, Jing H, Raychaudhuri S, Kusick GF, Imoto Y, Li S, Itoh K, Ma Y, Jafri H, Dalva MB, Chapman ER, Ha T, Watanabe S, Liu J (2023) Membrane compression by synaptic vesicle exocytosis triggers ultrafast endocytosis. Nat Commun 14:2888.

O'Neil SD, Rácz B, Brown WE, Gao Y, Soderblom EJ, Yasuda R, Soderling SH (2021) Action potential-coupled Rho GTPase signaling drives presynaptic plasticity. eLife 10:e63756.

O'Shaughnessy EC, Lam M, Ryken SE, Wiesner T, Lukasik K, Zuchero JB, Leterrier C, Adalsteinsson D, Gupton SL (2024) pHusion: A robust and versatile toolset for automated detection and analysis of exocytosis. J Cell Sci 137:jcs261828.

Ovesný M, Křížek P, Borkovec J, Švindrych Z, Hagen GM (2014) ThunderSTORM: a comprehensive ImageJ plug-in for PALM and STORM data analysis and super-resolution imaging. Bioinformatics 30:2389–2390.

Papandréou M-J, Leterrier C (2018) The functional architecture of axonal actin. Mol Cell Neurosci 91:151–159.

Pietzsch T, Saalfeld S, Preibisch S, Tomancak P (2015) BigDataViewer: visualization and processing for large image data sets. Nat Methods 12:481–483.

Reshetniak S, Rizzoli SO (2019) Interrogating Synaptic Architecture: Approaches for Labeling Organelles and Cytoskeleton Components. Front Synaptic Neurosci 11:23.

Ries J (2020) SMAP: a modular super-resolution microscopy analysis platform for SMLM data. Nat Methods 17:870–872.

Sakamoto H, Ariyoshi T, Kimpara N, Sugao K, Taiko I, Takikawa K, Asanuma D, Namiki S, Hirose K (2018) Synaptic weight set by Munc13-1 supramolecular assemblies. Nat Neurosci 21:41–49.

Sankaranarayanan S, Atluri PP, Ryan TA (2003) Actin has a molecular scaffolding, not propulsive, role in presynaptic function. Nat Neurosci 6:127–135.

Schindelin J, Arganda-Carreras I, Frise E, Kaynig V, Longair M, Pietzsch T, Preibisch S, Rueden C, Saalfeld S, Schmid B, Tinevez J-Y, White DJ, Hartenstein V, Eliceiri K, Tomancak P, Cardona A (2012) Fiji: an open-source platform for biological-image analysis. Nat Methods 9:676–682.

Shupliakov O, Bloom O, Gustafsson JS, Kjaerulff O, Löw P, Tomilin N, Pieribone VA, Greengard P, Brodin L (2002) Impaired recycling of synaptic vesicles after acute perturbation of the presynaptic actin cytoskeleton. Proc Natl Acad Sci 99:14476–14481.

Sidenstein SC, D'Este E, Böhm MJ, Danzl JG, Belov VN, Hell SW (2016) Multicolour Multilevel STED nanoscopy of Actin/Spectrin Organization at Synapses. Sci Rep 6:26725.

Speiser A, Müller L-R, Hoess P, Matti U, Obara CJ, Legant WR, Kreshuk A, Macke JH, Ries J, Turaga SC (2021) Deep learning enables fast and dense single-molecule localization with high accuracy. Nat Methods 18:1082–1090.

Südhof TC (2012) The Presynaptic Active Zone. Neuron 75:11–25.

Tanaka H, Fujii S, Hirano T (2014) Live-cell imaging of receptors around postsynaptic membranes. Nat Protoc 9:76–89.

Tanaka H, Funahashi J, Hirano T (2023) Live-cell imaging of endocytosed synaptophysin around individual hippocampal presynaptic active zones. Front Cell Neurosci 17:1277729.

Tang A-H, Chen H, Li TP, Metzbower SR, MacGillavry HD, Blanpied TA (2016) A trans-synaptic nanocolumn aligns neurotransmitter release to receptors. Nature 536:210–214.

Théry M (2010) Micropatterning as a tool to decipher cell morphogenesis and functions. J Cell Sci 123:4201–4213.

Théry M, Piel M (2009) Adhesive Micropatterns for Cells: A Microcontact Printing Protocol. Cold Spring Harb Protoc 2009:pdb.prot5255.

Togashi H, Sakisaka T, Takai Y (2009) Cell adhesion molecules in the central nervous system. Cell Adhes Migr 3:29–35.

Urbina FL, Gomez SM, Gupton SL (2018) Spatiotemporal organization of exocytosis emerges during neuronal shape change. J Cell Biol 217.

Wang Y, Schnitzbauer J, Hu Z, Li X, Cheng Y, Huang Z-L, Huang B (2014) Localization events-based sample drift correction for localization microscopy with redundant cross-correlation algorithm. Opt Express 22:15982.

Watanabe S, Rost BR, Camacho-Pérez M, Davis MW, Söhl-Kielczynski B, Rosenmund C, Jorgensen EM (2013) Ultrafast endocytosis at mouse hippocampal synapses. Nature 504:242–247.

Weng S, Fu J (2011) Synergistic regulation of cell function by matrix rigidity and adhesive pattern. Biomaterials 32:9584–9593.

Werner C, Sauer M, Geis C (2021) Super-resolving Microscopy in Neuroscience. Chem Rev 121:11971–12015.

Wiedenmann B, Franke WW (1985) Identification and localization of synaptophysin, an integral membrane glycoprotein of Mr 38,000 characteristic of presynaptic vesicles. Cell 41:1017–1028.

Yan Z, Kim E, Datta D, Lewis DA, Soderling SH (2016) Synaptic Actin Dysregulation, a Convergent Mechanism of Mental Disorders? J Neurosci 36:11411–11417.

Yudowski GA, Puthenveedu MA, Leonoudakis D, Panicker S, Thorn KS, Beattie EC, Zastrow M von (2007) Real-Time Imaging of Discrete Exocytic Events Mediating Surface Delivery of AMPA Receptors. J Neurosci 27:11112–11121.

Supplementary material

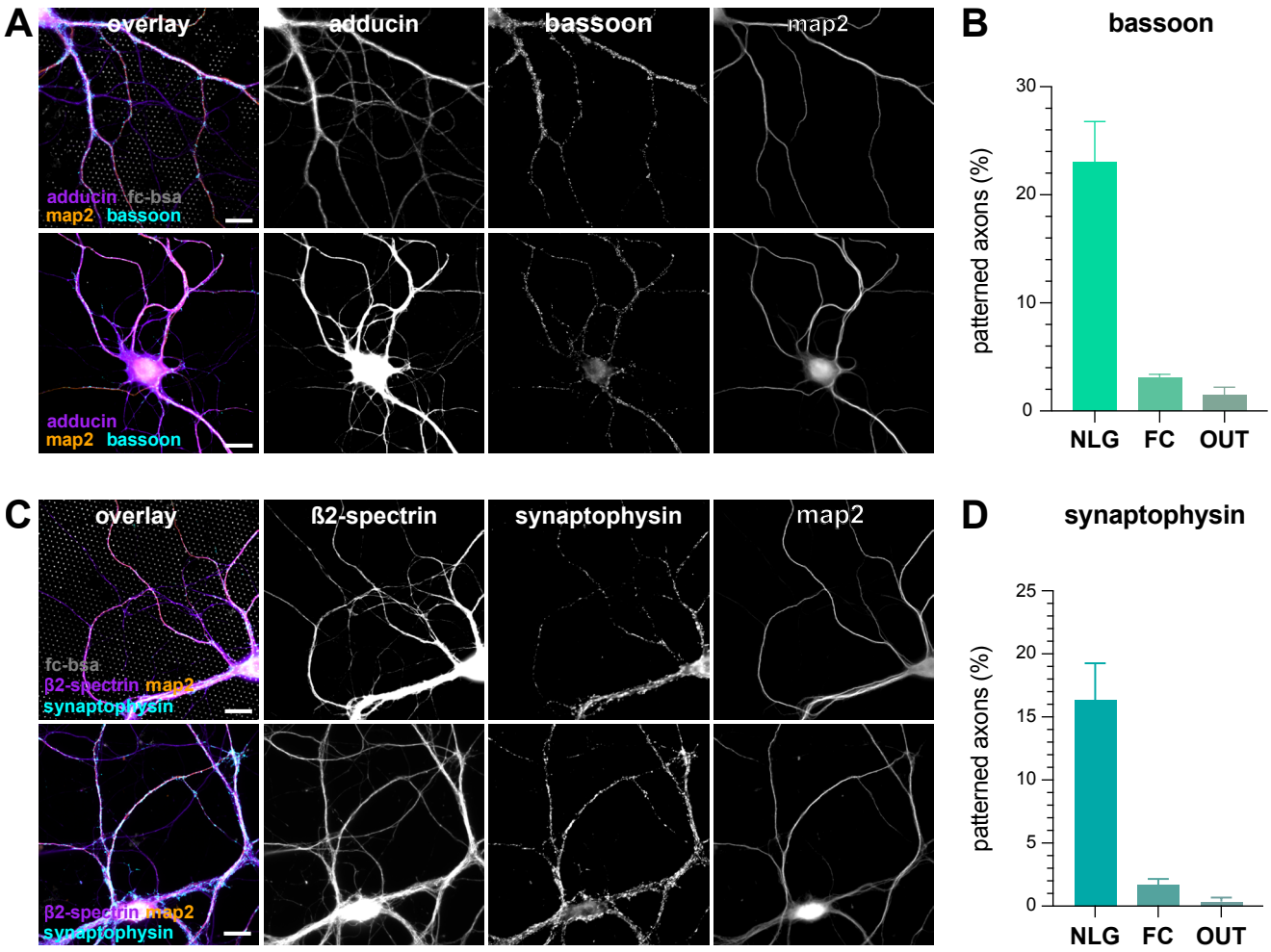

Figure S1: No induction of presynapses on Fc-BSA dots or outside the nlgn dots pattern.
A. Widefield fluorescence image of cultured neurons on top of the Fc-BSA micropattern (top row, gray) or outside of the pattern (bottom row) fixed at div 15 labeled for adducin (purple), bassoon (cyan), map2 (orange). Scale bar, 10 µm. **B.** Proportion of the length of isolated axons showing presynaptic bassoon specializations following the nlgn micropattern (patterned axon) over the total length of isolated axons selected within the experimental conditions (nlgn dots, N=5) compared to controls (Fc-BSA, N=3; outside of the nlgn dots pattern, N=4). **C.** Widefield fluorescence image of cultured neurons on top of the Fc-BSA micropattern (top row, gray) or outside of the pattern (bottom row) fixed at div 15 labeled for ß2-spectrin (purple), synaptophysin (cyan), map2 (orange). Scale bar, 10 µm. **D.** Proportion of the length of isolated axons showing presynaptic synaptophysin specializations following the nlgn micropattern (patterned axon) over the total length of isolated axons selected within the experimental conditions (nlgn dots, N=4) compared to controls (Fc-BSA dots, N=3; outside of the nlgn dots pattern, N=4).

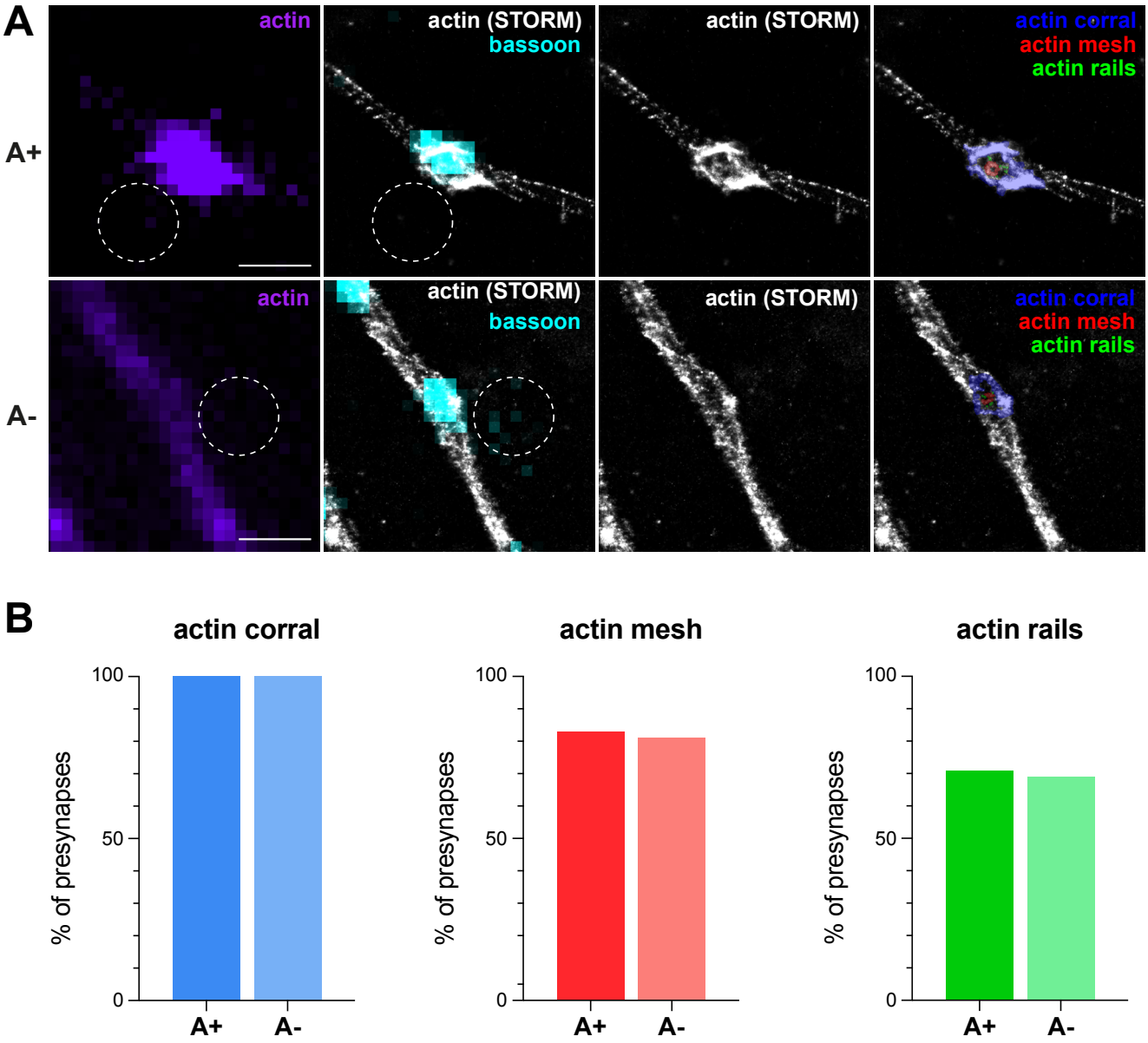

Figure S2: Presence of actin nanostructures in nlgn dot-induced presynapses enriched and non-enriched in actin.
A. Axon segments displaying actin-enriched (A+, first row) and actin-non-enriched presynapses (A-, second row). The left column displays the epifluorescence image of actin (purple) and the position of the nlgn dots (white dashed circle). Second column displays the STORM image of actin (gray), the epifluorescence image of bassoon (cyan) and the position of the nlgn dots (dotted circle in white). Third column shows the STORM image of actin (gray) alone. Fourth column shows colorized presynaptic actin nanostructures: actin corrals (blue), actin mesh (red) and actin rails (green). Scale bars, 1 µm. **B.** Proportion of presynapses where each nanostructure is detected for A+ and A- induced presynapses: actin corrals (blue), actin mesh (red), and actin rails (green).

9. Discussing Presynapse on Glass Model as The Optimal Tool to Decipher Presynaptic Actin Structure and Functions

9.1. Presynapse on Glass Model to Investigate Actin Role in Synaptic Vesicular Release

The work provided for my PhD project fulfilled its aim to find the correct tool to interrogate actin nanostructures at the presynapse. The novel presynapse-on-glass model induces presynapses oriented toward the glass, achieving the optical accessibility needed to decipher the roles presynaptic actin nanostructures may play in synaptic vesicular release using correlative live-cell imaging. Our preliminary data indicate the potential of this implemented model as an appropriate tool for investigations concerning presynaptic actin cytoskeleton and other presynaptic components. Due to the proximity of the presynapse to the glass we may take advantage of all the advances of super-resolution microscopy for better understanding of the architecture of presynapses and their related functions.

9.2. Structural and Functional Insights into Presynaptic Actin Nanostructures

Our observations point to roles underlying membrane modifications essential to ensure synaptic vesicle cycle. It is known that the actin cytoskeleton contributes to cell mechanics by generating driving forces underneath the plasma membrane, supporting changes in cellular morphology (Fletcher & Mullins, 2010). Together with the action of motor proteins moving along actin filaments, this cytoskeleton orchestrates the organization of cellular components (Venkatesh et al., 2020). The actin ultrastructure supports the nanoscopic organization of the presynaptic compartment, gathering crucial elements together and facilitating their trafficking (Chenouard et al., 2020). Moreover, my project interrogated the molecular architecture of the active zone scaffolding protein bassoon and actin nanostructures, demonstrating that the branched actin mesh is intertwined with bassoon clusters. These observations point to a structural role of actin mesh in supporting specialized presynaptic nanodomains. These findings were consistent for either actin-enriched or non-enriched induced presynapses. However, this role does

not exclude more direct involvement of actin nanostructures in vesicular fusion and release events, rather further studies are required to elucidate these potential roles. Live-cell imaging of the activity-dependent remodeling of actin using the presynapse-on-glass model offers new opportunities to address further questions related to actin's role in presynaptic functions.

9.2.1. Actin Distribution During Synaptic Vesicular Release

To investigate actin's role as an orchestrator of synaptic vesicular release, researchers studied activity-dependent dynamics of actin at presynapses. A study demonstrated that actin is recruited to presynapses upon stimulation, and subsequently redistributed along the surrounding axon. Meanwhile actin revert to pre-stimulation levels at presynaptic compartments. The intriguing variations of actin intensity are achieved in a few seconds and restored to baseline levels after 2 minutes in physiological conditions. These activity-dependent dynamics are abolished when actin monomers are sequestered and actin filaments depolymerize under pharmacological intervention. These drugs effects result in partial dispersion of presynaptic components underlying presynaptic actin scaffolding role (Sankaranarayanan et al., 2003). These findings are consistent with the observations made using our presynapse-on glass model. In our research, recycled vesicles are captured at a specific timepoint of presynapses activity, likely before or during vesicular release. Actin-enriched and non-enriched presynapses revealed significantly different vesicular cycling activity. Indeed, actin enriched presynapses yielded higher synaptic cycling activity and larger actin corrals as compared to non-enriched presynapses displaying lower amounts of actin and inferior cycling activity. These results are in line with actin recruitment observed by Sankaranarayanan and colleagues. Using diffraction-limited microscopy they detected a higher concentration of actin around the vesicle pools than within them. This work was realized using EGFP-tagged actin; it is important to mention that EGFP tags can affect endogenous dynamics and concentrations of actin cytoskeleton within cells, disrupting filamentous actin organization (Ignácz et al., 2023). The literature recognized LifeAct as an optimal tool labeling endogenous actin compared to EGFP-actin (Bhaskar et al., 2023; Nagasaki et al., 2017). Nevertheless, LifeAct can also create artifacts in live-cell experiments or induce modifications leading to severe functional or structural disruption in various cell types (Courtemanche et al., 2016b; Flores et al., 2019; R. Xu & Du, 2021). These findings emphasize that caution must be exercised when employing fluorescently tagged actin construct to investigate actin dynamics(Colombo et al., 2021; Mullins & Hansen, 2013; Riedl et al., 2008b; Smith et al., 2014). It is important to always consider the limitations of the experimental design and the microscopy technique used.

The diffraction-limit and the segmentation procedure employed by Sankaranarayanan and collaborators impeded the visualization of the smallest actin nanostructures and thus precluded interpretations of their further involvement in scaffolding presynaptic

compartments. However, super-resolution microscopy combined with our presynapse-on-glass model yielded similar results. We observed actin-dense corrals englobing induced presynapses, while less dense actin mesh and rails were found closer to the active zone where vesicles are known to dock.

9.2.2. Energy Demands of Actin Dynamics Defining Consistency Between Actin-Enriched and Non-Enriched Presynapses?

There is a striking consistency between the percentage of actin-enriched and non-enriched induced presynapses obtained using two distinct models of presynaptic induction. The same percentage (~60%) is also found in endogenously tagged natural presynapses (Bingham et al., 2023). This implies a biological constant that represents the amount of simultaneous highly cycling presynapses. Further, this suggests that the energy required for actin recruitment limits the amount of presynapses that can be highly cycling at once. Actin remodeling requires ATP consumption. However, the energy drain neurons undergo due to actin treadmilling remains a highly debated area of research. Historically, due to actin's high ATP consumption, the actin cytoskeleton has been considered one of the foremost drains of neuronal energy until very recently (Bernstein & Bamburg, 2002). Measurements made by indirectly tracking ATP revealed that actin dynamics play a significant role in ATP depletion. Pharmacologically inhibiting actin polymerization preserves intracellular ATP levels (Bernstein & Bamburg, 2002).

In contradicting findings, genetically encoded reporters were used to directly monitor ATP levels associated with actin dynamics in developing neurons M. Holand & G. Gallo (2023). Their results suggest that affecting actin dynamics does not impact ATP levels as previously reported. Holand, Gallo et al. suggested that certain compartments such as synapses could represent significant, but local, energy consumption explaining the controversial results found by researchers in the field. More studies employing fluorescent probes to analyze ATP levels in postnatal rodent hippocampal neurons quantified presynaptic ATP levels decrease upon synaptic activity (Pathak et al., 2015; Rangaraju et al., 2014). Though further investigation is needed to clarify actin's role, the current state of the field is evolving thanks to the advancement of recent technologies. Observing presynaptic 3D-live actin dynamics and ATP levels correlated with super-resolved capture of presynapses-on-glass actin nanostructures may explain the mechanisms underlying the distribution of actin enriched and non-enriched presynapses, and elucidate if this difference is related to the degree of energy consumption.

These future studies will help describe the functional differences between the actin-enriched and non-enriched presynapses. The higher concentration of synaptic proteins and cycling activity found in actin-enriched presynapses may represent more active, and thus ATP-demanding, synapses. The visualization of super-resolved nanostructures and

their energy-dependent modifications will deepen our understanding of these mechanisms.

9.2.3. Dynamics of Actin Nanostructures in Neurodevelopment During Different Synaptic States

The work I presented here provided time-frozen captures of the dynamic shift of actin nanostructures in mature presynapses. First, it would be interesting to investigate actin mesh, corrals and rails appearing across neuron developmental stages and corresponding presynaptic maturation. Second, highlighting their evolution over time may be critical to describe how presynaptic actin remodeling aligns with phases of synaptic strength. The micropattern of neuroligin dots is present throughout the whole culture duration. This feature of our implemented model enables the observation of actin dynamics in early aggregation of presynaptic components, firstly appearing around the day 7 *in vitro* (DIV) (Schätzle et al., 2012; W. Zhang & Benson, 2001b), when axonal growth and dendritic maturation is advanced. The subsequent steps of their development can be observed until the end stages of synaptic maturation (DIV 10; DIV 14; DIV 17; DIV 21). Both fixed and live-cell images of presynaptic formation at different stages of neuronal development are adapted to our goals. Additionally, observing actin dynamics and the evolution of presynaptic nanostructures over time will provide more insight regarding their specific roles. Inspired by the methodology developed by Schätzle and Zhang *(See Section 6.3.2.)*, it will be intriguing to adapt the automated segmentation algorithm to super-resolved presynaptic clusters. Examine the three-dimensional distribution of actin nanostructures and presynaptic proteins at different time points of presynaptic maturation could deepen our knowledge regarding actin roles. By first describing representations of the different stages of presynaptic maturation, the presynapse on glass model offers the opportunity to study these features in distinct synaptic states (i.e. long term potentiation or depression)*(See Section 3.4.)*.

Inducing presynapses using this innovative method of presynapse induction, gives us the ability to capture the actin distribution within time-frozen steps of its remodeling. The validation of this model further opens opportunities for multiple studies.

10. Advanced Microscopy Techniques for Real-Time Visualization of Presynaptic Vesicle Release and Actin using the Presynapse on Glass Model

Investigating presynaptic actin dynamics with advanced imaging techniques is crucial for understanding the role actin nanostructures might play in cellular processes like vesicle release. The novel presynapse-on-glass model implemented in my work already offers key advantages when investigating these intricate dynamics. Coupling the presynapse-on-glass model with single-molecule localization techniques allows accurate visualization of this cellular compartment at the nanoscale.

However, even with the use of our model of induction, neuroscientists face several methodological limitations to study their dynamics and involvement in synaptic functions related to active zone assembly or synaptic vesicle exocytosis. Altogether, with presynaptic actin treadmilling, these biological processes are millisecond-scale phenomena that remain difficult to interrogate (Carvalhais et al., 2021; Jackson et al., 2022; Nosov et al., 2020).

To argue which are the best tools to investigate presynaptic exocytosis and actin dynamics, we need to consider microscopy techniques that enable the visualization of these processes in living cells, using less-invasive methodologies with the highest resolution possible. The studying actin requires optimal four-dimensional resolution, meaning high spatial resolution, in both lateral and axial (x, y and z) as well as temporal (t) dimensions. Together with previously employed micropatterning techniques, I have employed and presented STORM and DNA-PAINT as ideal methods to interrogate presynapses structure and functions *(See Section 6)*. Nowadays, researchers have access to other imaging tools with similar properties (Butler-Hallissey Ciarán & Leterrier Christophe, 2024). Here, I will introduce other techniques that may also exploit the optical gain offered by our presynapse-on-glass model: Stimulated Emission Depletion (STED) and MINimal Emission FLUXes (MINFLUX).

10.1. Investigating Presynaptic Actin with STED

STED microscopy uses a high-intensity donut-shaped laser to reduce the excitation spot. Reducing the size of the depletion donut minimizes blur and out of focus light, enabling visualization of nanoscopic subcellular compartments such as synapses. The enhanced resolution provided by STED over traditional confocal microscopy makes this technique eligible to study intracellular structures in different cell types (Maraspini et al., 2020; Sidenstein et al., 2016). STED microscopy can achieve real-time imaging down to approximately 50 ms per frame, a feature essential for interrogating actin plasticity (Wegner et al., 2017). This temporal precision is adapted to study synaptic protein clustering at the active zone and exocytosis events. Reducing the size of the depletion beam enabled live imaging of synaptic vesicles at a restricted field of view (FOV) of 1.8um (Westphal et al., 2008), the approximate diameter of our micropatterned neuroligin dots. STED microscopy, thus, presents as an apt tool to leverage the advantages of our presynapse-on-glass model, and resolving presynaptic components down to 40 nm (Westphal et al., 2008).

The method used to track vesicle movement does not serve as an appropriate tool to study actin nanostructures, which are much more densely distributed. Advances have been made in the microscopy field to study the F-actin organization and remodeling within a plethora of different cell-types (reviewed in Phillips et al., 2024) as well as within synapses. However, most of them focus on the actin-dependent reshaping of dendritic spine morphology *(See Section 4.2.)*. In fact, STED microscopy has historically been used to study actin predominantly at the postsynapse, as this is an easier compartment to access in physiological conditions (Urban et al., 2011). However, these methods apply to study presynaptic actin and can be leveraged with the advent of our presynapse-on-glass model (Nosov et al., 2020; Oevel et al., 2024; Ogunmowo et al., 2023; Sidenstein et al., 2016; Urban et al., 2011; Willig et al., 2006).

Unfortunately, STED's high-power depletion beam constitutes an elevated risk of photobleaching and phototoxicity restricting the live-cell imaging capabilities. This characteristic also limits the compatible fluorophores available on the market, crucial to investigate actin and other components within presynapses. Despite this limitation, STED has been designated as a viable tool to studying cellular cytoskeletal structures by several researchers who used it to reveal neuronal periodicity and synaptic cytoskeleton (D'Este et al., 2015; J. C. Wang et al., 2018). Overcoming the obstacle of postsynapse presence, STED microscopy in combination with the presynapse-on-glass model will allow studies on the presynaptic compartment, unraveling still poorly understood dynamics.

10.2. MINFLUX and the Presynapse-on-Glass Model for Studying Presynaptic Actin Dynamics

An intriguing alternative for studying presynaptic actin dynamics is MINFLUX microscopy. It is an innovative technique that emerged in the field of super-resolution microscopy, combining the principles of single molecule localization microscopy (SMLM) and STED (Balzarotti et al., 2017). Instead of a depletion beam as in STED, MINFLUX uses a donut-shaped excitation beam that scans the sample, aiming to position the dark center of the donut as close to the fluorescent emitter as possible, allowing for more precise localization of the molecule's position. Its exceptional characteristics lead to optimal molecular localization precision at the nanometer scale down to approximately 1-3 nm in three dimensions (Schmidt et al., 2021; J. Wang et al., 2023) and makes this technology particularly interesting for the study of presynaptic components (Grabner et al., 2022).

MINFLUX appears also relevant for the investigation of cytoskeletal nanostructures in three dimensions. The sensitivity of its axial resolution would provide more precise visualization of actin mesh and rails. These are the smallest actin nanostructures we recognize in the presynaptic compartment using STORM microscopy, which can only achieve an axial resolution of 50 nm at best (Huang et al., 2009). The use of MINFLUX multicolor acquisition would highlight the precise organization of the active zone components and the intricate architecture of the branched actin belonging to the actin mesh. MILFLUX limitations impeding the visualizations of densely labeled structures, such as cytoskeletal elements, remains a subject of debate (Mihaila et al., 2022; Y. Le Wu et al., 2023). Recent findings using MINFLUX in postsynapses, underline its exceptional localization accuracy (Moosmayer et al., 2024) which could be exploited to investigate actin at induced presynapses. Despite the enhanced optical accessibility provided by our presynapse-on-glass model, distinguishing actin rails remains challenging. It is difficult to isolate them from other architectural elements when limited by conventional super-resolution imaging techniques. Improvements in labeling and quantitative analysis strategies of MINFLUX microscopy may help define the specific linearity and thickness of the actin rails in the future.

Additionally, MINFLUX's temporal resolution is approximated in the millisecond range when tracking a single fluorophore. It has allowed researchers to achieve remarkable observations of fast biological processes. Motor protein tracking along cytoskeletal elements were visualized in 2D and 3D live-cell imaging (Deguchi et al., 2023). By contrast, mapping structures such as actin filaments with MINFLUX require time consuming imaging sessions, but in the future, faster implementations may enable push further the current knowledge regarding actin role in presynaptic functions. However, MINFLUX application to biological processes is relatively new and requires highly photostable fluorophores. MINFLUX is a relatively new, yet promising, technique for future studies of presynaptic actin utilizing our novel presynapse-on-glass-model.

11. From Excitatory/Inhibitory Comparisons to Disease Models: Future Explorations of Presynaptic Actin Architectures and Methodology Implementations

Single molecule localization microscopy combined with the presynapse-on-glass model offers plenty of possible investigations to expand upon the current knowledge regarding presynaptic structural and functional aspects. Considering methodological limitations, implementations of our model will help build future experimental designs giving the opportunity to deepen our knowledge of active zone assembly and functions under physiological and pathological conditions.

The work realized during my PhD investigated presynaptic actin cytoskeletal arrangements and provided a model enabling their visualization with unprecedented optical accessibility. This study was conducted on induced excitatory presynapses which controlled orientation towards the glass ensured by the micropattern of periodically arranged dots of neuroligin-1. The extracellular epitope of this postsynaptic cell adhesion molecule (CAM) is known to interact with is presynaptic counterpart, neurexin-1, previously used by researchers for specific *in vitro* synapse formation (Funahashi et al., 2018; H. Tanaka et al., 2023). The properties of these two transsynaptic CAMs allowed studies of the synaptic compartment forming either onto the glass or in co-cultures with other transfected cell-types (Funahashi et al., 2018; Scheiffele et al., 2000). Neuroligins are involved in synapse formation and in the specification of synapses, that is either excitatory or inhibitory. Neuroligin-1 induces excitatory synapse specifications, while neuroligin-2 triggers inhibitory synapses. Replacing neuroligin-1 with neuroligin-2 and reproducing our experimental design may be useful to compare actin nanostructures between these two types of presynapses. Employing automated segmentation analysis to better distinguish actin clusters may uncover significant differences in actin nanostructure distribution between synaptic types. Quantitative characterizations are essential to highlight structural and functional relationships of the presynaptic actin nanostructures, but the conventional analysis has only allowed for determining the order of magnitude distinguishing actin corrals, mesh and rails. A new image analysis tool relying on point pattern analysis instead of the manual analysis used in my study could be appropriate to construct a detailed map of the presynaptic cytoskeletal architecture (Hugelier et al., 2024; Y. Le Wu et al., 2023). Depicting the spatial relationship of nearest neighbor distances between single point emitters rather than their overlap may discern

which localization belongs to the dense actin corrals, the faint actin mesh, or the linear rails. Spatial Pattern Analysis using Closest Events (SPACE) is appropriate to analyze images of dense presynaptic compartments. This tool may provide maps of presynaptic features, which will help define discrete structural differences between excitatory and inhibitory presynapses (Soltisz et al., 2024). This map, representing physiological conditions, can be compared to that of neuropathological presynapses. For instance, neuroligin and neurexin mutations are involved in cognitive diseases (Südhof, 2008). Genetically modified versions of neuroligins, mimicking mutations found in patients with familial autism-spectrum disorders, (Jamain et al., 2003; Laumonnier et al., 2004; Song et al., 1999; Zoghbi, 1986) may underpin significant differences in synaptic architecture between physiological and pathological conditions. Printing these mutated neuroligins onto the glass may enable the observation of presynaptic actin dynamics.

Moreover, comparing the established map of actin nanostructures and synaptic components to the pathological maps may address unanswered questions in the field. By exploiting the advantages of super-resolution microscopy and our presynapse-on-glass model, we may begin to address inquiries regarding actin cytoskeleton remodeling in human disease using patient-derived pluripotent stem cells from Down's syndrome, Alzheimer's disease and Autism Spectrum Disorder patients (Bamburg & Bernstein, 2016; Bernstein et al., 2011; Griesi-Oliveira et al., 2018; Maloney et al., 2005; Wurz et al., 2022). Achieving this nuanced understanding of how presynaptic actin structures and other components contribute to synaptic demands, will ultimately pave the way for understanding disease mechanisms and developing novel therapeutic strategies in the neuroscience field.

Conclusions

My PhD research successfully established the presynapse-on-glass model as an essential tool to decipher presynaptic actin nanoarchitecture and for investigating the relationship between structural elements and their functional implications.

This innovative model not only enhances the optical accessibility for super-resolution microscopy but also facilitates explorations combining live-cell imaging of dynamic processes like exocytosis and single molecule localization of actin at the presynaptic compartment. Three-dimensional imaging techniques successfully capture the spatial arrangement of actin corrals, mesh and rails and their localization in relation to presynaptic proteins. The findings indicate that our implemented model of induction affords controlled orientation of presynapses towards the glass as underlined by the aggregation of active zone scaffolding protein bassoon against the glass. We confirmed the presence of actin-enriched and actin non-enriched presynapses and correlated their fluorescence intensity levels with relative enrichment of presynaptic components as well as with cycling activity.

Future experiments leveraging our presynapse-on-glass model will be critical to elucidate the dynamics of actin nanostructures across synaptic states to enhance our comprehension of synaptic plasticity. As we await adequate advancements in imaging capabilities to capture actin remodeling processes with optimal spatial and temporal precision, the groundwork laid by my PhD research offers opportunities for new explorations. Further understanding of the complex interplay between actin structures and presynaptic components between different synaptic types, as well as between physiological and pathological model of presynapses, is now accessible.

My PhD research focused on understanding the presynaptic actin cytoskeleton by developing and employing our presynapse-on-glass model. The simplicity and adaptability of this approach, which enables printing a variety of molecules, expands its application potential – limited only by the creativity of the experimental designer.

Bibliography

Alberti, P., Semperboni, S., Cavaletti, G., & Scuteri, A. (2022). Neurons: The Interplay between Cytoskeleton, Ion Channels/Transporters and Mitochondria. In *Cells* (Vol. 11, Issue 16). MDPI. https://doi.org/10.3390/cells11162499

Albrecht, D., Winterflood, C. M., Sadeghi, M., Tschager, T., Noé, F., & Ewers, H. (2016). Nanoscopic compartmentalization of membrane protein motion at the axon initial segment. *Journal of Cell Biology*, *215*(1). https://doi.org/10.1083/jcb.201603108

Allison, D. W., Gelfand, V. I., Spector, I., & Craig, A. M. (1998). *Role of Actin in Anchoring Postsynaptic Receptors in Cultured Hippocampal Neurons: Differential Attachment of NMDA versus AMPA Receptors*.

Anggono, V., & Huganir, R. L. (2012). Regulation of AMPA receptor trafficking and synaptic plasticity. In *Current Opinion in Neurobiology* (Vol. 22, Issue 3, pp. 461–469). https://doi.org/10.1016/j.conb.2011.12.006

Baas, P. W., Deitch, J. S., Black, M. M., & Banker, G. A. (1988). Polarity orientation of microtubules in hippocampal neurons: Uniformity in the axon and nonuniformity in the dendrite. In *Proc. Nati. Acad. Sci. USA* (Vol. 85).

Baas, P. W., & Lin, S. (2011). Hooks and comets: The story of microtubule polarity orientation in the neuron. *Developmental Neurobiology*, *71*(6), 403–418. https://doi.org/10.1002/dneu.20818

Balzarotti, F., Eilers, Y., Gwosch, K. C., Gynnå, A. H., Westphal, V., Stefani, F. D., Elf, J., & Hell, S. W. (2017). Nanometer resolution imaging and tracking of fluorescent molecules with minimal photon fluxes. *Science*, *355*(6325), 606–612. https://doi.org/10.1126/science.aak9913

Bamburg, J. R., & Bernstein, B. W. (2010). Roles of ADF/cofilin in actin polymerization and beyond. In *F1000 Biology Reports* (Vol. 2, Issue 1). https://doi.org/10.3410/B2-62

Bamburg, J. R., & Bernstein, B. W. (2016). Actin dynamics and cofilin-actin rods in alzheimer disease. In *Cytoskeleton* (Vol. 73, Issue 9, pp. 477–497). John Wiley and Sons Inc. https://doi.org/10.1002/cm.21282

Banker, G. (2018). The development of neuronal polarity: A retrospective view. In *Journal of Neuroscience* (Vol. 38, Issue 8, pp. 1867–1873). Society for Neuroscience. https://doi.org/10.1523/JNEUROSCI.1372-16.2018

Bär, J., Kobler, O., Van Bommel, B., & Mikhaylova, M. (2016). Periodic F-actin structures shape the neck of dendritic spines. *Scientific Reports*, *6*. https://doi.org/10.1038/srep37136

Benoıˆt Zuber, B., Nikonenko, I., Klauser, P., Muller, D., & Dubochet, J. (2005). *The mammalian central nervous synaptic cleft contains a high density of periodically organized complexes*. www.pnas.orgcgidoi10.1073pnas.0509527102

Bernstein, B. W., & Bamburg, J. R. (2002). *Actin-ATP Hydrolysis Is a Major Energy Drain for Neurons*.

Bernstein, B. W., Maloney, M. T., & Bamburg, J. R. (2011). *Actin and Diseases of the Nervous System* (pp. 201–234). https://doi.org/10.1007/978-1-4419-7368-9_11

Bhaskar, H., Kleinjan, D. J., Oi, C., Gidden, Z., Rosser, S. J., Horrocks, M. H., & Regan, L. (2023). Live-cell super-resolution imaging of actin using LifeAct-14 with a PAINT-based approach. *Protein Science*, *32*(2). https://doi.org/10.1002/pro.4558

Bingham, D., Elise Jakobs, C., Wernert, F., Boroni-Rueda, F., Jullien, N., Schentarra, E.-M., Friedl, K., da Costa Moura, J., Michelle van Bommel, D., Caillol, G., Da Costa Moura, J., Ogawa, Y., Papandréou, M.-J., & Leterrier, C. (2023). Presynapses contain distinct actin nanostructures. *Journal of Cell Biology*, *2023*(10). https://doi.org/10.1083/jcb.202208110ï

Bloom, O., Evergren, E., Tomilin, N., Kjaerulff, O., Löw, P., Brodin, L., Pieribone, V. A., Greengard, P., & Shupliakov, O. (2003). Colocalization of synapsin and actin during synaptic vesicle recycling. *Journal of Cell Biology*, *161*(4), 737–747. https://doi.org/10.1083/jcb.200212140

Bodakuntla, S., Nedozralova, H., Basnet, N., & Mizuno, N. (2021). Cytoskeleton and Membrane Organization at Axon Branches. In *Frontiers in Cell and Developmental Biology* (Vol. 9). Frontiers Media S.A. https://doi.org/10.3389/fcell.2021.707486

Breitsprecher, D., & Goode, B. L. (2013). Formins at a glance. In *Journal of Cell Science* (Vol. 126, Issue 1, pp. 1–7). https://doi.org/10.1242/jcs.107250

Brose, N., Brunger, A., Cafiso, D., Chapman, E. R., Diao, J., Hughson, F. M., Jackson, M. B., Jahn, R., Lindau, M., Ma, C., Rizo, J., Shin, Y. K., Söllner, T. H., Tamm, L., Yoon, T. Y., & Zhang, Y. (2019). Synaptic vesicle fusion: today and beyond. In *Nature structural & molecular biology* (Vol. 26, Issue 8, pp. 663–668). NLM (Medline). https://doi.org/10.1038/s41594-019-0277-z

Brown, A., Slaughter, T., & Black, M. M. (1992). *Newly Assembled Microtubules Are Concentrated in the Proximal and Distal Regions of Growing Axons*.

Bu, Y., Wang, N., Wang, S., Sheng, T., Tian, T., Chen, L., Pan, W., Zhu, M., Luo, J., & Lu, W. (2015). Myosin IIb-dependent regulation of actin dynamics is required for N-Methyl-D-aspartate receptor trafficking during synaptic plasticity. *Journal of Biological Chemistry*, *290*(42), 25395–25410. https://doi.org/10.1074/jbc.M115.644229

Burry, R. W., & Matthew, W. D. (1986). Presynaptic elements formed on polylysine-coated beads contain synaptic vesicle antigens. In *Journal of Neurocytology* (Vol. 15).

Bury, L. A. D., & Sabo, S. L. (2011). Coordinated trafficking of synaptic vesicle and active zone proteins prior to synapse formation. *Neural Development*, *6*(1). https://doi.org/10.1186/1749-8104-6-24

Butler-Hallissey Ciarán, & Leterrier Christophe. (2024). Super-resolution imaging of the neuronal cytoskeleton. *J Cell Science*. https://zenodo.org/records/13171364

Carlsson, A. E. (2018). Membrane bending by actin polymerization. In *Current Opinion in Cell Biology* (Vol. 50, pp. 1–7). Elsevier Ltd. https://doi.org/10.1016/j.ceb.2017.11.007

Carvalhais, L. G., Martinho, V. C., Ferreiro, E., & Pinheiro, P. S. (2021). Unraveling the Nanoscopic Organization and Function of Central Mammalian Presynapses With

Super-Resolution Microscopy. In *Frontiers in Neuroscience* (Vol. 14). Frontiers Media S.A. https://doi.org/10.3389/fnins.2020.578409

Chenouard, N., Xuan, F., & Tsien, R. W. (2020). Synaptic vesicle traffic is supported by transient actin filaments and regulated by PKA and NO. *Nature Communications*, *11*(1). https://doi.org/10.1038/s41467-020-19120-1

Chia, P. H., Chen, B., Li, P., Rosen, M. K., & Shen, K. (2014). Local F-actin network links synapse formation and axon branching. *Cell*, *156*(1–2), 208–220. https://doi.org/10.1016/j.cell.2013.12.009

Chou, F.-S., & Wang, P.-S. (2016). The Arp2/3 complex is essential at multiple stages of neural development. *Neurogenesis*, *3*(1), e1261653. https://doi.org/10.1080/23262133.2016.1261653

Cingolani, L. A., & Goda, Y. (2008). Actin in action: The interplay between the actin cytoskeleton and synaptic efficacy. In *Nature Reviews Neuroscience* (Vol. 9, Issue 5, pp. 344–356). https://doi.org/10.1038/nrn2373

Cole JC, Villa BR, & Wilkinson RS. (2000). Disruption of actin impedes transmitter release in snake motor terminals. *J Physiology* , *525*(Pt 3), 579–586.

Colombo, J., Antkowiak, A., Kogan, K., Kotila, T., Elliott, J., Guillotin, A., Lappalainen, P., & Michelot, A. (2021). A functional family of fluorescent nucleotide analogues to investigate actin dynamics and energetics. *Nature Communications*, *12*(1). https://doi.org/10.1038/s41467-020-20827-4

Costa, A. R., & Sousa, M. M. (2021). The role of the membrane-associated periodic skeleton in axons. In *Cellular and Molecular Life Sciences* (Vol. 78, Issue 13, pp. 5371–5379). Springer Science and Business Media Deutschland GmbH. https://doi.org/10.1007/s00018-021-03867-x

Costa, M., Draper, B. W., & Priess, J. R. (1997). The Role of Actin Filaments in Patterning the Caenorhabditis elegans Cuticle. In *DEVELOPMENTAL BIOLOGY* (Vol. 184).

Courtemanche, N. (2018). Mechanisms of formin-mediated actin assembly and dynamics. In *Biophysical Reviews* (Vol. 10, Issue 6, pp. 1553–1569). Springer Verlag. https://doi.org/10.1007/s12551-018-0468-6

Courtemanche, N., Pollard, T. D., & Chen, Q. (2016a). Avoiding artefacts when counting polymerized actin in live cells with LifeAct fused to fluorescent proteins. *Nature Cell Biology*, *18*(6), 676–683. https://doi.org/10.1038/ncb3351

Courtemanche, N., Pollard, T. D., & Chen, Q. (2016b). Avoiding artefacts when counting polymerized actin in live cells with LifeAct fused to fluorescent proteins. *Nature Cell Biology*, *18*(6), 676–683. https://doi.org/10.1038/ncb3351

Cunningham, K. L., & Littleton, J. T. (2023). Mechanisms controlling the trafficking, localization, and abundance of presynaptic Ca2+ channels. In *Frontiers in Molecular Neuroscience* (Vol. 15). Frontiers Media S.A. https://doi.org/10.3389/fnmol.2022.1116729

Czöndör, K., Garcia, M., Argento, A., Constals, A., Breillat, C., Tessier, B., & Thoumine, O. (2013). Micropatterned substrates coated with neuronal adhesion molecules for high-content study of synapse formation. *Nature Communications*, *4*. https://doi.org/10.1038/ncomms3252

Dalva, M. B., McClelland, A. C., & Kayser, M. S. (2007). Cell adhesion molecules: Signalling functions at the synapse. In *Nature Reviews Neuroscience* (Vol. 8, Issue 3, pp. 206–220). https://doi.org/10.1038/nrn2075

Dani, A., Huang, B., Bergan, J., Dulac, C., & Zhuang, X. (2010). Superresolution Imaging of Chemical Synapses in the Brain. *Neuron*, *68*(5), 843–856. https://doi.org/10.1016/j.neuron.2010.11.021

Deguchi, T., Iwanski, M. K., Schentarra, E. M., Heidebrecht, C., Schmidt, L., Heck, J., Weihs, T., Schnorrenberg, S., Hoess, P., Liu, S., Chevyreva, V., Noh, K. M., Kapitein, L. C., & Ries, J. (2023). Direct observation of motor protein stepping in living cells using MINFLUX. *Science*, *379*(6636), 1010–1015. https://doi.org/10.1126/science.ade2676

Desroches, S., & Harris, A. R. (2023). Quantifying cytoskeletal organization from optical microscopy data. In *Frontiers in Cell and Developmental Biology* (Vol. 11). Frontiers Media SA. https://doi.org/10.3389/fcell.2023.1327994

D'Este, E., Kamin, D., Göttfert, F., El-Hady, A., & Hell, S. W. (2015). STED Nanoscopy Reveals the Ubiquity of Subcortical Cytoskeleton Periodicity in Living Neurons. *Cell Reports*, *10*(8), 1246–1251. https://doi.org/10.1016/j.celrep.2015.02.007

D'Este, E., Kamin, D., Velte, C., Göttfert, F., Simons, M., & Hell, S. W. (2016). Subcortical cytoskeleton periodicity throughout the nervous system. *Scientific Reports*, *6*. https://doi.org/10.1038/srep22741

Ding, E. A., & Kumar, S. (2024). Neurofilament Biophysics: From Structure to Biomechanics. In *Molecular Biology of the Cell* (Vol. 35, Issue 5). American Society for Cell Biology. https://doi.org/10.1091/mbc.E23-11-0438

Doerr, A. (2016). Cryo-electron tomography. In *Nature Methods* (Vol. 14, Issue 1, p. 34). Nature Publishing Group. https://doi.org/10.1038/nmeth.4115

Dotti, C. G., Sullivan, C. A., & Banker, G. A. (1988). The Establishment of Polarity by Hippocampal Neurons in Culture. In *The Journal of Neuroscience: Vol. I* (Issue 4).

E Bocinelli. (2005). Neuroscience. *Encyclopedia of Condensed Matter Physics, Elsevier*, 64–69. https://doi.org/https://doi.org/10.1016/B0-12-369401-9/00394-6

EL-Husseini ALaa EL-Din, Schnell Eric, Chetkovich Dane M., Nicoll Roger A., & Bredt David S. (2000). PSD-95 Involvement in Maturation of Excitatory Synapses. *Science*, *290*, 1364–1368.

Fenster, S. D., Kessels, M. M., Qualmann, B., Chung, W. J., Nash, J., Gundelfinger, E. D., & Garner, C. C. (2003). Interactions between Piccolo and the actin/dynamin-binding protein Abp1 link vesicle endocytosis to presynaptic active zones. *Journal of Biological Chemistry*, *278*(22), 20268–20277. https://doi.org/10.1074/jbc.M210792200

Fernández-Busnadiego, R., Zuber, B., Maurer, U. E., Cyrklaff, M., Baumeister, W., & Lučić, V. (2010). Quantitative analysis of the native presynaptic cytomatrix by cryoelectron tomography. *Journal of Cell Biology*, *188*(1), 145–156. https://doi.org/10.1083/jcb.200908082

Fischer, M., Kaech, S., Knutti, D., & Matus, A. (1998). Rapid Actin-Based Plasticity in Dendritic Spines. In *Neuron* (Vol. 20). http://www.neuron.org/supplemental/20/5/847

Fish, K. N. (2009). Total internal reflection fluorescence (TIRF) microscopy. In *Current Protocols in Cytometry* (Issue SUPPL.50). John Wiley and Sons Inc. https://doi.org/10.1002/0471142956.cy1218s50

Fletcher, D. A., & Mullins, R. D. (2010). Cell mechanics and the cytoskeleton. In *Nature* (Vol. 463, Issue 7280, pp. 485–492). https://doi.org/10.1038/nature08908

Flores, L. R., Keeling, M. C., Zhang, X., Sliogeryte, K., & Gavara, N. (2019). Lifeact-GFP alters F-actin organization, cellular morphology and biophysical behaviour. *Scientific Reports*, *9*(1). https://doi.org/10.1038/s41598-019-40092-w

Flynn, K. C., Hellal, F., Neukirchen, D., Jacob, S., Tahirovic, S., Dupraz, S., Stern, S., Garvalov, B. K., Gurniak, C., Shaw, A. E., Meyn, L., Wedlich-Söldner, R., Bamburg, J. R., Small, J. V., Witke, W., & Bradke, F. (2012). ADF/Cofilin-Mediated Actin Retrograde Flow Directs Neurite Formation in the Developing Brain. *Neuron*, *76*(6), 1091–1107. https://doi.org/10.1016/j.neuron.2012.09.038

Flynn, K. C., Pak, C. W., Shaw, A. E., Bradke, F., & Bamburg, J. R. (2009). Growth cone-like waves transport actin and promote axonogenesis and neurite branching. *Developmental Neurobiology*, *69*(12), 761–779. https://doi.org/10.1002/dneu.20734

Frank Bradke, & Calros G. Dotti. (1999). *The Role of Local Actin Instability in Axon Formation*. http://dx.doi.org/10.1126/science.283.5409.1931

Frost, N. A., Shroff, H., Kong, H., Betzig, E., & Blanpied, T. A. (2010). Single-molecule discrimination of discrete perisynaptic and distributed sites of actin filament assembly within dendritic spines. *Neuron*, *67*(1), 86–99. https://doi.org/10.1016/j.neuron.2010.05.026

Funahashi, J., Tanaka, H., & Hirano, T. (2018). Visualization of synchronous or asynchronous release of single synaptic vesicle in active-zone-like membrane formed on neuroligin-coated glass surface. *Frontiers in Cellular Neuroscience*, *12*. https://doi.org/10.3389/fncel.2018.00140

Gallo, G. (2016). Encyclopedia of Signaling Molecules. In *Encyclopedia of Signaling Molecules*. Springer International Publishing. https://doi.org/10.1007/978-3-319-67199-4

Ganguly, A., Tang, Y., Wang, L., Ladt, K., Loi, J., Dargent, B., Leterrier, C., & Roy, S. (2015). A dynamic formin-dependent deep F-actin network in axons. *Journal of Cell Biology*, *210*(3), 401–417. https://doi.org/10.1083/jcb.201506110

Gentile, J. E., Carrizales, M. G., & Koleske, A. J. (2022). Control of Synapse Structure and Function by Actin and Its Regulators. In *Cells* (Vol. 11, Issue 4). MDPI. https://doi.org/10.3390/cells11040603

Ghose, A., & Pullarkat, P. (2023). The role of mechanics in axonal stability and development. In *Seminars in Cell and Developmental Biology* (Vol. 140, pp. 22–34). Elsevier Ltd. https://doi.org/10.1016/j.semcdb.2022.06.006

Gilman, S. R., Iossifov, I., Levy, D., Ronemus, M., Wigler, M., & Vitkup, D. (2011). Rare De Novo Variants Associated with Autism Implicate a Large Functional Network of Genes Involved in Formation and Function of Synapses. *Neuron*, *70*(5), 898–907. https://doi.org/10.1016/j.neuron.2011.05.021

Glebov, O. O., Jackson, R. E., Winterflood, C. M., Owen, D. M., Barker, E. A., Doherty, P., Ewers, H., & Burrone, J. (2017). Nanoscale Structural Plasticity of the Active Zone Matrix Modulates Presynaptic Function. *Cell Reports*, *18*(11), 2715–2728. https://doi.org/10.1016/j.celrep.2017.02.064

Golgi, C. (1903). golgioperaomniav3. *Ulrico Hoepli*, *Volume 1*.

Grabner, C. P., Jansen, I., Neef, J., Weihs, T., Schmidt, R., Riedel, D., Wurm, C. A., & Moser, T. (2022). Resolving the molecular architecture of the photoreceptor active zone with 3D-MINFLUX. In *Sci. Adv* (Vol. 8). https://www.science.org

Griesi-Oliveira, K., Suzuki, A. M., Alves, A. Y., Mafra, A. C. C. N., Yamamoto, G. L., Ezquina, S., Magalhães, Y. T., Forti, F. L., Sertie, A. L., Zachi, E. C., Vadasz, E., & Passos-Bueno, M. R. (2018). Actin cytoskeleton dynamics in stem cells from autistic individuals. *Scientific Reports*, *8*(1). https://doi.org/10.1038/s41598-018-29309-6

Han, B., Zhou, R., Xia, C., & Zhuang, X. (2017). Structural organization of the actin-spectrin–based membrane skeleton in dendrites and soma of neurons. *Proceedings of the National Academy of Sciences of the United States of America*, *114*(32), E6678–E6685. https://doi.org/10.1073/pnas.1705043114

Hanley, J. G. (2014). Actin-dependent mechanisms in AMPA receptor trafficking. In *Frontiers in Cellular Neuroscience* (Vol. 8, Issue November). Frontiers Research Foundation. https://doi.org/10.3389/fncel.2014.00381

Hirokawa, N., Sobue, K., Kanda, K., Harada, A., & Yorifuji, H. (1989). *The Cytoskeletal Architecture of the Presynaptic Terminal and Molecular Structure of Synapsin 1*. http://rupress.org/jcb/article-pdf/108/1/111/1461210/111.pdf

Holland, S. M., & Gallo, G. (2023). Actin cytoskeletal dynamics do not impose an energy drain on growth cone bioenergetics. *Journal of Cell Science*, *136*(16). https://doi.org/10.1242/jcs.261356

Hotulainen, P., Llano, O., Smirnov, S., Tanhuanpää, K., Faix, J., Rivera, C., & Lappalainen, P. (2009). Defning mechanisms of actin polymerization and depolymerization during Dendritic spine morphogenesis. *Journal of Cell Biology*, *185*(2), 323–339. https://doi.org/10.1083/jcb.200809046

Huang, B., Bates, M., & Zhuang, X. (2009). Super-resolution fluorescence microscopy. In *Annual Review of Biochemistry* (Vol. 78, pp. 993–1016). https://doi.org/10.1146/annurev.biochem.77.061906.092014

Hugelier, S., Tang, Q., Kim, H. H. S., Gyparaki, M. T., Bond, C., Santiago-Ruiz, A. N., Porta, S., & Lakadamyali, M. (2024). ECLiPSE: a versatile classification technique for structural and morphological analysis of 2D and 3D single-molecule localization microscopy data. *Nature Methods*. https://doi.org/10.1038/s41592-024-02414-3

Hughes, C. A., & Bennett, V. (1995). Adducin: A physical model with implications for function in assembly of spectrin-actin complexes. *Journal of Biological Chemistry*, *270*(32), 18990–18996. https://doi.org/10.1074/jbc.270.32.18990

Igarashi, M., Nozumi, X., Wu, L. G., Zanacchi, F. C., Katona, X., Barna, X. L., Xu, P., Zhang, M., Xue, F., & Boyden, E. (2018). New observations in neuroscience using superresolution microscopy. *Journal of Neuroscience*, *38*(44), 9459–9467. https://doi.org/10.1523/JNEUROSCI.1678-18.2018

Ignácz, A., Nagy-Herczeg, D., Hausser, A., & Schlett, K. (2023). Dendritic effects of genetically encoded actin-labeling probes in cultured hippocampal neurons. *Molecular Biology of the Cell*, *34*(7). https://doi.org/10.1091/mbc.E22-08-0331

Insuk Song, R. L. H. (2002). Regulation of AMPA receptors during synaptic plasticity. In *TRENDS in Neurosciences* (Vol. 25, Issue 11). http://tins.trends.com

Iwanski, M. K., & Kapitein, L. C. (2023). Cellular cartography: Towards an atlas of the neuronal microtubule cytoskeleton. In *Frontiers in Cell and Developmental Biology* (Vol. 11). Frontiers Media SA. https://doi.org/10.3389/fcell.2023.1052245

Jackson, R. E., Compans, B., & Burrone, J. (2022). Correlative Live-Cell and Super-Resolution Imaging to Link Presynaptic Molecular Organisation With Function. *Frontiers in Synaptic Neuroscience*, *14*. https://doi.org/10.3389/fnsyn.2022.830583

Jamain, S., Quach, H., Betancur, C., Råstam, M., Colineaux, C., Gillberg, C., Soderstrom, H., Giros, B., Leboyer, M., Gillberg, C., Bourgeron, T., Nydén, A., Philippe, A., Cohen, D., Chabane, N., Mouren-Siméoni, M. C., Brice, A., Sponheim, E., Spurkland, I., … Van Maldergem, L. (2003). Mutations of the X-linked genes encoding neuroligins NLGN3 and NLGN4 are associated with autism. *Nature Genetics*, *34*(1), 27–29. https://doi.org/10.1038/ng1136

Jang, Y., Soekmadji, C., Mitchell, J. M., Thomas, W. G., & Thorn, P. (2012). Real-time measurement of f-actin remodelling during exocytosis using lifeact-EGFP transgenic animals. *PLoS ONE*, *7*(7). https://doi.org/10.1371/journal.pone.0039815

Jung, M., Kim, D., & Mun, J. Y. (2020). Direct Visualization of Actin Filaments and Actin-Binding Proteins in Neuronal Cells. In *Frontiers in Cell and Developmental Biology* (Vol. 8). Frontiers Media S.A. https://doi.org/10.3389/fcell.2020.588556

Kapitein, L. C., & Hoogenraad, C. C. (2015). Building the Neuronal Microtubule Cytoskeleton. In *Neuron* (Vol. 87, Issue 3, pp. 492–506). Cell Press. https://doi.org/10.1016/j.neuron.2015.05.046

Kim, E. J., Jeon, C. S., Lee, S. Y., Hwang, I., & Chung, T. D. (2016). Robust Type-specific Hemisynapses Induced by Artificial Dendrites. *Scientific Reports*, *6*. https://doi.org/10.1038/srep24210

Komada, M., & Soriano, P. (2002). βIV-spectrin regulates sodium channel clustering through ankyrin-G at axon initial segments and nodes of Ranvier. *Journal of Cell Biology*, *156*(2), 337–348. https://doi.org/10.1083/jcb.200110003

Krstić, R. V. (1985). General Histology of the Mammal. In *General Histology of the Mammal: Vol. Plate 168. Synapses.* Springer Berlin Heidelberg. https://doi.org/10.1007/978-3-642-70420-8

Kudryashova, I. V. (2021). The Reorganization of the Actin Matrix as a Factor of Presynaptic Plasticity. *Neurochemical Journal*, *15*(3), 217–225. https://doi.org/10.1134/s1819712421030089

Kuriu, T., Inoue, A., Bito, H., Sobue, K., & Okabe, S. (2006). Differential control of postsynaptic density scaffolds via actin-dependent and -independent mechanisms. *Journal of Neuroscience*, *26*(29), 7693–7706. https://doi.org/10.1523/JNEUROSCI.0522-06.2006

Lamprecht, R. (2021). Actin cytoskeleton role in the maintenance of neuronal morphology and long-term memory. In *Cells* (Vol. 10, Issue 7). MDPI. https://doi.org/10.3390/cells10071795

Landis, D. M. D., Hall, A. K., Weinstein, L. A., & Reese, T. S. (1988). The Organization of Cytoplasm at the Presynaptic Active Zonk df a Central Nervous System Synapse_. In *Neuron* (Vol. 1).

Laumonnier, F., Bonnet-Brilhault, F., Gomot, M., Blanc, R., David, A., Moizard, M.-P., Raynaud, M., Ronce, N., Lemonnier, E., Calvas, P., Laudier, B., Chelly, J., Fryns, J.-P., Ropers, H.-H., Hamel, B. C. J., Andres, C., Barthélémy, C., Moraine, C., & Briault, S. (2004). Report X-Linked Mental Retardation and Autism Are Associated with a Mutation in the NLGN4 Gene, a Member of the Neuroligin Family. In *Am. J. Hum. Genet* (Vol. 74).

Lavoie-Cardinal, F., Bilodeau, A., Lemieux, M., Gardner, M. A., Wiesner, T., Laramée, G., Gagné, C., & De Koninck, P. (2020). Neuronal activity remodels the F-actin based submembrane lattice in dendrites but not axons of hippocampal neurons. *Scientific Reports*, *10*(1). https://doi.org/10.1038/s41598-020-68180-2

Lei, W., Omotade, O. F., Myers, K. R., & Zheng, J. Q. (2016). Actin cytoskeleton in dendritic spine development and plasticity. In *Current Opinion in Neurobiology* (Vol. 39, pp. 86–92). Elsevier Ltd. https://doi.org/10.1016/j.conb.2016.04.010

Leite, S. C., Pinto-Costa, R., & Sousa, M. M. (2021). Actin dynamics in the growth cone: a key player in axon regeneration. In *Current Opinion in Neurobiology* (Vol. 69, pp. 11–18). Elsevier Ltd. https://doi.org/10.1016/j.conb.2020.11.015

Leite, S. C., Sampaio, P., Sousa, V. F., Nogueira-Rodrigues, J., Pinto-Costa, R., Peters, L. L., Brites, P., & Sousa, M. M. (2016). The Actin-Binding Protein α-Adducin Is Required for Maintaining Axon Diameter. *Cell Reports*, *15*(3), 490–498. https://doi.org/10.1016/j.celrep.2016.03.047

Leite, S. C., & Sousa, M. M. (2016). The neuronal and actin commitment: Why do neurons need rings? *Cytoskeleton*, *73*(9), 424–434. https://doi.org/10.1002/cm.21273

Lelek, M., Gyparaki, M. T., Beliu, G., Schueder, F., Griffié, J., Manley, S., Jungmann, R., Sauer, M., Lakadamyali, M., & Zimmer, C. (2021). Single-molecule localization microscopy. In *Nature Reviews Methods Primers* (Vol. 1, Issue 1). Springer Nature. https://doi.org/10.1038/s43586-021-00038-x

Leterrier, C. (2018). The axon initial segment: An updated viewpoint. *Journal of Neuroscience*, *38*(9), 2135–2145. https://doi.org/10.1523/JNEUROSCI.1922-17.2018

Leterrier, C. (2021a). A pictorial history of the neuronal cytoskeleton. *Journal of Neuroscience*, *41*(1), 11–27. https://doi.org/10.1523/JNEUROSCI.2872-20.2020

Leterrier, C. (2021b). Putting the axonal periodic scaffold in order. In *Current Opinion in Neurobiology* (Vol. 69, pp. 33–40). Elsevier Ltd. https://doi.org/10.1016/j.conb.2020.12.015

Leterrier, C., Dubey, P., & Roy, S. (2017). The nano-architecture of the axonal cytoskeleton. In *Nature Reviews Neuroscience* (Vol. 18, Issue 12, pp. 713–726). Nature Publishing Group. https://doi.org/10.1038/nrn.2017.129

Leterrier, C., Potier, J., Caillol, G., Debarnot, C., Rueda Boroni, F., & Dargent, B. (2015). Nanoscale Architecture of the Axon Initial Segment Reveals an Organized and Robust Scaffold. *Cell Reports*, *13*(12), 2781–2793. https://doi.org/10.1016/j.celrep.2015.11.051

Letourneau, P. C. (2009). Actin in axons: Stable scaffolds and dynamic filaments. *Results and Problems in Cell Differentiation*, *48*, 65–90. https://doi.org/10.1007/400_2009_15

Liaci, C., Camera, M., Caslini, G., Rando, S., Contino, S., Romano, V., & Merlo, G. R. (2021). Neuronal cytoskeleton in intellectual disability: From systems biology and modeling to therapeutic opportunities. *International Journal of Molecular Sciences*, *22*(11). https://doi.org/10.3390/ijms22116167

Liu, C. H., & Rasband, M. N. (2019). Axonal spectrins: Nanoscale organization, functional domains and spectrinopathies. In *Frontiers in Cellular Neuroscience* (Vol. 13). Frontiers Media S.A. https://doi.org/10.3389/fncel.2019.00234

Lorenzo, D. N., Edwards, R. J., & Slavutsky, A. L. (2023). Spectrins: molecular organizers and targets of neurological disorders. In *Nature Reviews Neuroscience* (Vol. 24, Issue 4, pp. 195–212). Springer Nature. https://doi.org/10.1038/s41583-022-00674-6

Lucido, A. L., Sanchez, F. S., Thostrup, P., Kwiatkowski, A. V., Leal-Ortiz, S., Gopalakrishnan, G., Liazoghli, D., Belkaid, W., Lennox, R. B., Grutter, P., Garner, C. C., & Colman, D. R. (2009). Rapid assembly of functional presynaptic boutons triggered by adhesive contacts. *Journal of Neuroscience*, *29*(40), 12449–12466. https://doi.org/10.1523/JNEUROSCI.1381-09.2009

Lüscher, C., & Malenka, R. C. (2012). NMDA receptor-dependent long-term potentiation and long-term depression (LTP/LTD). *Cold Spring Harbor Perspectives in Biology*, *4*(6), 1–15. https://doi.org/10.1101/cshperspect.a005710

Lyser, K. M. (1968). Early Differentiation of Motor Neuroblasts in the Chick Embryo as Studied by Electron Microscopy II. Microtubules and Neurofilamentsl. In *ELOP3IFXTAL BIOLOGY* (Vol. 17).

Maloney, M. T., Minamide, L. S., Kinley, A. W., Boyle, J. A., & Bamburg, J. R. (2005). β-secretase-cleaved amyloid precursor protein accumulates at actin inclusions induced in neurons by stress or amyloid β: A feedforward mechanism for alzheimer's disease. *Journal of Neuroscience*, *25*(49), 11313–11321. https://doi.org/10.1523/JNEUROSCI.3711-05.2005

Maraspini, R., Wang, C. H., & Honigmann, A. (2020). Optimization of 2D and 3D cell culture to study membrane organization with STED microscopy. *Journal of Physics D: Applied Physics*, *53*(1). https://doi.org/10.1088/1361-6463/ab45df

Markham, J. A., & Fifkova, E. (1986). Actin filament organization within dendrites and dendritic spines during development. In *Developmental Brain Research* (Vol. 27).

Maschi, D., Gramlich, M. W., & Klyachko, V. A. (2018). Myosin V functions as a vesicle tether at the plasma membrane to control neurotransmitter release in central synapses. *ELife*. https://doi.org/10.7554/eLife.39440.001

Matus, A., Ackermann, M., Pehling, G., Byerst, H. R., & Fujiwarat, K. (1982). High actin concentrations in brain dendritic spines and postsynaptic densities

cytoskeleton/immunocytochemistry/dendritesi/synaptic junction/synaptic plasticity). In *Proc. Natd Acad. Sci. USA* (Vol. 79). https://www.pnas.org

McGough, A., Pope, B., Chiu, W., Weeds, A., & McLean, M. (1997). Cofilin Changes the Twist of F-Actin: Implications for Actin Filament Dynamics and Cellular Function. In *The Journal of Cell Biology* (Vol. 138, Issue 4). http://www.jcb.org

Mihaila, T. S., B€, C., Ostersehlt, L. M., Pape, J. K., Keller-Findeisen, J., Sahl, S. J., & Hell, S. W. (2022). *Enhanced incorporation of subnanometer tags into cellular proteins for fluorescence nanoscopy via optimized genetic code expansion*. https://doi.org/10.1073/pnas

Moosmayer, T., Kiszka, K. A., Westphal, V., Pape, J. K., Leutenegger, M., Steffens, H., Grant, S. G. N., Sahl, S. J., & Hell, S. W. (2024). *MINFLUX fluorescence nanoscopy in biological tissue*. https://doi.org/10.1101/2024.07.06.602333

Morachevskaya, E. A., & Sudarikova, A. V. (2021). Actin dynamics as critical ion channel regulator: ENaC and Piezo in focus. In *American Journal of Physiology - Cell Physiology* (Vol. 320, Issue 5, pp. C696–C702). American Physiological Society. https://doi.org/10.1152/ajpcell.00368.2020

Morales, M., Colicos, M. A., & Goda, Y. (2000). Actin-Dependent Regulation of Neurotransmitter Release at Central Synapses presynaptic nerve terminals (Fifkova and Delay, 1982; Gotow et al., 1991). Since most F-actin appears to oc-cupy the internal space of presynaptic nerve terminals formed many puncta that colocalized with a presynaptic. In *Neuron* (Vol. 27).

Morris, R. L., & Hollenbeck, P. J. (n.d.). *Axonal Transport of Mitochondria along Microtubules and F-Actin in Living Vertebrate Neurons*.

Mullins, R. D., & Hansen, S. D. (2013). In vitro studies of actin filament and network dynamics. In *Current Opinion in Cell Biology* (Vol. 25, Issue 1, pp. 6–13). Elsevier Ltd. https://doi.org/10.1016/j.ceb.2012.11.007

Muñoz-Lasso, D. C., Romá-Mateo, C., Pallardó, F. V., & Gonzalez-Cabo, P. (2020). Much More Than a Scaffold: Cytoskeletal Proteins in Neurological Disorders. In *Cells* (Vol. 9, Issue 2). NLM (Medline). https://doi.org/10.3390/cells9020358

Nagasaki, A., Kijima, S. T., Yumoto, T., Imaizumi, M., Yamagishi, A., Kim, H., Nakamura, C., & Uyeda, T. Q. P. (2017). The Position of the GFP Tag on Actin Affects the Filament Formation in Mammalian Cells. In *CELL STRUCTURE AND FUNCTION* (Vol. 42).

Negi, A. S., Gautam, Y., Alam, S., Chanda, D., Luqman, S., Sarkar, J., Khan, F., & Konwar, R. (2015). Natural antitubulin agents: Importance of 3,4,5-trimethoxyphenyl fragment. In *Bioorganic and Medicinal Chemistry* (Vol. 23, Issue 3, pp. 373–389). Elsevier Ltd. https://doi.org/10.1016/j.bmc.2014.12.027

Nonaka, M., Doi, T., Fujiyoshi, Y., Takemoto-Kimura, S., & Bito, H. (2006). Essential contribution of the ligand-binding βB/βC loop of PDZ1 and PDZ2 in the regulation of postsynaptic clustering, scaffolding, and localization of postsynaptic density-95. *Journal of Neuroscience*, *26*(3), 763–774. https://doi.org/10.1523/JNEUROSCI.2489-05.2006

Nosov, G., Kahms, M., & Klingauf, J. (2020). The Decade of Super-Resolution Microscopy of the Presynapse. In *Frontiers in Synaptic Neuroscience* (Vol. 12). Frontiers Media S.A. https://doi.org/10.3389/fnsyn.2020.00032

Oevel, K., Hohensee, S., Kumar, A., Rosas-Brugada, I., Bartolini, F., Soykan, T., & Haucke, V. (2024). Rho GTPase signaling and mDia facilitate endocytosis via presynaptic actin. *ELife*, *12*. https://doi.org/10.7554/eLife.92755

Ogunmowo, T. H., Jing, H., Raychaudhuri, S., Kusick, G. F., Imoto, Y., Li, S., Itoh, K., Ma, Y., Jafri, H., Dalva, M. B., Chapman, E. R., Ha, T., Watanabe, S., & Liu, J. (2023). Membrane compression by synaptic vesicle exocytosis triggers ultrafast endocytosis. *Nature Communications*, *14*(1). https://doi.org/10.1038/s41467-023-38595-2

Ohashi, K. (2015). Roles of cofilin in development and its mechanisms of regulation. In *Development Growth and Differentiation* (Vol. 57, Issue 4, pp. 275–290). Blackwell Publishing. https://doi.org/10.1111/dgd.12213

Okamoto, K. I., Nagai, T., Miyawaki, A., & Hayashi, Y. (2004). Rapid and persistent modulation of actin dynamics regulates postsynaptic reorganization underlying bidirectional plasticity. *Nature Neuroscience*, *7*(10), 1104–1112. https://doi.org/10.1038/nn1311

O'neil, S. D., Rácz, B., Brown, W. E., Gao, Y., Soderblom, E. J., Yasuda, R., & Soderling, S. H. (2021). Action potential-coupled rho gtpase signaling drives presynaptic plasticity. *ELife*, *10*. https://doi.org/10.7554/eLife.63756

Opazo, P., Sainlos, M., & Choquet, D. (2012). Regulation of AMPA receptor surface diffusion by PSD-95 slots. In *Current Opinion in Neurobiology* (Vol. 22, Issue 3, pp. 453–460). https://doi.org/10.1016/j.conb.2011.10.010

O'Rourke, N. A., Weiler, N. C., Micheva, K. D., & Smith, S. J. (2012). Deep molecular diversity of mammalian synapses: Why it matters and how to measure it. In *Nature Reviews Neuroscience* (Vol. 13, Issue 6, pp. 365–379). https://doi.org/10.1038/nrn3170

Papandréou, M. J., & Leterrier, C. (2018). The functional architecture of axonal actin. In *Molecular and Cellular Neuroscience* (Vol. 91, pp. 151–159). Academic Press Inc. https://doi.org/10.1016/j.mcn.2018.05.003

Pathak, D., Shields, L. Y., Mendelsohn, B. A., Haddad, D., Lin, W., Gerencser, A. A., Kim, H., Brand, M. D., Edwards, R. H., & Nakamura, K. (2015). The role of mitochondrially derived ATP in synaptic vesicle recycling. *Journal of Biological Chemistry*, *290*(37), 22325–22336. https://doi.org/10.1074/jbc.M115.656405

Penazzi, L., Bakota, L., & Brandt, R. (2016). Microtubule Dynamics in Neuronal Development, Plasticity, and Neurodegeneration. In *International Review of Cell and Molecular Biology* (Vol. 321, pp. 89–169). Elsevier Inc. https://doi.org/10.1016/bs.ircmb.2015.09.004

Perge, J. A., Niven, J. E., Mugnaini, E., Balasubramanian, V., & Sterling, P. (2012). Why do axons differ in caliber? *Journal of Neuroscience*, *32*(2), 626–638. https://doi.org/10.1523/JNEUROSCI.4254-11.2012

Phillips, T. A., Marcotti, S., Cox, S., & Parsons, M. (2024). Imaging actin organisation and dynamics in 3D. In *Journal of Cell Science* (Vol. 137, Issue 2). Company of Biologists Ltd. https://doi.org/10.1242/jcs.261389

Poliak, S., & Peles, E. (2003). The local differentiation of myelinated axons at nodes of ranvier. In *Nature Reviews Neuroscience* (Vol. 4, Issue 12, pp. 968–980). European Association for Cardio-Thoracic Surgery. https://doi.org/10.1038/nrn1253

Purves, D. , Augustine, G. J. , Fitzpatrick, D. , Hall, W. C. , LaMantia, A.-S. , & & White, L. E. (2018). *Neuroscience* (D. , Purves, G. J. , Augustine, D. , Fitzpatrick, W. C. , Hall, A.-S. , LaMantia, & L. E. White, Eds.; 6th edition). Oxford University Press.

Rangaraju, V., Calloway, N., & Ryan, T. A. (2014). Activity-driven local ATP synthesis is required for synaptic function. *Cell*, *156*(4), 825–835. https://doi.org/10.1016/j.cell.2013.12.042

Rao, T. C., Nawara, T. J., & Mattheyses, A. L. (2022). Live-Cell Total Internal Reflection Fluorescence (TIRF) Microscopy to Investigate Protein Internalization Dynamics. In *Methods in Molecular Biology* (Vol. 2438, pp. 45–58). Humana Press Inc. https://doi.org/10.1007/978-1-0716-2035-9_3

Renz, M. (2013). Fluorescence microscopy-A historical and technical perspective. In *Cytometry Part A* (Vol. 83, Issue 9, pp. 767–779). Wiley-Liss Inc. https://doi.org/10.1002/cyto.a.22295

Reshetniak, S., & Rizzoli, S. O. (2019). Interrogating Synaptic Architecture: Approaches for Labeling Organelles and Cytoskeleton Components. In *Frontiers in Synaptic Neuroscience* (Vol. 11). Frontiers Media S.A. https://doi.org/10.3389/fnsyn.2019.00023

Riedl, J., Crevenna, A. H., Kessenbrock, K., Yu, J. H., Neukirchen, D., Bista, M., Bradke, F., Jenne, D., Holak, T. A., Werb, Z., Sixt, M., & Wedlich-Soldner, R. (2008a). Lifeact: A versatile marker to visualize F-actin. *Nature Methods*, *5*(7), 605–607. https://doi.org/10.1038/nmeth.1220

Riedl, J., Crevenna, A. H., Kessenbrock, K., Yu, J. H., Neukirchen, D., Bista, M., Bradke, F., Jenne, D., Holak, T. A., Werb, Z., Sixt, M., & Wedlich-Soldner, R. (2008b). Lifeact: A versatile marker to visualize F-actin. *Nature Methods*, *5*(7), 605–607. https://doi.org/10.1038/nmeth.1220

Rizo, J. (2022). *Molecular Mechanisms Underlying Neurotransmitter Release*. https://doi.org/10.1146/annurev-biophys-111821

Rust, M. J., Bates, M., & Zhuang, X. (2006). Sub-diffraction-limit imaging by stochastic optical reconstruction microscopy (STORM). *Nature Methods*, *3*(10), 793–795. https://doi.org/10.1038/nmeth929

Ruthel, G., & Banker, G. (1999). Role of Moving Growth Cone-Like "Wave" Structures in the Outgrowth of Cultured Hippocampal Axons and Dendrites. In *J Neurobiol* (Vol. 39).

Saifetiarova, J., Taylor, A. M., & Bhat, M. A. (2017). Early and late loss of the cytoskeletal scaffolding protein, ankyrin G reveals its role in maturation and maintenance of nodes of Ranvier in myelinated axons. *Journal of Neuroscience*, *37*(10), 2524–2538. https://doi.org/10.1523/JNEUROSCI.2661-16.2017

Sainio, M. T., Rasila, T., Molchanova, S. M., Järvilehto, J., Torregrosa-Muñumer, R., Harjuhaahto, S., Pennonen, J., Huber, N., Herukka, S. K., Haapasalo, A., Zetterberg, H., Taira, T., Palmio, J., Ylikallio, E., & Tyynismaa, H. (2022). Neurofilament Light

Regulates Axon Caliber, Synaptic Activity, and Organelle Trafficking in Cultured Human Motor Neurons. *Frontiers in Cell and Developmental Biology*, *9*. https://doi.org/10.3389/fcell.2021.820105

Sakamoto, H., Ariyoshi, T., Kimpara, N., Sugao, K., Taiko, I., Takikawa, K., Asanuma, D., Namiki, S., & Hirose, K. (2018). Synaptic weight set by Munc13-1 supramolecular assemblies. In *Nature Neuroscience* (Vol. 21, Issue 1, pp. 41–55). Nature Publishing Group. https://doi.org/10.1038/s41593-017-0041-9

Sankaranarayanan, S., Atluri, P. P., & Ryan, T. A. (2003). Actin has a molecular scaffolding, not propulsive, role in presynaptic function. *Nature Neuroscience*, *6*(2), 127–135. https://doi.org/10.1038/nn1002

Sasaki, Y. (2020). Local translation in growth cones and presynapses, two axonal compartments for local neuronal functions. In *Biomolecules* (Vol. 10, Issue 5). MDPI AG. https://doi.org/10.3390/biom10050668

Schätzle, P., Wuttke, R., Ziegler, U., & Sonderegger, P. (2012). Automated quantification of synapses by fluorescence microscopy. *Journal of Neuroscience Methods*, *204*(1), 144–149. https://doi.org/10.1016/j.jneumeth.2011.11.010

Scheiffele, P., Fan, J., Choih, J., Fetter, R., & Serafini, T. (2000). Neuroligin Expressed in Nonneuronal Cells Triggers Presynaptic Development in Contacting Axons. In *Cell* (Vol. 101).

Schikorski, T., & Stevens, C. F. (1997). *Quantitative Ultrastructural Analysis of Hippocampal Excitatory Synapses*.

Schmidt, R., Weihs, T., Wurm, C. A., Jansen, I., Rehman, J., Sahl, S. J., & Hell, S. W. (2021). MINFLUX nanometer-scale 3D imaging and microsecond-range tracking on a common fluorescence microscope. *Nature Communications*, *12*(1). https://doi.org/10.1038/s41467-021-21652-z

Schneider, F., Metz, I., & Rust, M. B. (2023). Regulation of actin filament assembly and disassembly in growth cone motility and axon guidance. In *Brain Research Bulletin* (Vol. 192, pp. 21–35). Elsevier Inc. https://doi.org/10.1016/j.brainresbull.2022.10.019

Schneider, J., & Jasnin, M. (2022). Capturing actin assemblies in cells using in situ cryo-electron tomography. *European Journal of Cell Biology*, *101*(3). https://doi.org/10.1016/j.ejcb.2022.151224

Sharonov, A., & Hochstrasser, R. M. (2006). *Wide-field subdiffraction imaging by accumulated binding of diffusing probes*. www.pnas.orgcgidoi10.1073pnas.0609643104

Sheng, M., & Hoogenraad, C. C. (2007). The postsynaptic architecture of excitatory synapses: A more quantitative view. In *Annual Review of Biochemistry* (Vol. 76, pp. 823–847). https://doi.org/10.1146/annurev.biochem.76.060805.160029

Sidenstein, S. C., D'Este, E., Böhm, M. J., Danzl, J. G., Belov, V. N., & Hell, S. W. (2016). Multicolour multilevel STED nanoscopy of actin/spectrin organization at synapses. *Scientific Reports*, *6*. https://doi.org/10.1038/srep26725

Siksou, L., Rostaing, P., Lechaire, J. P., Boudier, T., Ohtsuka, T., Fejtová, A., Kao, H. T., Greengard, P., Gundelfinger, E. D., Triller, A., & Marty, S. (2007). Three-dimensional

architecture of presynaptic terminal cytomatrix. *Journal of Neuroscience*, *27*(26), 6868–6877. https://doi.org/10.1523/JNEUROSCI.1773-07.2007

Smith, B. A., Gelles, J., & Goode, B. L. (2014). Single-molecule studies of actin assembly and disassembly factors. In *Methods in Enzymology* (Vol. 540, pp. 95–117). Academic Press Inc. https://doi.org/10.1016/B978-0-12-397924-7.00006-6

Soltisz, A. M., Craigmile, P. F., & Veeraraghavan, R. (2024). Spatial Pattern Analysis using Closest Events (SPACE)-A Nearest Neighbor Point Pattern 2 Analysis Framework for Assessing Spatial Relationships from Image Data Brief Title Spatial Pattern Analysis using Closest Events Author Names 8 Primary Institutions. *Microscopy and Microanalysis, University Press on Behalf of the Microscopy Society of America*, *Volume 30*(Issue 2), 306–317. https://doi.org/10.1101/2023.05.17.541131

Song, J.-Y., Ichtchenko, K., Su¨dhofsu¨dhof, T. C., & Brose, N. (1999). *Neuroligin 1 is a postsynaptic cell-adhesion molecule of excitatory synapses* (Vol. 96). www.pnas.org.

Spence, E. F., Kanak, D. J., Carlson, B. R., & Soderling, S. H. (2016). The Arp2/3 complex is essential for distinct stages of spine synapse maturation, including synapse unsilencing. *Journal of Neuroscience*, *36*(37), 9696–9709. https://doi.org/10.1523/JNEUROSCI.0876-16.2016

Spence, E. F., & Soderling, S. H. (2015). Actin out: Regulation of the synaptic cytoskeleton. In *Journal of Biological Chemistry* (Vol. 290, Issue 48, pp. 28613–28622). American Society for Biochemistry and Molecular Biology Inc. https://doi.org/10.1074/jbc.R115.655118

Stefanou, M. I. (2020). The footprints of neuroscience in Alexandria during the 3rd-century BC: Herophilus and Erasistratus. *Journal of Medical Biography*, *28*(4), 186–194. https://doi.org/10.1177/0967772018789349

Steffens, H., Mott, A. C., Li, S., Wegner, W., Švehla, P., Kan, V. W. Y., Wolf, F., Liebscher, S., & Willig, K. I. (2021). Stable but not rigid: Chronic in vivo STED nanoscopy reveals extensive remodeling of spines, indicating multiple drivers of plasticity. In *Sci. Adv* (Vol. 7). https://www.science.org

Stockwell, I., Watson, J. F., & Greger, I. H. (2024). Tuning synaptic strength by regulation of AMPA glutamate receptor localization. *BioEssays*, *46*(7). https://doi.org/10.1002/bies.202400006

Südhof, T. C. (2008). Neuroligins and neurexins link synaptic function to cognitive disease. In *Nature* (Vol. 455, Issue 7215, pp. 903–911). Nature Publishing Group. https://doi.org/10.1038/nature07456

Südhof, T. C. (2012). The presynaptic active zone. In *Neuron* (Vol. 75, Issue 1, pp. 11–25). https://doi.org/10.1016/j.neuron.2012.06.012

Südhof, T. C., & Rizo, J. (2011). Synaptic vesicle exocytosis. *Cold Spring Harbor Perspectives in Biology*, *3*(12). https://doi.org/10.1101/cshperspect.a005637

Tanaka, H., Funahashi, J., & Hirano, T. (2023). Live-cell imaging of endocytosed synaptophysin around individual hippocampal presynaptic active zones. *Frontiers in Cellular Neuroscience*, *17*. https://doi.org/10.3389/fncel.2023.1277729

Tanaka, K., Takeda, S., Mitsuoka, K., Oda, T., Kimura-Sakiyama, C., Maéda, Y., & Narita, A. (2018). Structural basis for cofilin binding and actin filament disassembly. *Nature Communications*, *9*(1). https://doi.org/10.1038/s41467-018-04290-w

Tang, A. H., Chen, H., Li, T. P., Metzbower, S. R., MacGillavry, H. D., & Blanpied, T. A. (2016). A trans-synaptic nanocolumn aligns neurotransmitter release to receptors. *Nature*, *536*(7615), 210–214. https://doi.org/10.1038/nature19058

Tas, R. P., & Kapitein, L. C. (2018). Exploring cytoskeletal diversity in neurons. In *Science* (Vol. 361, Issue 6399, pp. 231–232). American Association for the Advancement of Science. https://doi.org/10.1126/science.aat5992

Trouillon, R., & Ewing, A. G. (2014). Actin controls the vesicular fraction of dopamine released during extended kiss and run exocytosis. *ACS Chemical Biology*, *9*(3), 812–820. https://doi.org/10.1021/cb400665f

Uchida, A., Peng, J., & Brown, A. (2023). Regulation of neurofilament length and transport by a dynamic cycle of phospho-dependent polymer severing and annealing. *Molecular Biology of the Cell*, *34*(7). https://doi.org/10.1091/mbc.E23-01-0024

Unsain, N., Stefani, F. D., & Cáceres, A. (2018). The actin/spectrin membrane-associated periodic skeleton in neurons. In *Frontiers in Synaptic Neuroscience* (Vol. 10, Issue MAY). Frontiers Media S.A. https://doi.org/10.3389/fnsyn.2018.00010

Urban, N. T., Willig, K. I., Hell, S. W., & Nägerl, U. V. (2011). STED nanoscopy of actin dynamics in synapses deep inside living brain slices. *Biophysical Journal*, *101*(5), 1277–1284. https://doi.org/10.1016/j.bpj.2011.07.027

Vassilopoulos, S., Gibaud, S., Jimenez, A., Caillol, G., & Leterrier, C. (2019). Ultrastructure of the axonal periodic scaffold reveals a braid-like organization of actin rings. *Nature Communications*, *10*(1). https://doi.org/10.1038/s41467-019-13835-6

Venkatesh, K., Mathew, A., & Koushika, S. P. (2020). Role of actin in organelle trafficking in neurons. In *Cytoskeleton* (Vol. 77, Issues 3–4, pp. 97–109). John Wiley and Sons Inc. https://doi.org/10.1002/cm.21580

Wang, J. C., Bolger-Munro, M., & Gold, M. R. (2018). Visualizing the actin and microtubule cytoskeletons at the b-cell immune synapse using stimulated emission depletion (STED) microscopy. *Journal of Visualized Experiments*, *2018*(134). https://doi.org/10.3791/57028

Wang, J., Zhang, Z., Shen, H., Wu, Q., & Gu, M. (2023). Application and development of fluorescence probes in MINFLUX nanoscopy (invited paper). In *Journal of Innovative Optical Health Sciences* (Vol. 16, Issue 1). World Scientific. https://doi.org/10.1142/S1793545822300117

Wang, L., Ho, C.-L., Sun, D., Liem, R. K. H., & Brown, A. (2000). Rapid movement of axonal neurofilaments interrupted by prolonged pauses. In *NATURE CELL BIOLOGY* (Vol. 2).

Wegner, W., Ilgen, P., Gregor, C., Van Dort, J., Mott, A. C., Steffens, H., & Willig, K. I. (2017). In vivo mouse and live cell STED microscopy of neuronal actin plasticity using far-red emitting fluorescent proteins. *Scientific Reports*, *7*(1). https://doi.org/10.1038/s41598-017-11827-4

Wen, P. J., Grenklo, S., Arpino, G., Tan, X., Liao, H. S., Heureaux, J., Peng, S. Y., Chiang, H. C., Hamid, E., Zhao, W. D., Shin, W., Näreoja, T., Evergren, E., Jin, Y., Karlsson, R., Ebert, S.

N., Jin, A., Liu, A. P., Shupliakov, O., & Wu, L. G. (2016). Actin dynamics provides membrane tension to merge fusing vesicles into the plasma membrane. *Nature Communications*, *7*. https://doi.org/10.1038/ncomms12604

Westphal, V., Rizzoli, S. O., Lauterbach, M. A., Kamin, D., Jahn, R., & Hell, S. W. (2008). Video-rate far-field optical nanoscopy dissects synaptic vesicle movement. *Science*, *320*(5873), 246–249. https://doi.org/10.1126/science.1154228

Willig, K. I., Rizzoli, S. O., Westphal, V., Jahn, R., & Hell, S. W. (2006). STED microscopy reveals that synaptotagmin remains clustered after synaptic vesicle exocytosis. *Nature*, *440*(7086), 935–939. https://doi.org/10.1038/nature04592

Wu, L. G., & Chan, C. Y. (2022). Multiple Roles of Actin in Exo- and Endocytosis. In *Frontiers in Synaptic Neuroscience* (Vol. 14). Frontiers Media S.A. https://doi.org/10.3389/fnsyn.2022.841704

Wu, Y. Le, Hoess, P., Tschanz, A., Matti, U., Mund, M., & Ries, J. (2023). Maximum-likelihood model fitting for quantitative analysis of SMLM data. *Nature Methods*, *20*(1), 139–148. https://doi.org/10.1038/s41592-022-01676-z

Wulf, E., Debobent, A., Bautz, F. A., Faulsticht, H., & Wielandtt, T. H. (1979). Fluorescent phallotoxin, a tool for the visualization of cellular actin (microfilaments/rat kangaroo PtK1 cells/bovine kidney MDBK cells). In *Cell Biology* (Vol. 76, Issue 9). https://www.pnas.org

Wurz, A. I., Schulz, A. M., O'Bryant, C. T., Sharp, J. F., & Hughes, R. M. (2022). Cytoskeletal dysregulation and neurodegenerative disease: Formation, monitoring, and inhibition of cofilin-actin rods. In *Frontiers in Cellular Neuroscience* (Vol. 16). Frontiers Media S.A. https://doi.org/10.3389/fncel.2022.982074

Xu, K., Zhong, G., & Zhuang, X. (2013). Actin, spectrin, and associated proteins form a periodic cytoskeletal structure in axons. *Science*, *339*(6118), 452–456. https://doi.org/10.1126/science.1232251

Xu, R., & Du, S. (2021). Overexpression of Lifeact-GFP Disrupts F-Actin Organization in Cardiomyocytes and Impairs Cardiac Function. *Frontiers in Cell and Developmental Biology*, *9*. https://doi.org/10.3389/fcell.2021.746818

Yau, K. W., Schätzle, P., Tortosa, E., Pagès, S., Holtmaat, A., Kapitein, L. C., & Hoogenraad, C. C. (2016). Dendrites In vitro and In vivo contain microtubules of opposite polarity and axon formation correlates with uniform plus-end-out microtubule orientation. *Journal of Neuroscience*, *36*(4), 1071–1085. https://doi.org/10.1523/JNEUROSCI.2430-15.2016

Yokobori, S., Nakae, R., & Yokota, H. (2020). Neurofilaments light chain/Neurofilaments heavy chain. In *Biomarkers for Traumatic Brain Injury* (pp. 193–203). Elsevier. https://doi.org/10.1016/B978-0-12-816346-7.00013-0

York, G. K., & Steinberg, D. A. (2009). Chapter 3 Neurology in Ancient Egypt. In *Handbook of Clinical Neurology* (Vol. 95, Issue C, pp. 29–36). Elsevier B.V. https://doi.org/10.1016/S0072-9752(08)02103-9

Yu, W., & Baas, P. W. (1994). Changes in Microtubule Number and Length during Axon Differentiation. In *The Journal of Neuroscience* (Vol. 14, Issue 5).

Yuste, R. (2015). From the neuron doctrine to neural networks. In *Nature Reviews Neuroscience* (Vol. 16, Issue 8, pp. 487–497). Nature Publishing Group. https://doi.org/10.1038/nrn3962

Zhang, S. X., Duan, L. H., Qian, H., & Yu, X. (2016). Actin Aggregations Mark the Sites of Neurite Initiation. *Neuroscience Bulletin*, *32*(1), 1–15. https://doi.org/10.1007/s12264-016-0012-2

Zhang, W., & Benson, D. L. (2001a). *Stages of Synapse Development Defined by Dependence on F-Actin*.

Zhang, W., & Benson, D. L. (2001b). *Stages of Synapse Development Defined by Dependence on F-Actin*.

Zhao, B., Meka, D. P., Scharrenberg, R., König, T., Schwanke, B., Kobler, O., Windhorst, S., Kreutz, M. R., Mikhaylova, M., & Calderon De Anda, F. (2017). Microtubules Modulate F-actin Dynamics during Neuronal Polarization. *Scientific Reports*, *7*(1). https://doi.org/10.1038/s41598-017-09832-8

Zhong, G., He, J., Zhou, R., Lorenzo, D., Babcock, H. P., Bennett, V., & Zhuang, X. (2014). Developmental mechanism of the periodic membrane skeleton in axons. *ELife*, *3*. https://doi.org/10.7554/eLife.04581

Zhou, Q., Homma, K. J., & Poo, M. M. (2004). Shrinkage of dendritic spines associated with long-term depression of hippocampal synapses. *Neuron*, *44*(5), 749–757. https://doi.org/10.1016/j.neuron.2004.11.011

Zhou, Q., Zhou, P., Wang, A. L., Wu, D., Zhao, M., Südhof, T. C., & Brunger, A. T. (2017). The primed SNARE-complexin-synaptotagmin complex for neuronal exocytosis. *Nature*, *548*(7668), 420–425. https://doi.org/10.1038/nature23484

Zhou, R., Han, B., Nowak, R., Lu, Y., Heller, E., Xia, C., Chishti, A. H., Fowler, V. M., & Zhuang, X. (2022). Proteomic and functional analyses of the periodic membrane skeleton in neurons. *Nature Communications*, *13*(1). https://doi.org/10.1038/s41467-022-30720-x

Zigmond, S. H. (2004). Formin-induced nucleation of actin filaments. In *Current Opinion in Cell Biology* (Vol. 16, Issue 1, pp. 99–105). https://doi.org/10.1016/j.ceb.2003.10.019

Zocchi, R., Compagnucci, C., Bertini, E., & Sferra, A. (2023). Deciphering the Tubulin Language: Molecular Determinants and Readout Mechanisms of the Tubulin Code in Neurons. In *International Journal of Molecular Sciences* (Vol. 24, Issue 3). MDPI. https://doi.org/10.3390/ijms24032781

Zoghbi, H. Y. (1986). Postnatal Neurodevelopmental Disorders: Meeting at the Synapse? In *Proc. Natl. Acad. Sci. U.S.A* (Vol. 19, Issue 2). Plenum. www.sciencemag.org